Arak University
1972
JGERI
Journal of Green Energy Research and Innovation
ISSN: 3041-9018

# Journal of Green Energy Research and Innovation

Volume 2, Issue 1, Winter 2025

PUBLISHER
**Arak University**

# Journal of Green Energy Research and Innovation (JGERI)

Publisher: **Arak University**

Director-in-Charge: **Dr. Ali Asghar Ghadimi**

Editor-in-Chief: **Prof. Gevork B. Gharehpetian**

Deputy Editor: **Dr. Abolghasem Daeichian**

Managing and Executive Editor**: Dr. Mahyar Abasi**

Coverage area: **International**

Journal Type: **Scientific and technical**

Scientific Rank (Iran MSRT): **B**

Language: **English**

Frequency: **Quarterly**

Review Time: **4-8 Weeks**

Publication Type: **Electronic**

Open Access: **Yes**



Policy: **Peer-Reviewed**

DOI**: 10.61186/jgeri**

E-mails: **jgeri@araku.ac.ir**

Website: **https://jgeri.araku.ac.ir/**

Address: **Department of Electrical Engineering, Faculty of Engineering, Arak University, Arak, Iran.**

P.O. Box: **38156-8-8349**

Tel: **086-32625099**

# Editorial Board

# About Journal

**JGERI** is an international, open-access, and free-of-charge journal in the field of green and renewable energies, published quarterly, only electronically, in cooperation with the Renewable Energy Research Institute (**RERI**) of Arak University and Iranian Association of Electrical and Electronics Engineers (**IAEEE**). Articles accepted and published by **JGERI** are in three formats: research articles, review articles, and applied articles. **JGERI** accepts manuscripts that provide results of scientific achievements in a very wide scope of fundamental, engineering, and industrial research focusing on green energy.

The following articles are acceptable:

- **Research articles** are expected to present innovative solutions, new concepts, or creative ideas that can help solve existing or emerging technical challenges in the field of green and renewable energy.
- **Review articles** are expected to provide enlightening and specialized reviews, trainings, or case studies on an important topic, timely and widely in the field of green and renewable energies.
- **Applied articles** are expected to share the results of the industry's valuable experiences in dealing with challenging technical issues, developing/adopting new standards, applying new technologies or solving complex problems in the field of green and renewable energies. These articles can have a significant impact on the strategic plans of the industry in the coming years.

# Aims and Scope

JGERI is interested on the qualified international multidisciplinary research results related to all aspects of green energy. The scope of JGERI is very broad, and welcomes original, novel fundamental and engineering research. We also publish reviews and industrial reports of green energy and its impact on the eco-environment.

We welcome research papers that focus on, but are not limited to, the following areas:

- Policies and Strategies for Green Energy Systems
- Fundamental And Industrial Applications for Green Energy Systems
- Energy Conversion, Control Techniques, and Grid Interactive Systems for Green Energy Systems
- Environmental Impacts of Energy Technologies and Pollution Control
- Materials And Catalysis for Green Energy Systems
- Green Energy Consumption
- Artificial Intelligence, Machine Learning, and Computational Methods in Green Energy Systems
- Public Awareness and Education for Green Energy Systems
- Solar Energy and Photovoltaic
- Wind Energy
- Hydrogen Energy and Energy Storage
- Biofuel and Bioenergy
- Utilization of Green Energies in the Structure of Power Systems
- Development of Manufacturing Technology for Green Energy Production Tools
- Electricity Market in the Presence of Green Energies
- The Effects of Green Energy Production on Power Quality of the Power System
- Impact of Expansion Planning of Power Systems on the Development of Green Energy Generation
- Operation of Green Energy-Based Microgrids
- Control and Protection of Power Systems in Networks Equipped with Green and Renewable Generation
- Energy Management in Networks Consisting of Green Energies
- Studies on the Technology of Hybrid Vehicles Based on Green Energy Fuels
- The Future Perspective of the Electricity Industry in the Presence of Production-Based Technologies and Green Energy-Based Consumers
- Green Energy Storage Technologies
- Communication Infrastructures and Protocols and Internet in Green Energy-Based Power Systems
- Cyber Security and Defense Activities in the Field of Green Energy Management

Each manuscript will go through a rigors peer-review process. you can visit our Guide for Authors page for information on preparing your manuscript.

# Guide for Authors

1. **Important points and rules for manuscript submission and publication**

-Submitting a manuscript to a journal means that the manuscript is not under review or has not been published anywhere in any other language before.
-The submission of the manuscript for publication by the author, implicitly or explicitly, implies the approval of the organization or body where the author works and has used its affiliation.
-By submitting the manuscript, all authors officially declare their agreement to grant the copyright of the manuscript in case of acceptance to Arak University and JGERI. However, the authors are responsible for all the contents published in the manuscript, and the journal is only a reviewer and publisher.
- All authors are required to declare any actual or potential conflicts of interest, including financial, personal, or relationships with individuals or organizations that could affect their work.
- Each of the authors must declare their contribution and role in the manuscript on the Title Page to the journal. The statement of approval of all authors and their role in the manuscript is the responsibility of the corresponding author.
- Authors should note that all manuscripts sent to JGERI are checked with Authenticate's CrossCheck software to analyze the authenticity of the content. In this analysis, the overlap and similar texts presented in the submitted manuscripts will be determined.
- JGERI makes its manuscripts open to access after publication and there is no charge (APC) for reviewing and publication of manuscripts, and readers can download and use the articles for free.
- All authors, if they had financial support in conducting research related to this manuscript, should briefly state their role. If financial source(s) have no role in the results of the research published by the article, this should also be mentioned by the authors.
- Acknowledgments to individuals and institutions can be mentioned in a separate section at the end of the manuscript before References, and they must not be included as footnotes or in any other form. In this section, it is recommended to mention the names of those who have collaborated during the research (such as those helping in the language correctness aspect of the manuscript, assisting in writing the manuscript or proofreading it, and other cases).
- Non-commercial use of the manuscript will be governed by the Creative Commons Attribution-NonCommercial 4.0 International License, which is currently available at the link (https://creativecommons.org/licenses/by-nc/4.0/). This certificate allows others to use the authors' work in a non-commercial way and utilize it in their research work, although in the new work, they need to acknowledge the authors and mention its non-commercial nature.

## 2. Initial submission of the manuscript

Submission to this journal is online and you will be accompanied in all the steps of creating a user account and uploading files. All correspondence, including notification of the editor's decision and request for revision, will be made via email. To submit your manuscript, just click on the **Submit Manuscript** option on the journal page. Then, click on **Register** to create an author account. A message will be sent to your email containing your username and password. Then, log in to the manuscript submission system on the Users login page, where you need to enter the username and password and submit your new manuscript. Once you are logged in, you can change your password by clicking on My Home in the top menu. For the next time, just log in to your account. Please include the names, addresses, and email addresses of at least three potential academic reviewers with the paper. Please include reviewers' names and their academic rank, affiliation, and contact information (mail address is mandatory). However, only the editor has the right to decide on the use of suggested reviewers. All the submitted manuscripts undergo the process of plagiarism check with IThenticate software and the review process begins. According to the journal policy, there is a difference between the requirements for initial and revised submission files. Required files for initial submission include three files: **JGERI_Main_Manuscript**, **JGERI_Form_for _Copyright_Transfer_Statement and Conflict_ of_ Interest_ Disclosure** and **JGERI_Cover_Letter**, all three of which must be sent to the journal in PDF format. You can use the links below to download the requirements and suggestions files of these three files.

- JGERI_Guideline_for_Main_Manuscript
- JGERI_Guideline_for_Cover_Letter
- JGERI_Form_for_Copyright_Transfer_Statement and Conflict_ of_ Interest_ Disclosure

## 3. Submission of the revised manuscript

If the submitted manuscript, after going through the initial review process, is evaluated by the officials and reviewers of the journal and a decision is made to make corrections and revisions in the form of minor or major, the authors are obliged to make the corrections and prepare the response letter to the reviewers within the time specified by the journal. Three files must be sent to the journal at this stage: WORD and PDF files of the revised manuscript (changes should be highlighted), PDF file of the response to the reviewers (including the comments and responses of each of the reviewers separately), Title Page and Authorship file in WORD format (containing two main forms: Title Page and Authorship). The link to download the necessary files along with their requirements and instructions is given below. Points raised in the file **JGERI_Revised_Manuscript** must be followed for compiling the revised manuscript.

The authors are obliged to submit the revised file in PDF and WORD format to the journal. Also, different parts of the file **JGERI_Form_for_Title_Page_ and_ Authorship** needs to be completed and signed by the corresponding author, but **JGERI_Response_to_the_Reviewers_Comments** is suggested by the journal and it is not necessary to follow all the points of that file. It should be noted that all the stages of page layout and editing in the form of final publication are the responsibility of the journal. In the completion stages of this process, the cooperation of the authors is needed, and we will inform you at each stage. Thus, the minimum requirements for file compilation are provided in the template file.

- JGERI_Guideline_for_Revised_Manuscript
- JGERI_Form_for_Title_Page_ and_ Authorship
- JGERI_Guideline_for_Response_to_the_Reviewers_Comments

## 4. After the final acceptance of the manuscript

After announcing the final acceptance of the manuscript (reviews may happen several times), the files **JGERI_Revised_Manuscript** and **JGERI_Form_for_ Title_Page_ and_ Authorship** will be sent to the paging unit for page layout and final editing. After the final acceptance announcement, the authors will be asked to send a graphic abstract included in a single file. Then, the process of compilation of the manuscript will be completed by the journal and finally, the proof version of the manuscript will be sent to the authors. The authors are obliged to check the proof file completely and report to the journal if they find any ambiguity or error in the final file. In some cases, along with the final proof file of the manuscript, there may be a series of errors and ambiguities in the manuscript, which are sent to the author in the form of comments along with the proof version of the manuscript. The corresponding author is obliged to clarify and resolve these problems and ambiguities in the specified time.

## 5. After publication on the journal's website

After announcing the initial acceptance, the information of the article without its content will be indexed in the Articles in the Press section of the website. After including the article in the issue selected by the journal, the desired article will be indexed in the Current Issue unit along with Vol., No., and pp. Also, the electronic file of the article can be introduced in all scientific references through the DOI link. The important point is that, after acceptance and indexing, the names of the authors cannot be changed, that is, it will not be possible to add, delete, or change the order of the names of the authors and their organizational affiliations.

# Cooperative Publication Organization

**Renewable Energy Research Institute of Arak University**
http://araku.ac.ir/web/riren

**Iranian Association of Electrical and Electronics Engineers**
https://iaeee.ir/

**Iranian Wind Energy Association**
https://www.irwea.org/fa/

# Indexing Databases and Social Networks

**Iran MSRT:** https://journals.msrt.ir/home/detail/21538/

**Magiran:** https://www.magiran.com/magazine/8484

**Google Scholar:** https://scholar.google.com/citations?user=47bsJFoAAAAJ&hl=en

**Linkedin:** https://www.linkedin.com/in/jgeri-arak-university-0818872b9

**Academia:** https://independent.academia.edu/JournalofGreenEnergyResearchandInnovationJGERI

**MyScineceWork:** https://www.mysciencework.com/profile/j.green.energy.res.innov.jgeri

# Contents

Journal of Green Energy Research and Innovation

# Optimal Operation and Management of Energy Resources in Microgrids in the Presence of Renewable Resources and Energy Storage by Modified Grey Wolf Optimization Algorithm

Javad Nikoukar, Shokoofeh Mohammadi, Hamid Reza Hanif, Reza Aminpour Gogani, Masoumeh Ghafari, Abdolreza Behvandi

## Highlights

- Modified Grey Wolf Optimization (MGWO) algorithm optimizes microgrid energy management.
- MGWO beats Particle Swarm Optimization (PSO) in two scenarios, reducing costs and improving efficiency.
- Negative energy costs indicate economic gains from electricity sales, especially with renewables.

## Graphical Abstract


Use your device to scan and read the article online

Citation
J. Nikoukar, S. Mohammadi, et al.," Optimal Operation and Management of Energy Resources in Microgrids in the Presence of Renewable Resources and Energy Storage by Modified Grey Wolf Optimization Algorithm," *Journal of Green Energy Research and Innovation*, vol. 2, no. 1, pp. 1-13, 2025.

https://doi.org/10.61186/jgeri.2.1.1

JGERI Journal of Green Energy Research and Innovation

Journal of Green Energy Research and Innovation 2.1 (2025) 1-13

Online ISSN: 3041-9018

Journal of Green Energy Research and Innovation

Journal Homepage: www.jgeri.araku.ac.ir

# Optimal Operation and Management of Energy Resources in Microgrids in the Presence of Renewable Resources and Energy Storage by Modified Grey Wolf Optimization Algorithm

Javad Nikoukar [1], Shokoofeh Mohammadi [1,2], Hamid Reza Hanif [3,*], Reza Aminpour Gogani [4], Masoumeh Ghafari [5], Abdolreza Behvandi [6]

[1] *Department of Electrical Engineering, Saveh Branch, Islamic Azad University, Saveh, Iran.*
[2] *Department of Electrical Engineering, Science and Research Branch, Islamic Azad University, Tehran, Iran.*
[3] *Iran University of Science and Technology (IUST), Tehran, Iran.*
[4] *Resilient Smart Grid Research Lab, Department of Electrical Engineering, Azarbaijan Shahid Madani University, Tabriz, Iran.*
[5] *Electrical and Computer Engineering Department, Babol Noshirvani University of Technology, Babol, Iran.*
[6] *Department of Electrical Engineering, Ramhormoz Branch, Islamic Azad University, Ramhormoz, Iran.*

A R T I C L E I N F O

***Keywords:***
Microgrid Energy Management,
Distributed Generation Resources,
Reliability,
Gray Wolf Algorithm.

***Article History:***
Received: 15 April 2024;
Revised: 23 May 2024;
Accepted: 31 May 2024.

***Article type:***
Research Article

* ***Corresponding author***
*E-mail address:*
h.hanif.iustz@gmail.com (H. R. Hanif)

A B S T R A C T

This paper delves into the meticulous optimization of distributed energy resources and their storage within a conventional microgrid framework. The optimization endeavor leverages an array of cutting-edge technologies including photovoltaic, wind, fuel cells, micro-turbines, and batteries, with the dual objectives of curtailing operational expenses and fortifying system reliability. To attain these objectives, the article employs a refined algorithm derived from the Grey Wolf Optimization technique. Furthermore, simulations are executed under two distinct scenarios. In the first scenario, the presumption is that all distributed energy resources within the microgrid are exploitable, whereas in the second scenario, spatial constraints necessitate the exclusion of photovoltaic and wind turbine resources. Simulation outcomes evince that post-implementation of energy management via metaheuristic algorithms, there is a discernible reduction in the operational costs of the microgrid alongside an enhancement in system reliability. Additionally, the elimination of photovoltaic and wind resources results in escalated costs and grid blackout within the microgrid. In summary, the simulation findings affirm the superior efficacy of the proposed modified Grey Wolf algorithm in addressing energy management quandaries in comparison to the Particle Swarm Optimization algorithm.

## 1. Introduction

The energy sector is witnessing a crucial shift towards decentralized renewable sources [1] due to the environmental and economic challenges posed by diminishing fossil fuels. This shift aims to combat rising global temperatures and environmental degradation. Recent research has focused on developing efficient energy systems, reducing power losses by utilizing decentralized generation resources, also known as Distributed Energy Resources (DERs) [2]. DERs, equipped with power electronics, can actively manage grid parameters when integrated.

Microgrids represent a significant advancement in aggregating these DERs [3]. They are self-contained networks comprising various renewable sources, storage, and controllable loads, with the capability to operate independently. Microgrids are designed with power electronic converters to ensure flexibility and seamless operation. Engineers advocate for decentralized generation within microgrids to reduce energy costs, especially in remote areas, where they can harness wind, solar, and other renewable sources. This approach offers multiple benefits, including cost savings, load optimization, and improved system stability [4], while also reducing environmental impacts. The successful integration of DERs into microgrids is a key strategy for a sustainable energy future, addressing both economic and environmental concerns. A variety of solutions has been developed for optimal microgrid operation management, predominantly falling under the following categories delineated in research spanning the last two decades:

A variety of solutions has been developed for optimal microgrid operation management, predominantly falling under the following categories delineated in research spanning the last two decades:

A) Traditional Optimization Methods:

• Nonlinear programming [5,6]
• Linear programming [7]
• Mixed-integer programming [8]
• Modified interior point method [9]

B) Intelligent Optimization Methods:

• Genetic algorithm [10]
• Particle swarm optimization algorithm [11]
• Artificial neural network [12]

Conventional optimization algorithms employed for microgrid operation planning typically employ diverse search techniques, capable of addressing second-degree objective optimization problems with singular minima. In recent years, sophisticated optimization methodologies grounded in artificial intelligence have gained traction in optimal microgrid management, aimed at ameliorating the local optimum conundrum and addressing uncertainties inherent in the problem [13-16].

This paper focuses on the optimal management of renewable energy and electrical energy storage within standard microgrids to reduce operational costs while upholding reliability metrics. A refined and enhanced iteration of the Grey Wolf Optimization (GWO) technique, dubbed the Modified Grey Wolf Optimization (MGWO) algorithm, is proposed herein for this purpose. The subsequent sections delineate the mathematical formulation of the problem, elucidate the proposed algorithm, and present simulation results derived from the implementation of the algorithm under two scenarios, with and without renewable resources.

## 2. Microgrid

Microgrids constitute an integral component of the power distribution framework, encompassing diverse arrays of distributed energy resources and consumers of both electricity and thermal energy. Outfitted with switchgear and transformers, these grids possess the capability to seamlessly connect to or disconnect from the primary network, catering to a spectrum of subscribers spanning residential, commercial, and industrial domains. Illustrated in Figure 1, a microgrid interfaces with the upstream network while offering not only energy provision for local demands but also ancillary services and thermal energy, exemplifying its multifunctionality. The foundational configuration of a microgrid, as depicted in Figure 1, features a pivotal node, facilitated by a switch, establishing connection with the upstream network.

In contrast to traditional power systems reliant on centralized operation of large-scale thermal power plants, microgrids exert significantly lesser environmental strain. Leveraging non-fossil energy sources, microgrids play a pivotal role in curbing greenhouse gas emissions, constituting one of their most notable advantages. Moreover, the proximity of consumers to energy sources fosters heightened awareness regarding optimal energy utilization, thereby augmenting overall efficiency.

In the market milieu, two overarching policies govern the integration of microgrids. Firstly, the microgrid's entire energy demand is met through local resources, disregarding interactions with the upstream network. Under this paradigm, the microgrid operator endeavors to minimize operational costs on an hourly basis. Secondly, the operator retains the option to engage in power exchange within the market, striving to optimize cost efficiency and production output for sale to the upstream network, thereby maximizing revenue.

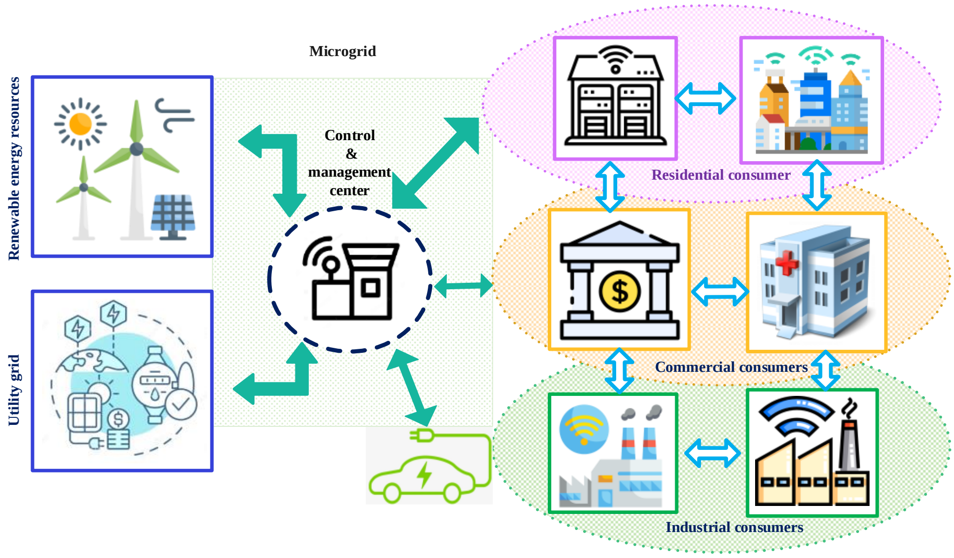


**Figure 1.** A model of a sample microgrid.

Effective planning and operation of microgrids necessitate consideration of both short-term exigencies and long-term imperatives. Short-term operational constraints encompass load shedding protocols, transient voltage and frequency modulation, dynamic response adequacy, and power quality standards for sensitive loads. Control architecture within microgrids is dichotomized into centralized and decentralized frameworks, each comprising three hierarchical tiers: Distribution Network Operator (DNO), potentially accompanied by a Market Operator (MO), Microgrid Central Controller (MGCC) incorporating the microgrid operator, and local controllers affiliated with individual distributed generation units or loads.

Seamless bidirectional communication between local controllers and the microgrid's central controller constitutes a fundamental requisite, feasibly facilitated through telecommunications infrastructure, power transmission channels, or wireless mediums. The central controller of the microgrid is vested with the responsibility of optimizing power interchange with the primary network and maximizing production, informed by prevailing market dynamics and security constraints. Planning activities undertaken by the central controller occur at predefined intervals, such as every 15 minutes for forthcoming hours.

In alignment with market-oriented strategies, the microgrid operator orchestrates planning and execution processes based on a plethora of inputs, encompassing market prices, proposed pricing structures, and priority delineations for local supply, iteratively coordinated with local controllers. Additionally, the operator devises strategies and implements proposed pricing mechanisms alongside production levels stipulated by controllers of dispersed generation resources, while adhering to network security imperatives and leveraging predictive analytics for renewable energy sources.

## 3. Model of Cascading Networks Under Study

This article delves into the intricacies of managing microgrid energy, as depicted by the schematic in Figure 2. The microgrid under examination harnesses a blend of photovoltaic panels, wind turbines, and microturbines as its distributed generation sources. To store the electrical bounty, it relies on fuel cells and batteries. Seamless integration with the main power grid is enabled through a distribution transformer, ensuring fluid power exchange. Noteworthy is the microgrid's ability to monetize surplus energy by vending it to the grid, thus providing economic dividends for its operator. Operating at a voltage of 400 volts, it engages in power transactions with the upper grid through a 20/0.4 kilovolt distribution transformer, maintaining a frequency of 50 hertz. The microgrid's load peaks at approximately 1695 kilowatts, with a zenith of 90 kilowatts around hour 19.

Within the microgrid, loads are presumed to be temporally distributed and variable. Energy procurement costs from the grid are judiciously managed on a time-of-use (TOU) framework. Figure 3 meticulously outlines consumer energy demands juxtaposed against hourly electricity prices. The microgrid's energy tariff fluctuates between $0.14 and $0.4 per kilowatt-hour, aligning with grid loads ranging from 50 kilowatts to 90 kilowatts. The calculation of consumed energy costs involves a simple multiplication of hourly consumption with the corresponding electricity price, elegantly visualized in Figure 4.

Consequently, the total system cost, bereft of distributed generation sources, tallies up to $2164. Solar and wind generation capacities within the microgrid are intricately tied to solar irradiance, local wind speeds, and the installation density of solar panels and wind turbines. Consequently, the maximum generation capacities from these sources are meticulously derived and showcased in Figure 5. The microgrid's distributed generation and battery storage capabilities are bound by power constraints, meticulously laid out in Table 1. Negative power values for the battery denote storage operations. Moreover, accounting for startup costs in fuel cell and microturbine generation, power exchange with the main grid, capped at a maximum of 30 kilowatts, remains a viable option.

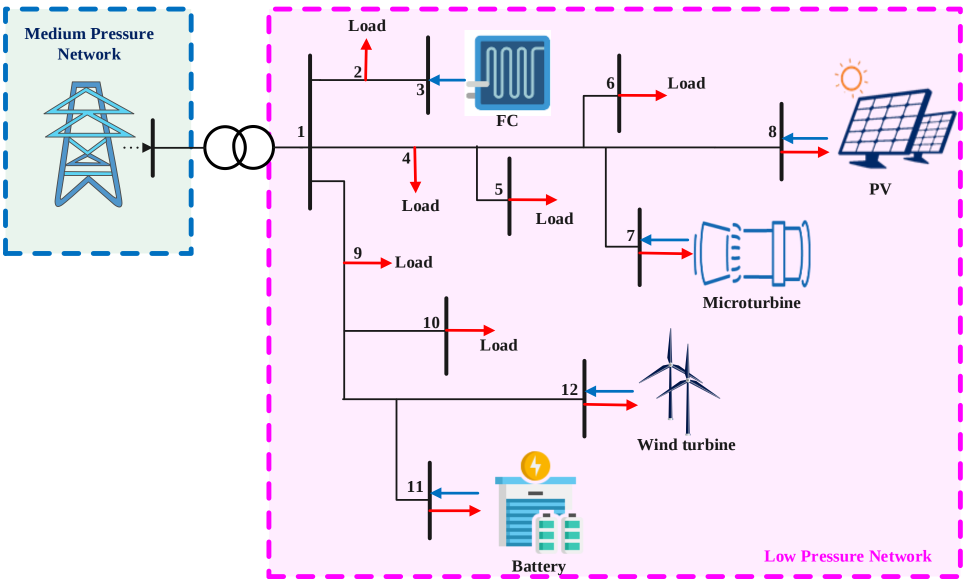


**Figure 2.** The studied microgrid model.

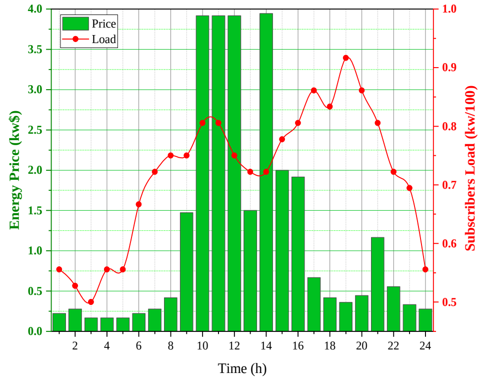


**Figure 3.** The amount of load and the price of electricity [17].

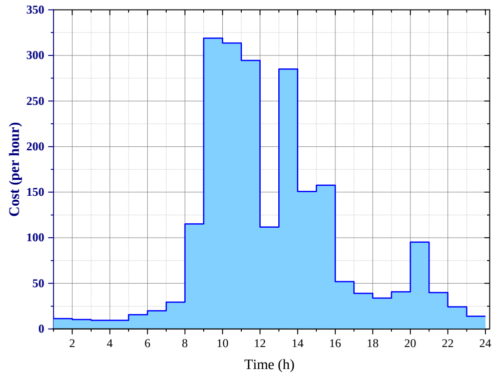


**Figure 4.** Cost of energy supply per hour in case of non-use of scattered products.

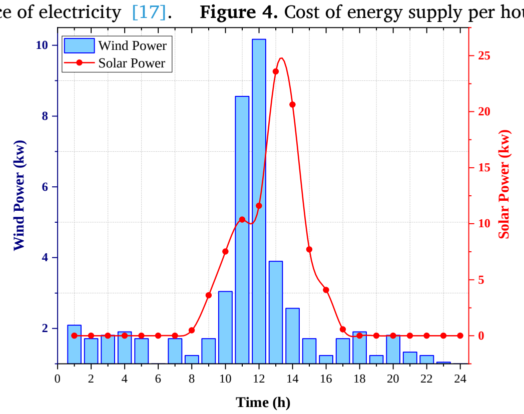


**Figure 5.** Maximum wind and photovoltaic power [17].

**Table 1.** The cost of generating power resources [17].

| Sources Cost | Solar Cells | Wind Turbine | Micro Turbine | Fuel Cell | Battery |
|---|---|---|---|---|---|
| Setup Fee ($) | 0 | 0 | 0.96 | 1.65 | 0 |
| Power Generation Cost ($/KWh) | 2.584 | 1.073 | 0.475 | 0.294 | 0.38 |
| Minimum Power (kwh) | 0 | 0 | 6 | 3 | -30 |
| Maximum Power (kwh) | Variable Every Hour | Variable Every Hour | 30 | 30 | 30 |

### *3.1. Operating Constraints*

To enhance microgrid efficiency, it is imperative to address crucial requisites. Within a microgrid, equilibrium between generated power and incoming power from the primary grid is paramount. This amalgamated power, comprising consumers' demand and losses, must align with the microgrid's generation input. To achieve this, we establish Equation (1):

$$\sum_{i=1}^{Ng} P_{Gi}(t) + \sum_{j=1}^{Ns} P_{Sj}(t) + P_{Grid}(t) = \sum_{k=1}^{Nk} P_{Lk}(t) - ENS(t) \quad (1)$$

Here, $P_{Lk}$ denotes the load for load K, and $N_k$ signifies the number of loads linked to the microgrid. During microgrid operation, it is essential to consider approximate power generation limits for each distributed generation. Imposing these constraints prevents unauthorized distributed generation activities during unauthorized intervals. Equation (2) outlines power generation capacity constraints, encompassing lower and upper limits for generator and energy storage capacities. Furthermore, it delineates constraints on battery charging and discharging within each time interval:

$$P_{min}^{gn}(t) \le P^{gn}(T) \le P_{max}^{gn}(t)$$
$$P_{min}^{sm}(t) \le P^{sm}(T) \le P_{max}^{sm}(t) \quad (2)$$
$$P_{min}^{grid}(t) \le P^{grid}(T) \le P_{max}^{grid}(t)$$

In Equation (3), $V_{tess}$ signifies the battery's stored energy at hour t, while $P^{charge}$ and $P^{discharge}$ denote permissible rates of battery charging and discharging over specific periods. Vmaxess and Vminess represent the maximum and minimum allowable energy storage values in batteries, and $P_{max}$ charge and $P_{min}$ charge denote the maximum and minimum limits of battery charging and discharging:

$$V_{min}^{ess} \leq V_t^{ess} \leq V_{max}^{ess}$$
$$P_t^{charge} \leq P_{max}^{charge} \quad (3)$$
$$P_t^{discharge} \leq P_{max}^{discharge}$$

### 3.2. Grey Wolf Algorithm

Grey wolves (Canis lupus), revered apex predators within the Canidae family, command a pivotal role in their ecosystem's intricate web of life. Occupying the zenith of the food chain, they wield dominance with grace. Group-oriented by nature, their packs, typically comprising 5 to 12 individuals, boast a sophisticated social fabric, crucial for decision-making and cohesion, vividly depicted in Figure 6.

At the helm of these packs stand alpha pairs, orchestrating the hunt, determining resting grounds, and dictating the rhythm of pack life. Despite their authoritative stance, glimpses of democracy surface, with alphas occasionally yielding to the collective wisdom. The pack, in turn, executes commands under alpha tutelage, underscoring their mastery in leadership and organizational finesse.

Nestled beneath the alphas lie the beta wolves, dutiful aides entrusted with executing decisions and upholding pack unity. Gender-neutral in their role, betas seamlessly transition to leadership in the absence or incapacity of alphas, deftly balancing deference with authority, providing invaluable counsel and feedback. In the depths of the hierarchy reside the omegas, bearing the weight of submission within the pack's dynamics. Often overlooked, they serve as the unassuming linchpin, their absence capable of unleashing turmoil within the pack's delicate equilibrium, a testament to their silent but profound influence. Beyond the intricacies of social order, Grey wolves exhibit a mesmerizing tapestry of group hunting tactics, weaving together search, pursuit, and ambush strategies, meticulously illustrated in Figure 7. This article delves into the quantitative modeling of these behaviors and hierarchical dynamics, culminating in the refinement and optimization of the groundbreaking GWO algorithm.

### 3.3. Algorithm and Mathematical Model

In this segment, we delve into mathematical models concerning social hierarchy, pursuit, entrapment, and prey attack, followed by an exposition on the GWO algorithm [18].

The objective of microgrid energy management lies in determining the hourly generation capacity of each resource to curtail costs. This article presents studies conducted under two scenarios. In the initial scenario, where the utilization of all dispersed generation resources is assumed, energy management is executed. Conversely, the second scenario explores spatial constraints for wind turbine and solar panel installation. To regulate energy resources in the microgrid, we employ the MGWO for optimization. Its operation ensures compliance with constraints pertinent to power generation from each resource. To validate algorithmic outcomes, results from the MGWO are juxtaposed with those derived from the Particle Swarm Optimization (PSO) algorithm. Parameter values for both algorithms are outlined in Table 2. Consistency in population size and iterations is maintained across both algorithms. The process of optimal management of dispersed generation resources in the microgrid, facilitated by intelligent algorithms, is depicted in Figure 8.

For intelligent management of dispersed generation resources in the microgrid, initial input entails monthly average load, geographical coordinates, and specific dates into the Homer software. The software outputs daily average load alongside wind and solar irradiation conditions. Leveraging this data, management is executed through the MGWO and PSO algorithms, aiming to achieve minimum costs with a high level of confidence [1].

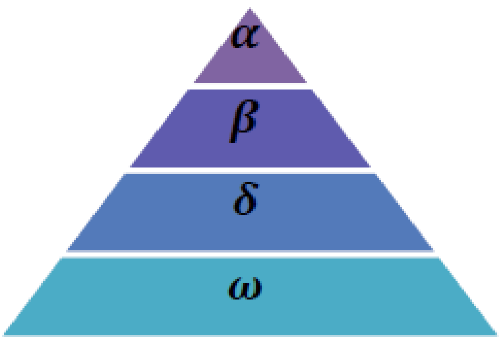


**Figure 6.** Grey wolf hierarchy [18].


**Figure 7.** Hunting behavior of Grey wolves: (A) tracking, chasing and approaching prey (B-D) chasing, boring and encirclement (E) standing position and attacking.

**Table 2.** Parameter of Grey wolf and particle swarm.

| Solution Method | Best Answer ($) | Worst Answer ($) | Average Responses ($) | Standard Deviation | Solution Method |
|---|---|---|---|---|---|
| Modified Grey Wolf | 163.8 | 172.9 | 166.9 | 4.14 | Modified Grey Wolf |
| Particle Swarm Optimization | 168.4 | 182.1 | 175.4 | 6.89 | Particle Swarm Optimization |
| Solution Method | Best Answer ($) | Worst Answer ($) | Average Responses ($) | Standard Deviation | Solution Method |
| Modified Grey Wolf | 163.8 | 172.9 | 166.9 | 4.14 | Modified Grey Wolf |

## 4. The Results Obtained from The Simulation

### *4.1. Analysis of the Results of Scenario One*

In the initial scenario, under the assumption of sufficient space for accommodating all distributed generation resources within the microgrid, the intricate task of supplying loads is delegated to a composite of distributed generation resources, battery storage, and the primary electricity grid. To finely tune energy supply costs, sophisticated algorithms such as MGWO and PSO have been harnessed for the astute management of distributed generation resources.

Through a rigorous regimen of thirty executions, the outcomes of these algorithms are laid bare in Figure 9. Impressively, across a majority of iterations, the GWO algorithm consistently outperforms its counterpart by yielding lower final objective function values. The minimum values achieved by the MGWO and PSO algorithms were $163.8 and $168.4 respectively, with the maximum values oscillating between $172.9 and $182.1 respectively over thirty executions.

Delving deeper, Table 3 unveils a comprehensive analysis encompassing the best and worst responses, average responses, and standard deviations across thirty optimization runs. Notably, the GWO algorithm's average responses and standard deviations exhibit superior performance over the PSO algorithm, affirming the efficacy of the proposed methodology. A diminutive standard deviation connotes a tighter convergence amongst responses across diverse iterations. Illustrated in Figure 10, the convergence trajectories of both algorithms depict the PSO algorithm reaching $168.4 after 137 iterations, while the GWO algorithm attains $163.8 after 146 iterations, emblematic of a lower final cost.

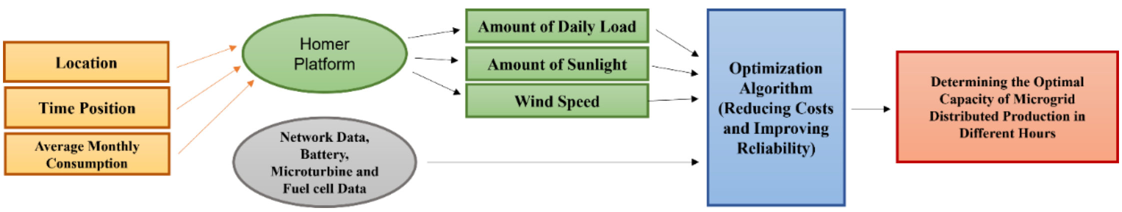


**Figure 8.** The trend of optimal resource management in microgrid.

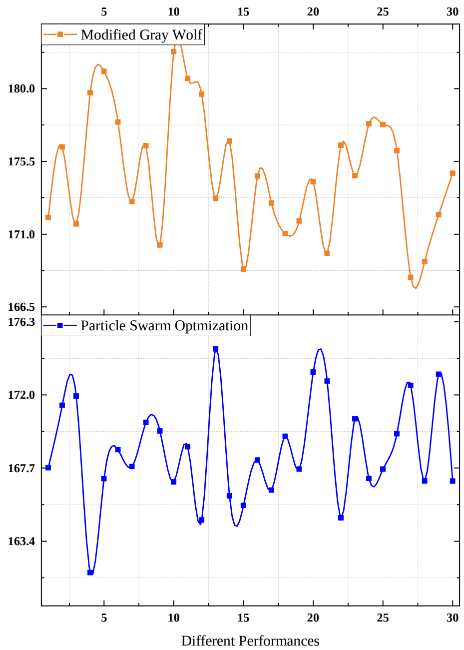


**Figure 9.** The final optimization values by Modified Grey Wolf Optimizer and Particle swarm optimizer in the first scenario in 30 different executions.

**Table 3.** Optimization results in 30 times of running the algorithms in the first scenario.

| Gray Wolf Algorithm | | | | |
|---|---|---|---|---|
| Number of Population | Algorithm Iterations | $\beta$ | $\alpha$ | $\gamma$ |
| 50 | 200 | 0.85 | 0.6 | 0.04 |
| **Particle Swarm Algorithm** | | | | |
| Number of Population | Algorithm Iterations | C1 = C2 | $w_{min}$ | $w_{max}$ |
| 50 | 200 | 2 | 0.6 | 0.9 |

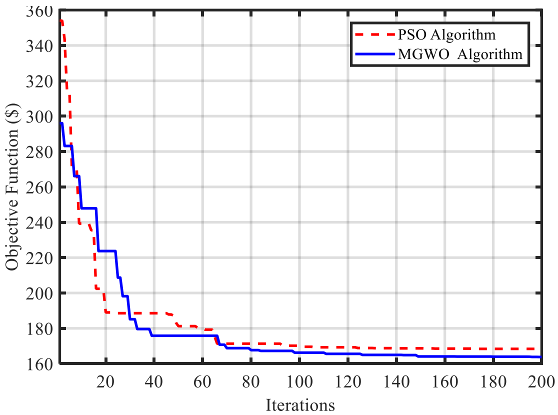


**Figure 10.** The process of convergence of Modified GWO and Particle swarm optimization algorithms in the first scenario.

Additionally, Figure 11 delineates the nuanced contribution of each distributed generation resource towards fulfilling the microgrid's electrical energy demands over a 24-hour timeframe post-optimization by MGWO and PSO algorithms. Strategically managing energy during specified hours significantly mitigates electricity costs by capitalizing on the upstream network and judiciously charging the battery during off-peak periods.

During peak hours characterized by escalated electricity prices, the microgrid's power requisites lean heavily on distributed generation and storage resources, with surplus energy judiciously sold back to the main grid. Consequently, hours 10 to 17 witness not only a cessation in energy procurement from the main grid but also a surplus sold back, as elucidated in Table 4.

Further dissected in Figure 12, the cost breakdown underscores negative costs for procuring energy from the main grid, indicative of a surplus income derived from electricity sales compared to procurement expenditures. Optimized energy management by the PSO algorithm yields an estimated income of $459.15 from exchanging electrical energy with the upstream network, while the proposed GWO algorithm amplifies this to $494.3. The penalty for unmet energy supply incurred by the MGWO algorithm towers at $74.23, surpassing that of the PSO algorithm standing at $68.45

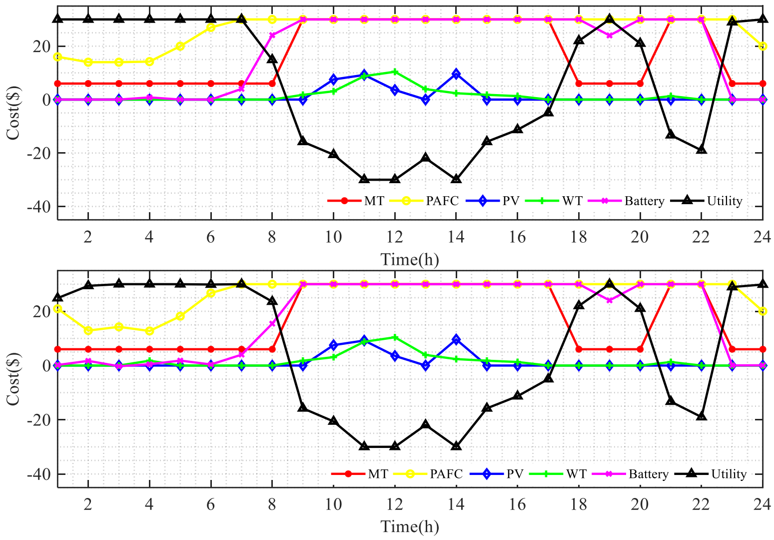


**Figure 11.** The contribution of each of the distributed production sources in the energy supply in the microgrid

a) Modified Grey Wolf Optimizer b) Particle swarm optimizer.

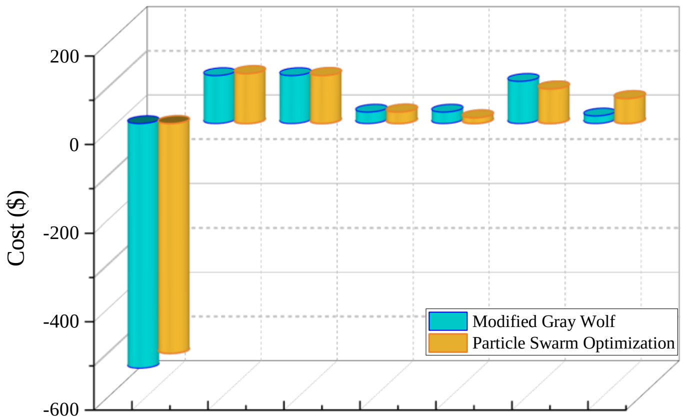


**Figure 12.** Disaggregated cost in the first scenario.

**Table 4.** Power resources and energy exchanged with the national electricity grid in the first scenario.

| Hour | 1 | 2 | 3 | 4 | 5 | 6 | 7 | 8 | 9 | 10 | 11 | 12 |
|---|---|---|---|---|---|---|---|---|---|---|---|---|
| NET | 25 | 29 | 30 | 30 | 30 | 30 | 30 | 24 | -15 | -20 | -30 | -30 |
| FC | 21 | 13 | 15 | 13 | 18 | 27 | 30 | 30 | 30 | 30 | 29 | 30 |
| MT | 6 | 6 | 6 | 6 | 6 | 6 | 6 | 6 | 30 | 30 | 30 | 30 |
| PV | 0 | 0 | 0 | 0 | 0 | 0 | 0 | 0 | 0 | 7 | 9 | 3 |
| WT | 0 | 0 | 0 | 0 | 2 | 0 | 0 | 0 | 0 | 1 | 3 | 9 |
| BAT | 0 | 2 | 0 | 0 | 1 | 0 | 4 | 15 | 30 | 30 | 30 | 30 |
| Hour | 13 | 14 | 15 | 16 | 17 | 18 | 19 | 20 | 21 | 22 | 23 | 24 |
| NET | -22 | -30 | -15 | -11 | -5 | 22 | 30 | 21 | -13 | -19 | 28 | 30 |
| FC | 30 | 30 | 30 | 30 | 30 | 30 | 30 | 30 | 30 | 30 | 30 | 20 |
| MT | 30 | 30 | 30 | 30 | 30 | 6 | 6 | 6 | 29 | 30 | 6 | 6 |
| PV | 0 | 9 | 0 | 0 | 0 | 0 | 0 | 0 | 0 | 0 | 0 | 0 |
| WT | 11 | 4 | 2 | 1 | 1 | 0 | 0 | 0 | -1 | 1 | 0 | 0 |
| BAT | 30 | 29 | 30 | 30 | 30 | 29 | 24 | 29 | 30 | 29 | 0 | 0 |

### 4.2. Analysis of the Results of Scenario Two

In the subsequent phase of simulations, the microgrid's spatial limitations precluded the installation of wind turbines and solar panels, compelling reliance on fuel cells, micro-turbines, batteries, and the main grid to meet subscribers' energy needs. To optimize the management of distributed generation resources, we employed two enhanced GWO algorithms alongside the PSO algorithm, with the primary objectives of cost reduction and system reliability enhancement.

Figure 13 vividly portrays the results of 30 iterations for both algorithms. It's noteworthy that throughout most iterations, the GWO algorithm consistently outperformed the PSO algorithm in achieving the final optimized objective function value. Post-optimization, the lowest attained value with MGWO and PSO algorithms in the second scenario stood at $9,276 and $4,282, respectively, marking a significant increase compared to analogous values in the first scenario. Conversely, the highest objective function value among the 30 different runs for both MGWO and PSO algorithms amounted to $9,285 and $3,294, respectively.

Table 5 succinctly summarizes the simulation outcomes of 30 optimization algorithm runs in the second scenario. The results indicate that the average responses and standard deviations from 30 runs of the proposed GWO algorithm were $6,280 and $45.4, respectively, demonstrating superior performance compared to the PSO algorithm.

Further insights into convergence patterns are provided in Figure 14, illustrating the optimization process's trajectory in the second scenario. Notably, the PSO algorithm converged to $4,282 after 143 iterations, while the modified GWO algorithm reached $9,276 after 137 iterations, reaffirming the former's superior efficiency.

Additionally, Figure 15 offers a detailed depiction of simulation trends, illustrating the respective contributions of distributed generation resources to supplying electrical energy to microgrid subscribers over a 24-hour study period post-optimization by MGWO and PSO algorithms. Notably, during peak consumption hours, the shortfall in generated energy results in an excess of over 20 kilowatts of electrical energy, impacting profitability from electricity sales. The stability of the energy supply pattern is evident, with procurement from the main power grid timed during cheaper hours and sales deferred to more expensive ones. The heightened operation of distributed generation capacities from 9 a.m. to 5 p.m. is primarily driven by the high electricity prices during those hours, albeit with reduced profitability compared to the first scenario.

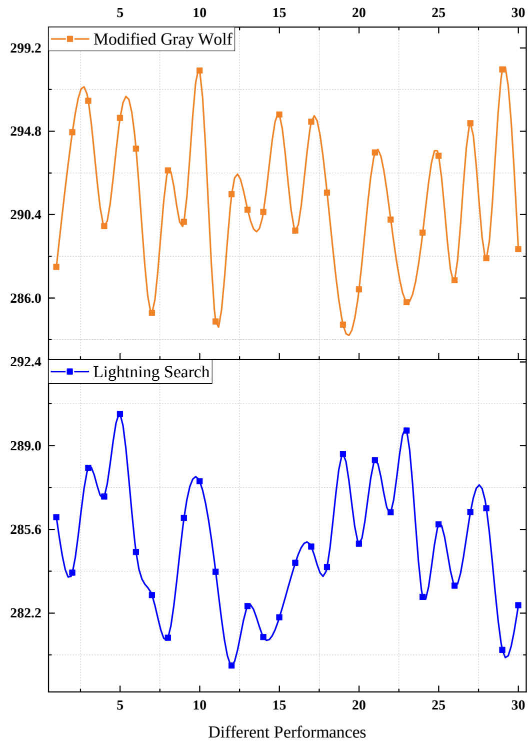


**Figure 13.** The final optimization values by Modified Grey Wolf Optimizer and PSO in the second scenario in 30 different executions.

**Table 5.** Optimization results in 30 executions of algorithms in the second scenario.

| Solution Method | Best Answer($) | Worst Answer($) | Average Responses($) | Standard Deviation |
|---|---|---|---|---|
| Gray Wolf Algorithm | 276.9 | 285.9 | 280.6 | 4.45 |
| Particle Swarm Algorithm | 282.4 | 294.3 | 289.8 | 6.11 |

Table 6 provides further insights into the production quantities of distributed generation sources and the exchanged power with the main power grid in the first scenario.

Moreover, Figure 16 delineates the individual component costs, underscoring the diminished profitability from selling electricity to the main grid compared to the first scenario. Post-optimization by the GWO algorithm, estimated profitability stands at approximately $6,362, while after optimization by the PSO algorithm, it amounts to $4,353. Conversely, optimal energy management by the proposed MGWO algorithm determines a penalty for unsupplied energy at $3,123, compared to approximately $2,156 after optimization by the PSO algorithm, reflecting the latter's enhanced microgrid reliability.

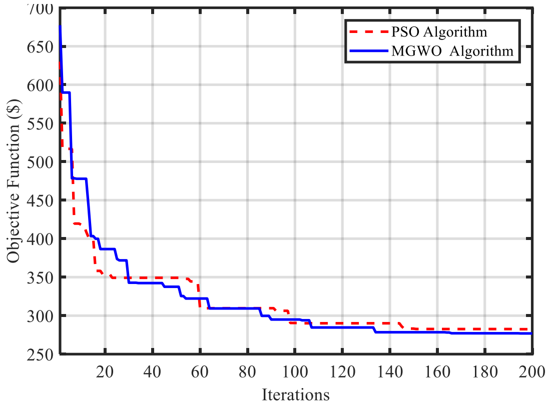


**Figure 14.** The process of convergence of MGWO and PSO optimization algorithms in the second scenario.

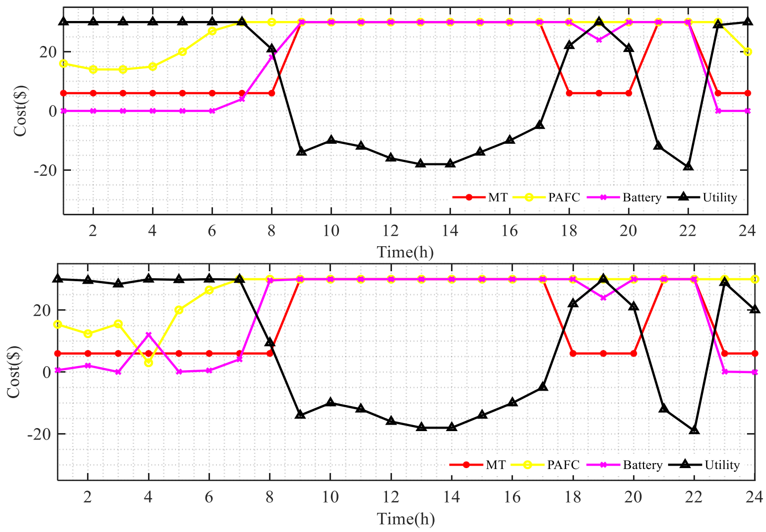


**Figure 15.** The contribution of each of the distributed production sources in the energy supply in the microgrid a) Modified Grey Wolf Optimization

b) Particle swarm optimization.

**Table 6.** Power resources and energy exchanged with the national electricity grid in the second scenario.

| Hour | 1 | 2 | 3 | 4 | 5 | 6 | 7 | 8 | 9 | 10 | 11 | 12 |
|---|---|---|---|---|---|---|---|---|---|---|---|---|
| NET | 30 | 29 | 28 | 30 | 29 | 30 | 30 | 9 | -14 | -10 | -12 | -16 |
| FC | 15 | 12 | 15 | 3 | 20 | 27 | 30 | 30 | 30 | 30 | 30 | 30 |
| MT | 6 | 6 | 6 | 6 | 6 | 5 | 6 | 6 | 30 | 30 | 30 | 30 |
| BAT | 1 | 1 | 0 | 12 | 0 | 0 | 4 | 30 | 30 | 30 | 31 | 30 |
| Hour | 13 | 14 | 15 | 16 | 17 | 18 | 19 | 20 | 21 | 22 | 23 | 24 |
| NET | -18 | -18 | -14 | -9 | -5 | 23 | 30 | 21 | -11 | -18 | 29 | 21 |
| FC | 30 | 30 | 30 | 30 | 30 | 30 | 30 | 30 | 30 | 30 | 30 | 30 |
| MT | 30 | 30 | 30 | 30 | 30 | 6 | 6 | 6 | 30 | 30 | 6 | 6 |
| BAT | 30 | 30 | 31 | 30 | 30 | 30 | 24 | 30 | 30 | 30 | 0 | 1 |

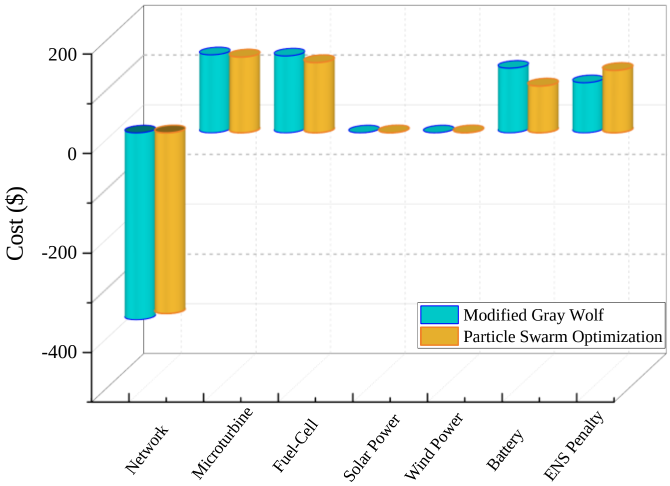


**Figure 16**. Separated cost in the second scenario.

### 4.3. *Comparison of Two Scenarios*

The quantification of power exchange through the national electricity grid has been meticulously calculated under two distinct scenarios, with their outcomes meticulously summarized in Table 7.

While the second scenario witnessed a decrease in profitability compared to the first, the reduction in exchanged power can be attributed to the exclusion of photovoltaic and wind renewable sources.

In the initial scenario, procurement from the national grid amounted to 357 kilowatt-hours, with 210 kilowatt-hours being sold. Conversely, the second scenario saw a decrease in exchanged power, with only 97 kilowatt-hours sold back to the national grid.

## 5. Conclusions

In this study, we meticulously orchestrated the energy management of a microgrid, utilizing advanced optimization algorithms—PSO and MGWO—to strategically mitigate costs. Our analysis encompassed a spectrum of distributed generation resources: solar panels, wind turbines, diesel generators, fuel cells, and battery storage systems.

Our investigation unfolded across two distinct scenarios: initially, a comprehensive exploration where all distributed generation resources were presumed operable, and subsequently, a more constrained scenario where spatial limitations precluded the installation of wind turbines and solar panels.

In the former scenario, we meticulously optimized energy distribution utilizing MGWO and PSO algorithms, with each algorithm subjected to 30 iterations. Impressively, the MGWO algorithm yielded a minimum optimized value of $163.8, outperforming the PSO algorithm, which yielded $168.4. Notably, the GWO Algorithm exhibited heightened efficiency and accuracy, evidenced by lower average and standard deviation values compared to PSO. The negative energy purchase cost from the main grid underscored a surplus in revenue from electricity sales—a promising indicator of economic viability.

Transitioning to the latter scenario, constrained by spatial limitations, we ingeniously leveraged a combination of fuel cells, microturbines, batteries, and the main grid to meet consumer energy demands. Despite the absence of wind turbines and solar panels, our optimization efforts persisted. Once again, both the GWO Algorithm and PSO were employed 30 times each, yielding minimum optimized values of $276.9 and $282.4, respectively—a marginally higher expenditure compared to the previous scenario. Demonstrating continued superiority, the GWO Algorithm maintained higher efficiency, as evidenced by lower average and standard deviation values. However, it's worth noting that profit from electricity sales to the main grid witnessed a decline compared to the first scenario, showcasing the nuanced impact of spatial constraints on economic outcomes.

Furthermore, our assessment encompassed penalties for unmet energy demands post-optimization, revealing the robustness of our approach. Specifically, penalties for unmet energy stood at $123.3 and $156.2 for MGWO and PSO algorithms, respectively, reaffirming the efficacy of our optimization strategies in addressing energy shortfalls.

**Table 7**. Power exchanged with the national electricity grid in two scenarios.

| Hour | 1 | 2 | 3 | 4 | 5 | 6 | 7 | 8 | 9 | 10 | 11 | 12 |
|---|---|---|---|---|---|---|---|---|---|---|---|---|
| First scenario | 30 | 30 | 29 | 30 | 30 | 30 | 30 | 15 | -15 | -21 | -30 | -30 |
| Second scenario | 30 | 30 | 30 | 30 | 30 | 29 | 29 | 20 | -14 | -11 | -13 | -17 |
| Hour | 13 | 14 | 15 | 16 | 17 | 18 | 19 | 20 | 21 | 22 | 23 | 24 |
| First scenario | -21 | -30 | -15 | -11 | -5 | 22 | 31 | 21 | -13 | -19 | 30 | 30 |
| Second scenario | -19 | -18 | -14 | -10 | -6 | 22 | 29 | 21 | -12 | -20 | 28 | 2 |

## References


[1] A. Alzahrani, K. Sajjad, et al., "Real-Time Energy Optimization and Scheduling of Buildings Integrated with Renewable Microgrid," *Applied Energy*, vol. 335, 120640, 2023.

[2] A. Arab Bafrani, A. Rezazade, and M. Sedighizadeh, "Robust Scheduling of Power System Considering Social Costs and Environmental Concerns," *IET Smart Cities*, vol. 5, no. 2, pp. 73–94, 2023.

[3] M. Jalili, M. Sedighizadeh, and A. S. Fini, "Stochastic Optimal Operation of a Microgrid Based on Energy Hub Including a Solar-Powered Compressed Air Energy Storage System and an Ice Storage Conditioner," *Journal of Energy Storage*, vol. 33, 102089, 2021.

[4] A. Salari, S. E. Ahmadi, M. Marzband, and M. Zeinali, "Fuzzy Q-Learning-Based Approach for Real-Time Energy Management of Home Microgrids Using Cooperative Multi-Agent System," *Sustainable Cities and Society*, vol. 95, 104528, 2023.

[5] R. Li, W. Wei, S. Mei, Q. Hu, and Q. Wu, "Participation of an Energy Hub in Electricity and Heat Distribution Markets: an MPEC Approach," *IEEE Transactions on Smart Grid*, vol. 10, no. 4, pp. 3641–3653, 2019.

[6] Z. Li, W. Wu, M. Shahidehpour, J. Wang, and B. Zhang, "Combined Heat and Power Dispatch Considering Pipeline Energy Storage of District Heating Network," *2017 IEEE Power & Energy Society General Meeting*, pp. 1–1, 2017.

[7] H. Zafarani, S. A. Taher, and M. Shahidehpour, "Robust Operation of a Multicarrier Energy System Considering Evs and CHP Units," *Energy*, vol. 192, 116703, 2020.

[8] M. Babaei, E. Azizi, M. T. Beheshti, and M. Hadian, "Data-Driven Load Management of Stand-Alone Residential Buildings Including Renewable Resources, Energy Storage System, and Electric Vehicle," *Journal of Energy Storage*, vol. 28, 101221, 2020.

[9] I. Jendoubi, and F. Bouffard, "Data-Driven Sustainable Distributed Energy Resources' Control Based on Multi-Agent Deep Reinforcement Learning," *Sustainable Energy, Grids and Networks*, vol. 32, 100919, 2022.

[10] M. Suresh, and R. Meenakumari, "An Improved Genetic Algorithm-Based Optimal Sizing of Solar Photovoltaic-Wind Turbine Generator-Diesel Generator-Battery Connected Hybrid Energy Systems for Standalone Applications," *International Journal of Ambient Energy*, pp. 1–8, 2019.

[11] Y. Cheng, H. Zheng, R. A. Juanatas, and M. J. Golkar, "Profitably Scheduling the Energy Hub of Inhabitable Houses Considering Electric Vehicles, Storage Systems, Revival Provenances and Demand Side Management Through a Modified Particle Swarm Optimization," *Sustainable Cities and Society*, vol. 92, 104487, 2023.

[12] G. Jelen, J. Babic, and V. Podobnik, "A Multi-Agent System for Context-Aware Electric Vehicle Fleet Routing: A Step Towards More Sustainable Urban Operations," *Journal of Cleaner Production*, vol. 374, 134047, 2022.

[13] E. Mohammadi, M. Alizadeh, M. Asgarimoghaddam, X. Wang, and M. G. Simões, "A Review on Application of Artificial Intelligence Techniques in Microgrids," *IEEE Journal of Emerging and Selected Topics in Industrial Electronics*, vol. 3, no. 4, pp. 878-890, 2022.

[14] S. Darvish Kermani, M. Fayazi, J. Barati, and M. Joorabian, "Percentage of Islanding and Peninsulating Detection in large Microgrids with Renewable Energy Resources with Multiple Connection Points to Different Grids," *Journal of Green Energy Research and Innovation*, vol. 1, no. 2, pp. 1–14, 2024.

[15] Y. Zheng, B. M. Jenkins, K. Kornbluth, A. Kendall, and C. Træholt, "Optimization of a Biomass-Integrated Renewable Energy Microgrid with Demand Side Management Under Uncertainty," *Applied Energy*, vol. 230, pp. 836–844, 2018.

[16] Y. Wu, Y. Wu, H. Cimen, J. C. Vasquez, and J. M. Guerrero, "Towards Collective Energy Community: Potential Roles of Microgrid and Blockchain to Go Beyond P2P Energy Trading," *Applied Energy*, vol. 314, 119003, 2022.

[17] N. Yin, R. Abbassi, H. Jerbi, A. Rezvani, and M. Müller, "A Day-ahead Joint Energy Management and Battery Sizing Framework Based On θ-Modified Krill Herd Algorithm for A Renewable Energy-Integrated Microgrid," *Journal of Cleaner Production*, vol. 282, p. 124435, 2021.

[18] H. Rezaei, O. Bozorg-Haddad, and X. Chu, "Grey Wolf Optimization (GWO) Algorithm," in *Advanced Optimization by Nature-Inspired Algorithms*, pp. 81-91, 2018.


## Declaration of competing interest

The authors declare that they have no known competing financial interests or personal relationships that could have appeared to influence the work reported in this paper. The ethical issues, including plagiarism, informed consent, misconduct, data fabrication and/or falsification, double publication and/or submission, redundancy, have been completely observed by the authors.

## Bibliography

**Javad Nikoukar** was born in Mashhad, Iran, in 1983. He received the B.S. degree in electrical power engineering from Ferdowsi University, Mashhad, Iran, in 2006 and the M.S. degree in electrical power engineering from the University of Tehran, Tehran, Iran, in 2008. He earned his Ph.D. degree in electrical power engineering from Sharif University of Technology, Tehran, Iran in 2013. Since 2015 he has been an assistant professor in Mashhad branch, Islamic Azad University, Mashhad, Iran. His primary research interests are electric machine analysis, modelling, and simulation, innovative electrical drive control approaches, and renewable energy systems.

**Email:** Javad.Nikoukar@iau.ac.ir
**ORCID:** 0000-0002-5142-0924
**Contribution Statement:** Conceptualization, Project administration, Visualization, Methodology.

**Shokoofeh Mohammadi** was born in Saveh, Iran, in 1988. She received the B.Sc., M.Sc., degrees in 2015, 2018, respectively, in Chemist and Energy systems engineering, energy systems modeling engineering, respectively. She is currently an, TA with the Department of mechanical engineering, Islamic Azad University, Saveh, Iran. And Ph.D. student at Science and Research Branch, Islamic Azad University, Tehran, Iran. Her main research interests are energy system analysis and reliability, Exergy Analysis, Modeling and Simulation. She has Active as a researcher/ QA manager in different Industrial Companies.

**Email:** Sh.mohammadi8959@gmail.com
**ORCID:** 0009-0004-0435-7426
**Contribution Statement:** Data curation, Formal analysis, Investigation, Resources, Writing-review & editing.

**Hamid Reza Hanif** received his B.Sc. and M.Sc. in Mathematics and PHD degrees in Electrical Power Engineering from Iran University of Science and Technology, Iran Tehran in 2014 and 2019 and 2023 respectively. He has authored and co-authored more than 75 papers in international journals and conferences. He has also published a book and co-authored some book chapters. His main research interests include renewable energy, technologies, Microgrids, Power System Planning, Power Systems, Smart grids, Electric vehicles, and fault location. Since 2018 he has been a reviewer and Editorial Board Member of several high-quality journals.

**Email:** h.hanif.iustz@gmail.com

**ORCID:** 0000-0001-9289-2947

**Contribution Statement:** Data curation, Funding acquisition, Visualization, Writing-review & editing.

**Reza Aminpour gogani** received his B.Sc. and M.Sc. and Ph.D. in Electrical Power Engineering from Azarbaijan Shahid Madani University. He has authored and co-authored more than 10 papers in international journals and conferences. He has also published a book and co-authored some book chapters. His main research interests include renewable energy, technologies, Microgrids, Power system Planning, Power Systems, Smart grids, Electric vehicles, and fault location. Since 2018 he has been a reviewer of several high-quality journals.

**Email:** Reza.aminpour@azaruniv.ac.ir

**ORCID:** 0009-0007-7013-6965

**Contribution Statement:** Methodology, Resources, Validation, Roles/Writing-original draft.

**Masoumeh Ghafari** was born in 2000 in Ilam, Iran. She received the bachelor's degree in Electrical Engineering from Malayer University, Malayer, Iran, in 2023. With a keen interest in advancing the field of Electrical Engineering, she is currently pursuing the master's degree at Babol Noshirvani University of Technology, Babol, Iran, Specializing in Electrical Engineering with a focus on Control Systems. her research interests include Smart Grids, Energy Optimization, and Application of Neural Networks in Renewable Energy Systems.

**Email:** ma.ghafari1379@gmail.com

**ORCID:** 0009-0000-4909-4616

**Contribution Statement:** Software, Resources, Software, Roles/Writing-original draft, Writing-review & editing.

**Abdolreza Behvandi** was born in 1987 in Iran. He received his B.Sc., M.Sc., and Ph.D. degrees all in Electrical Engineering (Power Systems) in 2010, 2012, and 2019 from Isfahan University of Technology, Isfahan University, and Shahid Chamran University of Ahvaz, respectively. Currently, he is an Assistant Professor at Department of Electrical Engineering, Ramhormoz Branch, Islamic Azad University, Ramhormoz, Iran. His special interests are power system studies, power system protection, renewable energy, and microgrids.

**Email:** rezabehvandi@gmail.com

**ORCID:** 0000-0002-4879-1994

**Contribution Statement:** Data curation, Formal analysis, Investigation, Resources, Validation.

Journal of Green Energy Research and Innovation

# Using Wastewater for Green Energy Production: A Review

Marzie Razavi

## Highlights

- Utilizing wastewater as an energy source.
- Generating bioelectricity through microorganisms in biomass.
- Reducing energy reliance and cutting wastewater treatment plant costs.
- Using green energy sources, including agricultural, industrial, and domestic wastewater.

## Graphical Abstract

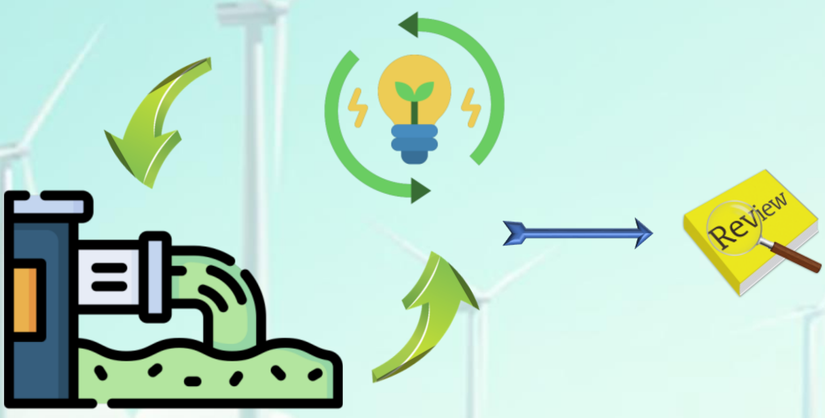


Use your device to scan and read the article online

Citation
M. Razavi," Using Wastewater for Green Energy Production: A Review," *Journal of Green Energy Research and Innovation*, vol. 2, no. 1, pp. 14-19, 2025.

https://doi.org/10.61186/jgeri.2.1.14

JGERI Journal of Green Energy Research and Innovation

Journal of Green Energy Research and Innovation 2.1 (2025) 14-19

Online ISSN: 3041-9018

Journal of Green Energy Research and Innovation

Journal Homepage: www.jgeri.araku.ac.ir

# Using Wastewater for Green Energy Production: A Review

Marzie Razavi *

*Department of Civil Engineering, Tafresh University, Tafresh, 39518 79611, Iran.*

A R T I C L E I N F O

***Keywords:***
Wastewater,
Green energy,
Microorganism,
Anaerobic bacteria,
Gas production.

***Article History:***
Received: 20 July 2024;
Revised: 12 August 2024;
Accepted: 17 August 2024.

***Article type:***
Review Article

* ***Corresponding author***
*E-mail address:*
m.razavi@tafreshu.ac.ir (M. Razavi)

A B S T R A C T

As oil resources become increasingly scarce, the need to transition to renewable energy sources is critical for sustainable living. The United Nations first emphasized the importance of sustainable development in 1987, highlighting the "central role" of energy in this effort. After years of research, innovative solutions for sustainable energy have emerged, with energy production from wastewater showing significant potential. Wastewater can be converted into biogas through anaerobic digestion, where microorganisms break down organic matter in the absence of oxygen to produce methane, which can be used for electricity, heat, or fuel. This process not only aids in reducing greenhouse gas emissions but also supports environmental protection and waste management. The growing demand for renewable energy has sparked significant interest in these techniques, which utilize bacteria to generate electricity, further demonstrating the potential of wastewater as a sustainable energy source. Using wastewater for energy not only lowers operational costs but also allows treatment plants to generate energy on-site, reducing reliance on external energy sources and lowering carbon emissions. Exploring these renewable energy sources is crucial, particularly given the large volumes of wastewater generated from agricultural, industrial, and domestic activities. This paper reviews the potential of wastewater as a green energy source, discussing specific technologies for treating various wastewater types and the associated challenges and opportunities. By examining successful case studies and emerging trends, it aims to advance green energy solutions that promote both environmental sustainability and economic growth.

## 1. Introduction

Non-renewable natural resources, such as oil, will end in the coming years, and therefore, humans must move towards the use of renewable energies to provide their energy needs. It seems that energy supply methods that do not require fossil fuel sources can be classified as sustainable energy [1]. The concept of sustainable development was officially introduced by the United Nations in 1987, where the significant role of energy in achieving sustainable development was acknowledged [2]. Today, researchers around the world are engaged in creating different solutions for sustainable energy production, which leads to the identification of different innovative approaches for green energy production. In this context, utilizing wastewater as a raw material for energy generation has garnered considerable interest [3,4]. Sustainable energy is energy that is produced and used in a way that "satisfies present human needs without hindering the capacity of future generations to satisfy their own needs". One of these methods is using wastewater and turning it into biogas and then producing energy from it. This method, known as green energy production, uses waste materials to produce energy and reduces greenhouse gas emissions.

In other words, in order to produce green energy from wastewater, environmentally friendly methods should be used [5,6]. The increasing energy demand highlights many concerns regarding environmental protection. Therefore, there is a need to develop and expand various clean and sustainable energy production technologies. Today, the use of wastewater as a source of energy production is viewed from a new perspective. In fact, using this method, waste materials and garbage become a valuable resource for energy production [7,8]. One of the newest methods of generating electricity is the use of microorganisms in biomass, which is also called bioelectricity production. In 1911, Potter made the first observation and discovery of the flow of electricity [9]. At that time, his work did not receive a special response, but in recent years, the ability of bacteria to produce energy has been discussed again. It seems that the need for renewable and new energy sources is one of the reasons for this return. In this method, the conversion of wastewater into biogas is generally done through anaerobic digestion and microorganisms decompose organic matter in the absence of oxygen [10].

Methane, which is the major part of the produced biogas, is used to generate electricity, heat or as a fuel. In addition to utilizing renewable and cost-effective energy sources, this method plays a crucial role in waste management, environmental protection, and the conservation of natural resources. It helps reduce the harmful environmental impacts of pollutants, supports green energy production, and contributes to enhancing the beauty of the landscape. Using the potential of wastewater reduces the harmful environmental effects of pollutants and produces green energy. The use of this method reduces the operational costs and also the energy produced in the treatment plant can be used in the facilities of the same place and eliminates the need to receive energy from external sources [11,12]. Also, this strategy is a means to compensate for energy consumption in sewage treatment plants and leads to the reduction of carbon emissions in the environment [11]. Considering that sustainable energy production from wastewater requires the use of new and advanced, cost-effective and scalable technologies, therefore there is a need to investigate and collect accurate and complete information in this field. Since all agricultural, industrial and domestic activities produce large amounts of wastewater, the need to investigate these rich and unique sources for green energy production is well felt. The purpose of this paper is to examine the diverse potential of wastewater as a source of green energy, along with the available technologies for treating different types of wastewaters—urban, industrial, and agricultural—while addressing their specific challenges and opportunities. In addition, various methods to convert these wastes into green energy will be investigated. This paper provides a comprehensive overview by showing successful case studies, advanced technologies and emerging trends. Comprehensive research, innovation and implementation in this critical area will help advance green energy generation solutions, thereby promoting environmental sustainability and supporting economic growth.

## 2. Wastewater Types and their Characteristics

All living organisms excrete waste materials from their bodies daily. In addition, industries, factories and agricultural activities also discharge amounts of waste materials into the environment every day. These waters are mainly known as sewage and have different quantitative and qualitative characteristics. Therefore, it is necessary to know the characteristics of different wastewater types in order to perform successful purification processes and generate energy from them. Table 1 generally lists some kinds of wastewater that are utilized to produce energy.

**Domestic Sewage:** Domestic sewage mainly includes human excreta, toilet waste, washing detergents and food residues [13,14]. According to the characteristics of domestic sewage, including the presence of organic materials for decomposition by bacteria, it has been used to produce different forms of renewable energy. Many researchers have achieved successful results in this field. For example, in 2011, Puig et al succeeded in purifying wastewater and simultaneously producing electricity using microbial fuel cell technology. In this study, which was conducted on a laboratory scale with a focus on the removal of organic matter and energy production, the testers succeeded in removing 80% of organic matter and producing 1.44 watts per cubic meter [15]. Table 2 presents the various compounds found in domestic wastewater.

**Agriculture Wastewater:** The wastewater generated in agriculture contains large organic loads, nutrients and pollutants. It usually contains high nitrogen and phosphorus which can cause eutrophication in water bodies when were not treated properly. Agricultural wastewater has always been a high BOD, COD waste water quality is good enough to be used as bio energy production.

**Industrial Wastewater:** Industrial wastewater varies widely depending on the industry [17,18]. There is a wide range of impurities in it, heavy metals, organic substances and inorganic compounds [19]. The high degree and diversity in the structure of industrial wastewaters require methods for specific treatment that can use their energy potential efficiently.

**Domestic Wastewater:** The main components of domestic or municipal sewage are organic household wastes, including human waste, food remains, soaps, and detergents [13,14]. Domestic wastewater represents a steady supply of organic matter that can be converted into biogas or any other renewable energy by means of anaerobic digestion.

**Agriculture Runoff:** This would refer to water that spills over from agricultural land during rainfall or irrigation [20]. This runoff often picks up soil, fertilizers, pesticides, and other chemicals used in farming.

**Table 1.** Wastewater Types

| |
|---|
| Domestic wastewater |
| Industrial wastewater |
| Septic tank wastewater |
| Leachate |
| Agricultural runoff |
| Urban runoff |

**Table 2.** Domestic wastewater components [16].

| | |
|---|---|
| Microorganisms | Pathogenic bacteria, virus and worm's egg |
| Biodegradable organic materials | Oxygen depletion in rivers, lakes and fjords |
| Other organic material | Detergents, pesticides, fat, oil and grease, color, solvents, phenols, cyanide |
| Nutrients | Nitrogen, phosphorus, ammonium |
| Metals | Hg, Pb, Cd, Cr, Cu, Ni |
| Other inorganic material | Acids, for example hydrogen sulphide, bases |

Runoff water often carries organic materials and nutrients from fertilizers, which can promote the growth of biomass in water bodies. This biomass, like algae, has been shown to be useful in being harvested and processed into biofuels by means of anaerobic digestion or fermentation [21]. This will give room for the production of green energy while managing nutrient pollution in water bodies.

**Sewage Sludge:** The semi-liquid by-product from treatment processes of wastewater that is generally further treated in an anaerobic digester, in which microorganisms break down organic matter in an oxygen-free environment to form biogas, largely composed of methane, used to run electricity, provide heat, or as biofuel in vehicles. Anaerobic digestion not only helps to produce renewable and cleaner energy [22] but also decreases the sludge volume while producing a nutrient-rich digestate for fertilizer applications.

## 3. Technologies for Green Energy Production

**Anaerobic Digestion:** Anaerobic digestion is one of the most studied and applied methods in the conversion of organic matter existing in wastewater into biogas. The final product consists basically of methane and carbon dioxide [23-28]. Simply, it involves a series of processes mediated by microbes: hydrolysis, acidogenesis, acetogenesis, and lastly, methanogenesis [29,30]. The produced methane could be utilized for electricity generation, heating, or even as a form of fuel for vehicles. Anaerobic digestion is a process whereby microorganisms break down organic matter in wastewater in the absence of oxygen, to yield biogas. This technology manages organic waste and recovers valuable energy, hence minimizing over-reliance on non-renewable resources. A number of studies have documented successful cases of WTE projects implemented around the world, covering different technologies and their efficacy in producing green energy. Gu et al. (2017) evaluated the possibility of WWTPs being energy self-sufficient and the challenges to be anticipated in such a scenario. They talked about integrating anaerobic digestion for the production of biogas from sewage sludge and its subsequent electricity and heat generation, touting huge reductions in the energy consumed by the plant [31]. WWTPs may be empowered with the potential to anaerobically digest organic matter in wastewater into biogas, mainly methane and carbon dioxide. This captured biogas can be put to use as a renewable energy supply in power and heat generation, hence reducing dependence on fossil fuels. Advanced treatment processes recover valuable nutrients such as nitrogen and phosphorus from wastewater for fertilizers. Modern WWTPs are designed to be energy-efficient, including technologies such as combined heat and power systems and energy-efficient pumps and motors. This contributes greatly to reducing the overall energy use and carbon footprint of a treatment process.

**Microbial Fuel Cells (MFCs):** MFCs harness electricity generation through bacteria involved in the metabolic activities directly converting organic matter present in wastewater into electricity [32]. The idea of bioelectricity production by MFC, initially discovered in 1911. The anodic chamber hosts bacteria that oxidize organic matter to release electrons, which then transit to the cathode through an external circuit and in the process generate electricity [33]. The benefits of using MFCs have thus far been wastewater treatment and power generation. It provides opportunities for continuous electricity generation through microbial activities, and potential uses of MFCs have been for in situ wastewater treatment systems that allow simultaneous pollutant removals with energy recovery [8]. There is ongoing work related to the development of MFCs in a way that allows performance improvement and the scaling up of the devices for real-life applications [34]. As stated above, Microbial Fuel Cells are an emerging means for producing electrical energy directly from organic matter in wastewater through the metabolism of microorganisms. This directly removes the requirement of an outside carbon-source that will provide energy along with the carbon footprints associated with energy generation. Generally; a lot of methane and carbon dioxide are said to be generated as a result of wastewater treatment. In contrast to other methods, where organic matter is directly converted into electricity in MFCs, there is a significantly lower release of methane. As a result, this process produces a reduced amount of greenhouse gases, contributing to a lesser overall impact on climate change. FCs work at ambient temperatures and pressures, which are low and do not utilize much energy input than conventional treatment. This further reduces the carbon print of the wastewater treatment process. MFCs have great potential and effectiveness in the degradation of a wide range of organic pollutants even for such which are less biodegradable in the conventional treatment process. This leads to better quality effluent water and less pollution in the receiving water body. There can be scaling of MFCs for different sizes of operations: small, on-site treatment systems or large municipal plants. It can serve its purpose with much flexibility for adoption and cumulative impact toward pollution reduction and the carbon footprint. MFCs have gained a lot of interest because they are able to generate electricity from wastewater. Electricity was also generated through MFCs employing floating air cathodes, hence proving the potential applicability of the technology [35]. Similarly, the activity of various inoculums was tested in urine-fed MFCs, which were monitored for power performance and microbial community dynamics. This study further demonstrated the adaptability and efficiency of MFCs in converting waste into electrical energy [36]. In the recent past, the electrochemical system has continuously improved and evolved with the development of new materials and better electrode configuration that leads to better performance of the microbial fuel cells. The use of nanomaterials and conductive polymer innovations has developed that offers increased power output and efficiency in treating wastewater. According to the study made by Mook et al. on 2014, electrochemical systems for wastewater treatments are combined or integrated with renewable sources of energy. One such approach focuses on the use of solar, wind, and bioenergy to power electrochemical processes for bettering wastewater treatment efficiency and sustainability. In this vein, this review presents an overview of the many technologies involved, advantages, challenges, and prospects of this area and underlines that renewable energy will play a key role in developing cost-effective and environmentally benign wastewater treatment solutions [37].

**Algal Biofuel Production:** Algal cultivation is particularly suited to nutrient-rich wastewater, which offers a combination of essential organic and inorganic nutrients. The biomass generated from algal growth can be harvested and further processed into various biofuels such as biodiesel, bioethanol, and biogas. Due to the high yields of algal biofuels and their ability to grow on non-agricultural land, they are considered one of the more sustainable renewable energy options. This method presents a promising avenue for renewable energy production [38]. Another well-established route is biogas production through anaerobic digestion (AD), which converts organic matter into biogas. Researchers have explored ways in which wastewater treatment plants (WWTPs) can achieve energy neutrality by optimizing energy recovery from internal sources, such as producing biogas from sewage sludge [39]. This approach not only aids in waste management but also helps reduce the energy footprint of WWTPs [40,41]. Additionally, studies have investigated the potential for increasing renewable energy use in WWTPs by examining the efficiency of biogas production through co-digestion processes that involve sewage sludge combined with other organic wastes[42]. This paper discusses the practical challenges and solutions for achieving energy self-sufficiency at wastewater treatment facilities.

**Hydrothermal Carbonization:** Hydrothermal carbonization is a kind of thermo-chemical process that allows the conversion of wet biomass under high pressure and moderate temperature into a carbon-rich solid called hydrochar. The technique finds its application mainly in the treatment of high moisture wastewater and for producing solid biofuels suitable for energy production. HTC offers an avenue to transform wet biomass into a possibly useful, reliable energy source—a term quite relevant in securing sustainable waste management and renewable energy generation. A 2024 article by Ho et al. discussed the challenges and innovations of HTC on the conversion of high-moisture waste into biofuels [43]. They investigated the feasibility of applying such a method from the laboratory scale up to real-scale application. This emphasized the environmental and economic benefits by upgrading the process. In research conducted by Gonzalez et al. in 2022, a comprehensive review of the parameters affecting HTC and its application in increasing the energy potential of biomass has been done. This paper describes how HTC can improve the properties of various biomass feedstocks for use as biofuels and other renewable energy sources [44].

**Photocatalytic hydrogen generation:** Photocatalytic production of hydrogen with wastewater is another prospective technique that dominates renewable energy generation coupled with environmental remediation. This process generates clean hydrogen fuel while treating wastewater by utilizing the organic pollutants present in wastewater and therefore contributes to the goals of sustainable energy with reduced pollution. Further research and development should be focused on the optimization and commercialization of large-scale processes. Zhang et al. provided an extensive review of photocatalyst materials and techniques for enhancing the efficiency of hydrogen production, along with thorough explanations of the underlying mechanisms and the challenges associated with this field [45]. According to a review by Penn et al. in 2020, photocatalytic hydrogen evolution is among the clean routes for solar energy conversion into hydrogen, suffering from inefficiencies in light absorption, carrier separation, and surface reactions [46].

**Integration of membrane bioreactors:** Membrane bioreactors (MBRs) represent the coupling of biological treatment and membrane filtration, therefore capable of providing high-efficiency wastewater treatment together with biogas production. Coupling MBRs with anaerobic digestion processes improves pollutant removal and enhances biogas production for optimal treatment and energy recovery. Neo et al. proved in 2016 that integrated MBR has future prospects to be a potential technology in treating wastewater and reducing its pollution, above all for the creation of new sources of energy and nutrients. They also showed that integrated MBR makes energy and nutrient recovery environmentally and economically feasible [47]. In 2020, Kalassov et al showed that classical technologies for gas processing in biofuel production are economically inefficient and lead to burning biogas for energy. Integrating biological gas production with membrane separation improves $CO_2$ emission elimination. MBRs offer environmental and economic advantages such as energy savings, low cost, less space occupation, and operational flexibility that make them ideal for biogas production [48].

**Hybrid Systems**: The combination of different technologies mentioned as hybrid systems can cause maximum energy recovery from wastewater. These systems are designed for repeated wastewater treatment and lead to increased energy production as well as treatment efficiency.

## 4. Future Challenges and Guidelines

Such potential for energy production from wastewater encounters a myriad of challenges: technical difficulties, high upfront costs, requires specialized maintenance and operation, variability in the composition of wastewater, and finally, complex regulatory frameworks. Another big barrier is the public resistance to health and safety concerns. This resource, however, is maximally exploited through technological development, integrated systems, public awareness, optimization of the wastewater streams, Business models yang sustainable, and international collaboration. Comprehensive life cycle assessments may further guide improvements and policy decisions to ultimately make the use of wastewater for energy production a prominent contributor to both sustainable development and environmental protection.

**Technical Challenges**: The diverse composition of wastewater presents significant challenges for sustainable energy production. The development of robust and adaptable technologies capable of managing diverse wastewater streams is crucial for their widespread adoption. Ensuring consistent performance across different wastewater types requires continuous innovation and optimization.

**Economic Considerations**: The initial investment required for establishing wastewater-to-energy systems can be substantial. However, the long-term benefits, including energy savings and reduced waste disposal costs, can offset these initial expenditures. Policies and incentives are necessary to support these investments and encourage the adoption of such technologies.

**Environmental Effects**: While wastewater-to-energy technologies offer significant environmental benefits, such as reduced greenhouse gas emissions and decreased water pollution, careful management is required to prevent potential negative impacts, such as the release of harmful by-products. Ensuring proper operation and monitoring of these systems is crucial to maximize their positive environmental contributions.

**Research and Development**: Continued research and development are vital for improving the efficiency and scalability of these technologies. Innovations in biotechnology, materials science, and process engineering will play a crucial role in overcoming current limitations and fully harnessing the potential of wastewater for green energy production. Investing in R&D will be key to advancing this field and achieving broader implementation.

## 5. Conclusions

Non-renewable natural resources will definitely run out, so there must be a reliance on renewable energy sources to supply human needs with energy in a sustainable manner. The increasing energy demand from all over the world accentuates the need for clean and sustainable technologies in this sector. Wastewater, once viewed merely as discharge waste, is now recognized as a valuable resource for energy production. The generation of bioelectricity by microorganisms present in biomass has regained attention as humanity continues its pursuit of renewable energy sources. This production of energy from wastewater decreases the cost of operation and lessens overdependence on an external source of energy, especially in treatment plants. The process offsets the energy used by sewage plants. However, this low carbon energy attainment from wastewater requires new advanced and affordable yet scalable technologies. It, therefore, calls for detailed research accompanied by accurate data collection. Given large volumes of wastewater originating from agricultural, industrial, and domestic activities, there is a need to exploit these rich sources of green energy production. This paper reviews the potential of wastewater as a green energy source through looking at various treatment technologies of wastewater and discussing associated challenges and opportunities. The paper discusses successful case studies, advanced technologies, and emerging trends to drive research, innovation, and the implementation of green energy solutions, all with the goal of promoting environmental sustainability and economic growth. It also aims to introduce several methods of producing cost-effective and readily available energy, commonly referred to as renewable or green energy.

## References


[1] D. Lal, "Microbes to Generate Electricity," *Indian Journal of Microbiology*, vol. 53, no. 1, pp. 120–122, 2013.

[2] I. Gunnarsdottir, B. Davidsdottir, E. Worrell, and S. Sigurgeirsdottir, "Sustainable Energy Development: History of the Concept and Emerging Themes," *Renewable and Sustainable Energy Reviews*, vol. 141, 110770, 2021.

[3] R. Kollmann, G. Neugebauer, et al., "Renewable Energy From Wastewater - Practical Aspects of Integrating a Wastewater Treatment Plant Into Local Energy Supply Concepts," *Journal of Cleaner Production*, vol. 155, pp. 119–129, 2017.

[4] P. F. Tee, M. O. Abdullah, I. A. W. Tan, C. Nolasco-Hipolito, and K. Bujang, "Review on Microbial Fuel (MFC) Hybrid Energy Systems for Wastewater Treatment and Bio-Energy Production," *Proceedings of the International Engineering Conference*, pp. 265–270, 2014.

[5] S. Periyasamy, T. Temesgen, et al., "Wastewater to Biogas Recovery," *Clean Energy and Resource Recovery*, pp. 301–314, 2022.

[6] M. Maktabifard, E. Zaborowska, and J. Makinia, "Achieving Energy Neutrality in Wastewater Treatment Plants Through Energy Savings and Enhancing Renewable Energy Production," *Reviews in Environmental Science and Bio/Technology*, vol. 17, no. 4, pp. 655–689, 2018.

[7] S. S. Siwal, Q. Zhang, et al., "Recovery Processes of Sustainable Energy Using Different Biomass and Wastes," *Renewable and Sustainable Energy Reviews*, vol. 150, 111483, 2021.

[8] A. Ebrahimi, D. Yousefi Kebria, and G. N. Darzi, "Improving Bioelectricity Generation and COD Removal of Sewage Sludge in Microbial Desalination Cell," *Environmental Technology*, vol. 39, no. 9, pp. 1188–1197, 2017.

[9] I. Kim, K. Chae, M. Choi, and W. Verstraete, "Microbial Fuel Cells: Recent Advances, Bacterial Communities and Application Beyond Electricity Generation," *Environmental Engineering Research*, vol. 13, no. 2, pp. 51–65, 2008.

[10] K. F. Adekunle, and J. A. Okolie, "A Review of Biochemical Process of Anaerobic Digestion," *Advances in Bioscience and Biotechnology*, vol. 6, no. 3, pp. 205–212, 2015.

[11] X. Guo, Y. Sun, and D. Ren, "Life Cycle Carbon Emission and Cost-Effectiveness Analysis of Electric Vehicles in China," *Energy for Sustainable Development*, vol. 72, pp. 1–10, 2023.

[12] S. Aftab, A. Shah, et al., "Marketability Prospects of Microbial Fuel Cells for Sustainable Energy Generation," *Energy & Fuels*, vol. 34, no. 8, pp. 9108–9136, 2020.

[13] R. L. Manasa, and A. Mehta, "Wastewater: Sources of Pollutants and Its Remediation," *Environmental Chemistry for a Sustainable World*, pp. 197–219, 2020.

[14] N. Singh, T. Poonia, et al., "Challenges of Water Contamination in Urban Areas," *Current Directions in Water Scarcity Research*, vol. 6, pp. 173–202, 2022.

[15] S. Puig, M. Serra, M. Coma, M. D. Balaguer, and J. Colprim, "Simultaneous Domestic Wastewater Treatment and Renewable Energy Production Using Microbial Fuel Cells (mfcs)," *Water Science and Technology*, vol. 64, no. 4, pp. 904–909, 2011.

[16] M. Henze, and Y. Comeau, "Wastewater Characterization," *Biological Wastewater Treatment: Principles, Modelling and Design*, vol. 7, 2008.

[17] J. Ahmed, A. Thakur, and A. Goyal, "Industrial Wastewater and Its Toxic Effects," *Biological Treatment of Industrial Wastewater*, pp. 1–14, 2021.

[18] D. Dutta, S. Arya, and S. Kumar, "Industrial Wastewater Treatment: Current Trends, Bottlenecks, and Best Practices," *Chemosphere*, vol. 285, 131245, 2021.

[19] T. O. Ajiboye, O. A. Oyewo, and D. C. Onwudiwe, "Simultaneous Removal of Organics and Heavy Metals from Industrial Wastewater: A Review," *Chemosphere*, vol. 262, 128379, 2021.

[20] J. Casalí, R. Gastesi, et al., "Runoff, Erosion, and Water Quality of Agricultural Watersheds in Central Navarre (spain)," *Agricultural Water Management*, vol. 95, no. 10, pp. 1111–1128, 2008.

[21] A. Ward, D. Lewis, and F. Green, "Anaerobic Digestion of Algae Biomass: A Review," *Algal Research*, vol. 5, pp. 204–214, 2014.

[22] P. V. Rao, S. S. Baral, R. Dey, and S. Mutnuri, "Biogas Generation Potential by Anaerobic Digestion for Sustainable Energy Development in India," *Renewable and Sustainable Energy Reviews*, vol. 14, no. 7, pp. 2086–2094, 2010.

[23] R. Kleerebezem, B. Joosse, R. Rozendal, and M. C. M. Van Loosdrecht, "Anaerobic Digestion Without Biogas?," *Reviews in Environmental Science and Bio/Technology*, vol. 14, no. 4, pp. 787–801, 2015.

[24] Mao, Y. Feng, X. Wang, and G. Ren, "Cheminform Abstract: Review on Research Achievements of Biogas from Anaerobic Digestion," *ChemInform*, vol. 47, no. 28, 2016.

[25] T. Z. D. de Mes, A. J. M. Stams, J. H. Reith, and G. Zeeman, "Methane Production by Anaerobic Digestion of Wastewater and Solid Wastes," Bio-methane & Bio-hydrogen, pp. 58-102, 2003.

[26] B. Deepanraj, V. Sivasubramanian, and S. Jayaraj, "Biogas Generation Through Anaerobic Digestion Process—An Overview," *Research Journal of Chemistry and Environment*, vol. 18, no. 1, 5, 2014.

[27] Y. Li, Y. Chen, and J. Wu, "Enhancement of Methane Production in Anaerobic Digestion Process: A Review," *Applied Energy*, vol. 240, pp. 120–137, 2019.

[28] L. Wu, W. Wei, et al., "Upgrading Biogas Produced in Anaerobic Digestion: Biological Removal and Bioconversion of CO2 in Biogas," *Renewable and Sustainable Energy Reviews*, vol. 150, 111448, 2021.

[29] M. C. Gould, "Bioenergy and Anaerobic Digestion," in *Bioenergy*, Academic Press, Jan. 2015, pp. 297-317.

[30] T. Induchoodan, I. Haq, and A. S. Kalamdhad, "Factors Affecting Anaerobic Digestion for Biogas Production: a Review," *Advanced Organic Waste Management*, pp. 223–233, 2022.

[31] Y. Gu, Y. Li, et al., "The Feasibility and Challenges of Energy Self-Sufficient Wastewater Treatment Plants," *Applied Energy*, vol. 204, pp. 1463–1475, 2017.

[32] B. E. Logan, and J. M. Regan, "Microbial Fuel Cells—challenges and Applications," *Environmental Science & Technology*, vol. 40, no. 17, pp. 5172–5180, 2006.

[33] B. E. Logan, B. Hamelers, et al., "Microbial Fuel Cells: Methodology and Technology," *Environmental Science & Technology*, vol. 40, no. 17, pp. 5181–5192, 2006.

[34] M. Razavi, D. Yousefi Kebria, and A. Ebrahimi, "Microbial Fuel Cell-enhanced Electrokinetic Process for Remediation of Chromium from Marine Sediments," *Environmental Progress & Sustainable Energy*, vol. 40, no. 1, 2020.

[35] S. Siddiqui, P. Bhatnagar, et al., "Wastewater Treatment and Energy Production by Microbial Fuel Cells," *Biomass Conversion and Biorefinery*, vol. 13, no. 5, pp. 3569-3592, 2023.

[36] M. J. Salar-Garcia, O. Obata, et al., "Impact of Inoculum Type on the Microbial Community and Power Performance of Urine-Fed Microbial Fuel Cells," *Microorganisms*,

vol. 8, no. 12, 1921, 2020.
[37] W. Mook, M. Aroua, and G. Issabayeva, "Prospective Applications of Renewable Energy Based Electrochemical Systems in Wastewater Treatment: A Review," *Renewable and Sustainable Energy Reviews*, vol. 38, pp. 36–46, 2014.
[38] J. K. Pittman, A. P. Dean, and O. Osundeko, "The Potential of Sustainable Algal Biofuel Production Using Wastewater Resources," *Bioresource Technology*, vol. 102, no. 1, pp. 17–25, 2011.
[39] K. Muylaert, A. Beuckels, et al., "Wastewater as a Source of Nutrients for Microalgae Biomass Production," *Biofuel and Biorefinery Technologies*, pp. 75–94, 2015.
[40] S. Borzooei, G. Campo, et al., "Optimization of the Wastewater Treatment Plant: From Energy Saving to Environmental Impact Mitigation," *Science of The Total Environment*, vol. 691, pp. 1182–1189, 2019.
[41] V. Aghabalaei, H. Nayeb, S. Mardani, M. Tabeshnia, and M. Baghdadi, "Minimizing Greenhouse Gases Emissions and Energy Consumption from Wastewater Treatment Plants Via Rational Design and Engineering Strategies: A Case Study in Mashhad, Iran," *SSRN Electronic Journal*, 2022.
[42] D. Elalami, H. Carrere, et al., "Pretreatment and Co-Digestion of Wastewater Sludge for Biogas Production: Recent Research Advances and Trends," *Renewable and Sustainable Energy Reviews*, vol. 114, 109287, 2019.
[43] T. T. Ho, A. Nadeem, and K. Choe, "A Review of Upscaling Hydrothermal Carbonization," *Energies*, vol. 17, no. 8, 1918, 2024.
[44] J. González-Arias, M. E. Sánchez, J. Cara-Jiménez, et al., "Hydrothermal Carbonization of Biomass and Waste: A Review," *Environmental Chemistry Letters*, vol. 20, pp. 211-221, 2022.
[45] Y. Zhang, Y. Heo, et al., "Photocatalytic Hydrogen Evolution Via Water Splitting: A Short Review," *Catalysts*, vol. 8, no. 12, 655, 2018.
[46] J. Pan, S. Shen, et al., "Recent Progress in Photocatalytic Hydrogen Evolution," *Acta Physico-Chimica Sinica*, vol. 36, 1905068, 2020.
[47] C. H. Neoh, Z. Z. Noor, N. S. A. Mutamim, and C. K. Lim, "Green Technology in Wastewater Treatment Technologies: Integration of Membrane Bioreactor with Various Wastewater Treatment Systems," *Chemical Engineering Journal*, vol. 283, pp. 582–594, 2016.
[48] N. Kalassov, D. Dzhonova, I. Tsibranska, S. Panyovska, and R. Manatbayev, "Application of Integrated Membrane Bioreactors in Renewable Energy Industry," *Journal of Chemical Technology and Metallurgy*, vol. 55, no. 2, 2020.

## Declaration of competing interest

The authors declare that they have no known competing financial interests or personal relationships that could have appeared to influence the work reported in this paper. The ethical issues, including plagiarism, informed consent, misconduct, data fabrication and/or falsification, double publication and/or submission, redundancy, have been completely observed by the authors.

## Bibliography

**Marzie Razavi** obtained her M.Sc. degree in Environmental Engineering from Iran University of Science and Technology (IUST), Tehran, Iran in 2012 and her Ph.D. degree in Environmental Engineering from Babol Noshirvani University of Technology, Babol, Iran in 2020. She is currently a member of the Faculty of Civil Engineering at Tafresh University. Her research interests include Water and Wastewater treatment, Electrokinetic Soil Remediation, Electrocoagulation and Energy production by Microbial Fuel Cell.
**Email:** M.razavi@tafreshu.ac.ir
**ORCID:** 0000-0003-4229-3502
**Contribution Statement:** Conceptualization, Funding acquisition, Investigation, Project administration, Resources, Supervision, Validation, Roles/Writing - original draft, Writing-review & editing.

Journal of Green Energy Research and Innovation

# Adaptive Backstepping Control of an Autonomous Multi-Bus Microgrid based on Grid-forming/Grid-following Strategy Under Unbalanced Load Conditions

Mohammad Mahdi Rezaei

## Highlights

- Microgrid Control: A robust strategy maintains voltage and frequency in multi-bus island microgrids.
- Grid-forming/Grid-following: Adaptive backstepping controls voltage and frequency, while direct power control manages active/reactive powers.
- Local Measurement-based Design: The system uses local measurements for control, independent of microgrid specifics.
- Stability and Robustness: The controllers ensure stable operation, handling disturbances and parameter uncertainties effectively.

## Graphical Abstract

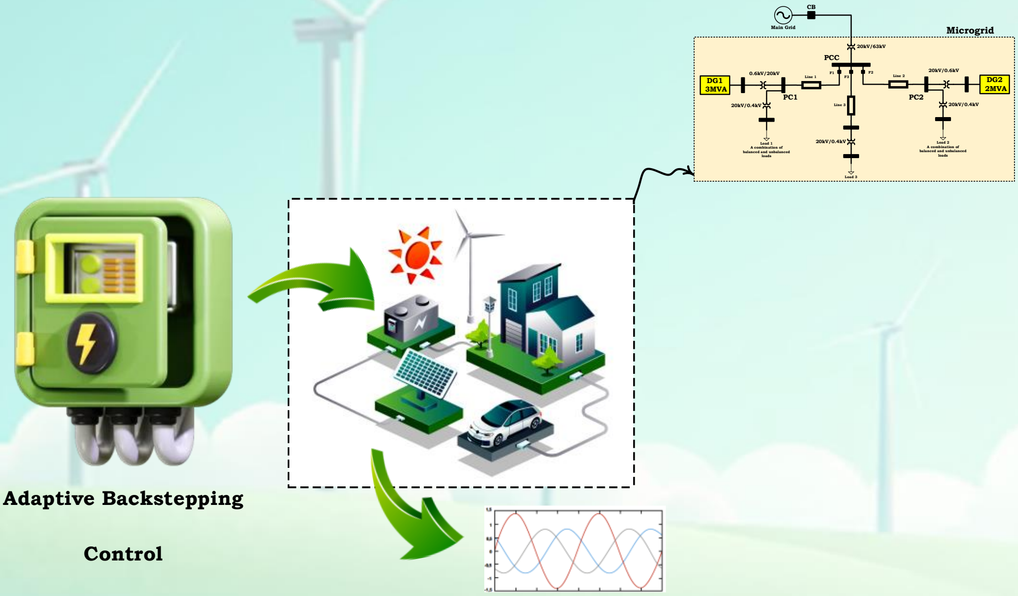


Use your device to scan and read the article online

Citation
M.M. Rezaie," Adaptive Backstepping Control of an Autonomous Multi-Bus Microgrid based on Grid-forming/Grid-following Strategy Under Unbalanced Load Conditions," *Journal of Green Energy Research and Innovation*, vol. 2, no. 1, pp. 20-31, 2025.

https://doi.org/10.61186/jgeri.2.1.20

JGERI Journal of Green Energy Research and Innovation

Journal of Green Energy Research and Innovation 2.1 (2025) 20-31

Online ISSN: 3041-9018

Journal of Green Energy Research and Innovation

Journal Homepage: www.jgeri.araku.ac.ir

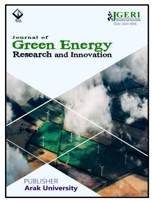

# Adaptive Backstepping Control of an Autonomous Multi-Bus Microgrid based on Grid-forming/Grid-following Strategy Under Unbalanced Load Conditions

Mohammad Mahdi Rezaei [*]

*Department of Electrical Engineering, Khomeinishahr Branch, Islamic Azad University, Khomeinishahr, Isfahan, Iran.*

A R T I C L E I N F O

***Keywords:***
Microgrid (MG),
Distributed Generation (DG),
Grid-forming/Grid-following control structure,
Adaptive Backstepping.

***Article History:***
Received: 26 June 2024;
Revised: 19 July 2024;
Accepted: 11 August 2024.

***Article type:***
Research Article

* ***Corresponding author***
*E-mail address:*
mm.rezaei@iaukhsh.ac.ir (M. Rezaie)

A B S T R A C T

In this article, in order to maintain the voltage and frequency of a multi-bus island microgrid, a robust control strategy is proposed. The microgrid under study is a medium voltage distribution system consisting of several inverter-based distributed generation (DG) units, and a combination of balanced and unbalanced local loads. Based on the Grid- forming/Grid-following structure, a robust voltage controller is designed based on the adaptive backstepping control method to keep the voltage and frequency of the Grid-forming unit at predefined values. In addition, to adjust the active/reactive powers of the Grid-following units, a direct power controller based on adaptive input-output feedback linearization control method is proposed. The negative sequence component of unbalanced local loads current is compensated by the proposed power controller. Only local measurements are used in designing of the controllers; therefore, the proposed method is independent of the topology of microgrid, the parameters of the system, and the dynamics of loads. The controllers presented in this article are robust and stable against various disturbances and parameter uncertainties. after outage of Grid-following unit, the power generated by the Grid-forming unit is adaptively adjusted so that the absence of generation at PC2 is offset. In addition, despite the mismatched filter resistance and accidental outage of Grid-following unit, even under non-local unbalanced load condition the proposed voltage controller robustly regulates the voltage waveform of MG with a reasonable transient. Validity and effectiveness of the proposed control strategy are shown based on time domain studies in MATLAB/Simulink environment.

## 1. Introduction

### *1.1. Problem statement*

Microgrids (MGs) are low- or medium-voltage local networks that include clusters of loads as well as distributed generation (DG) units [1-5]. Depending on the conditions, MGs can be operated both in grid connected mode and in islanded mode. In the mode of connected to the grid, the voltage of the buses and the frequency of the system are dictated by the main grid, and each DG unit generates predetermined values of active/reactive power [6-7]. Considering MG's performance as an independent system in islanded mode, it is necessary to perform a proper voltage and frequency control. To enhance the reliability of the MG, this process should be performed robust, fast, and locally [8-9].

### *1.2. Literature Review*

Several methods have been presented so far for the voltage/frequency control of islanded MGs [3-15, 19-25]. The main control strategies reported so far are methods based on Droop characteristic, and methods based on Grid-forming/Grid-following control structure [10]. Droop characteristic technique is the most well-known control strategy for MGs [3-15]. All DG units, in the methods based on Droop characteristic, participate in the voltage/frequency regulation of MG [11]. In this method, the total active/reactive power demand is shared locally among the DG units without using any MG communication. However, MG voltage and frequency deviations are unavoidable in this method [12]. In Grid-forming/Grid-following methods, the task of voltage and frequency regulation in MG is assigned to a DG unit, which usually has the highest power rating [14]. The name of this unit is called Grid-forming. Other units in MG, which are called Grid-following units, are responsible for generating predetermined active/reactive power.

Through appropriate control strategies, in addition to the main control purpose, the power quality of system can also be enhanced [15]. Voltage imbalance is the most common phenomenon among various power quality issues. Connection of unbalanced loads is the main cause of voltage unbalance in MGs. In actual distribution systems, due to the installation of a large number of unbalanced loads in different phases, the severity of overall load imbalance is not significant [16]. However, in MG systems, the problem of unbalanced loads is much more common and is caused by the unequal connection of unbalanced loads to the phases [17]. So, MGs are expected to be operated in such a way that they can perform properly even under unbalanced load conditions [18].

Therefore, both in the Droop and Grid-forming/Grid-following methods, to improve the dynamic behavior and achieve a disturbance rejection performance, the control scheme should be robust and fast in the island MG [19,23]. In the technical literature, various techniques have been reported for strong control of island MGs [19-24]. In [19], to improve the performance of MG, a changeable control structure in integration with the Droop characteristic technique is presented. A hierarchical two-stage control method is used in [20], which provides a centralized control strategy based on the cluster-oriented cooperative control strategy. By using this controller, it has been tried to optimize the sharing performance of power components in a multiple-MG system. However, the local controllers provided at the primary control level are based on the traditional droop method. In [21,22], the load dynamics is modeled with an RLC network and used in controller design process to achieve a suitable dynamic in the MG. Nevertheless, the stability and robustness of presented controllers cannot be cannot guaranteed against uncertainties in load configuration and dynamics.

In [23], a robust controller is proposed based on $H_\infty$ control technique, to voltage/frequency control of a single-bus elementary MG. Using the Grid-forming/Grid-following structure, the load disturbance is measured in real-time and the Grid-forming unit's controller uses it as a measurable external disturbance. However, because of high-bandwidth communications needed between the Grid-forming unit and all further loads in multi-bus MGs, for real-time measurement of the instantaneous load currents, the presented scheme in [23] can be impractical. The Grid-following unit is connected to some load buses to participate the demand of load. Although it is explained in [23] that the Grid-following unit is operated based on vector control method, no description is presented in this case. Moreover, the Grid-following unit during load disturbances is disconnected and the performance of the Grid-following units has not been studied against load disturbances. In addition, there is no guarantee for the stability and effectiveness of the control structure due to the parametric uncertainties of the system.

In [24] a combination of proportional-integrating-based (PI) and proportional-resonance-based (PR) methods are used to respectively control of the positive-sequence (PS) voltage and compensate the negative-sequence (NS) current components. Two equivalent circuits are presented in [24] for PS and NS load currents. However, since both the PS and NS voltages are linear functions of both the PS and NS currents, the presented equivalent circuits are coupled and cannot be used separately. In [25], a robust control strategy is presented for a multi-bus MG. In the control system presented in [25], the voltage regulation of MG is fulfilled by a sliding-mode voltage controller for the Grid-forming unit. However, the power controller designed for the Grid-following unit only regulates its own output power and does not play a role in compensating the effects of the imbalance of its local loads. This causes all the burden of load imbalance compensation to fall on the Grid-forming unit.

### *1.3. Research gap*

According to the conducted research, we realize that none of them used the adaptive backstepping control method to control the network. Also, few articles have designed their proposed controller based on unbalanced load control.

### *1.4. Main contribution and innovations*

The main contribution of this paper is to propose a robust voltage controller, based on adaptive backstepping control method, to force the voltage and frequency of the Grid-forming unit to track the relevant references, in the Grid-forming/Grid-following control structure of a multi-island MGs.

In addition, a direct power controller is proposed based on adaptive input-output feedback linearization (IOFL) for the Grid-following units, to control the PS active/reactive powers generated by these units. The presented power controller is designed to be able to compensate the NS current components (NSCCs) caused by unbalanced local loads. The presented control strategy is based on local measurements and is independent of topology, parameters and dynamics of microgrid loads. Performance of the presented control system have been shown through simulation studies in the MATLAB/Simulink.

## 2. Microgrid Structure Description

Figure 1 shows the single-line diagram of the studied MG, including three radial feeders [24-25]. MG is fed by two 0.6 kV DG units with capacity of 3 MVA (DG1) and 2 MVA (DG2), respectively. The DG units are modeled with a DC source that connected to medium voltage (MV) feeders through a power converter, an LC filter, and step-up transformers. A combination of balanced and unbalanced loads is also connected to MV feeders F1, F2 and F3 through step-down transformers. In this paper, MG operates in island mode. Table 1 shows the parameters of MG.

## 3. DG Unit Modeling

Figure 2(a) depicts an inverter-based DG unit connected to a microgrid interface through an LC filter. Taking into account the parameters under nominal conditions, the dynamic Equation (1,2) of output voltage and current can be derived in the synchronous ($dq$) reference frame, as shown in Figure 2(b).

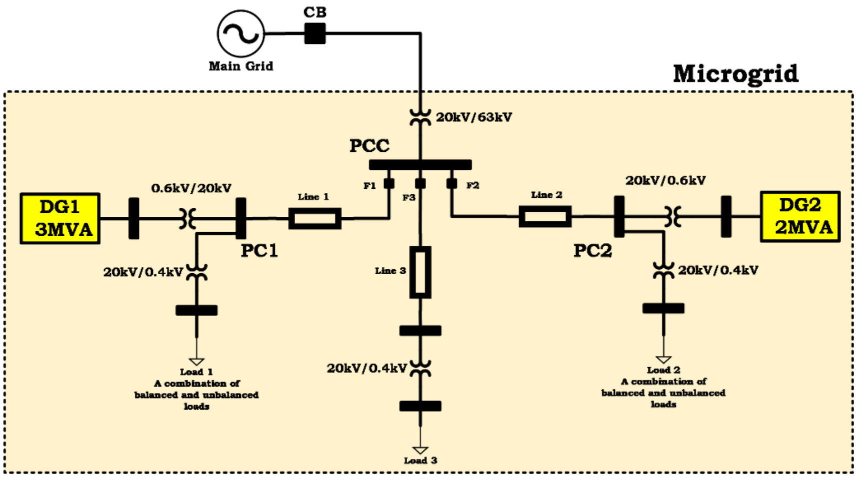


**Figure 1.** Schematic diagram of studied MG.

**Table 1.** Parameters of the studied system.

| Parameter | Value |
|---|---|
| Grid-forming DG nominal power | 3 MVA ($S_{base}$) |
| Grid-following DG nominal power | 2 MVA |
| VSC terminal voltage (line to line) | 600 V ($V_{base}$) |
| $R_{f1}$, $R_{f2}$ (Series filter resistance) | 0.002 Ω |
| $L_{f1}$, $L_{f2}$ (Series filter inductance) | 500 μH |
| $C_{f1}$, $C_{f2}$ (Filter capacitance) | 400 μF |
| $Z_{line1}$ (5.7 km overhead line) | 0.7 + j1.57 Ω |
| $Z_{line2}$ (4 km overhead line) | 0.5 + j1.25 Ω |
| $Z_{line3}$ (2 km overhead line) | 0.1 + j0 Ω |
| $V_{dc}$ (DC bus voltage) | 1500 V |
| $f_S$ (System frequency) | 50 Hz |
| $f_{SW}$ (Switching frequency) | 2 kHz |

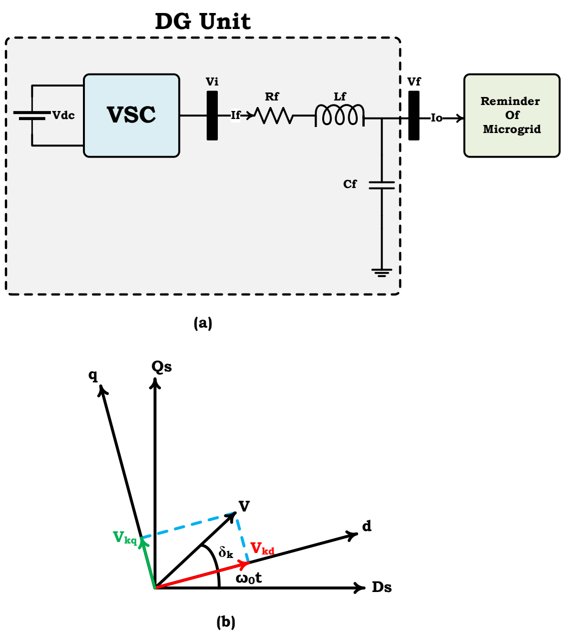


**Figure 2.** (a) Schematic diagram of a DG unit, (b) virtual synchronous reference frame.

$$\frac{d}{dt}I_f = a\left(V_i - bI_f - V_f\right) + \omega_0 I_f^{\perp}, \tag{1}$$

$$\frac{d}{dt}V_f = c\left(I_f - I_o\right) + \omega_0 V_f^{\perp}, \tag{2}$$

where the values of $a = \frac{1}{L_f}$ , $b = R_f$ and $c = \frac{1}{C_f}$ represent the parameters in nominal conditions; the symbols in bold denote $V = [V_d V_q]^T$ and $I = [I_d I_q]^T$ . Additionally, the superscript " $\perp$ " indicates a $90^\circ$ lag with respect to the original vector. By deviating the system's parameters with respect to nominal values, Equations (1,2) can be rewritten as Equations (3,4):

$$\frac{d}{dt}\mathrm{I}_f = a\left(\mathrm{V}_i - b\mathrm{I}_f - \mathrm{V}_f\right) + \omega_0 \mathrm{I}_f^{\perp} + \Theta_i, \tag{3}$$

$$\frac{d}{dt}\mathrm{V}_f = c\left(\mathrm{I}_f - \mathrm{I}_o\right) + \omega_0 \mathrm{V}_f^{\perp} + \Theta_v, \tag{4}$$

The lumped uncertainties, denoted as $\Theta_i = [\Theta_{id}\Theta_{iq}]^T$ and $\Theta_v = [\Theta_{vd}\Theta_{vq}]^T$ , can be expressed as Equations (5,6):

$$\Theta_i = \Delta a\left(\mathrm{V}_i - b\mathrm{I}_f - \mathrm{V}_f\right) - (a + \Delta a)\Delta b\mathrm{I}_f + \Lambda_i, \tag{5}$$

$$\Theta_v = \Delta c\left(\mathrm{I}_f - \mathrm{I}_o\right) + \Lambda_v, \tag{6}$$

where $\Delta$ denotes deviation from the expected value. In Equations (5,6), the terms $\Lambda_i$ and $\Lambda_v$ are introduced to address system dynamic disturbances and other unmodeled uncertainties.

## 4. Control Scheme

Based on Grid-forming/Grid-following control strategy in the context of a MG, $DG_1$ is specifically assigned the task of voltage control as a Grid-forming unit, and $DG_2$ has the specific role of generating predetermined levels of both active/reactive power components, as a Grid-following unit. In order to improve transient response and achieve desirable disturbance rejection and reference tracking performance, a robust voltage controller is specifically developed based on adaptive Backstepping for the Grid-forming unit. Additionally, a direct power controller has been developed based on adaptive IOFL. This controller ensures robust regulation of both active/reactive power levels that need to be supplied by Grid-following unit. In the subsequent subsections, a detailed explanation of the control design procedure is provided.

### *4.1. Adaptive Backstepping Control of Grid-forming Unit*

The primary control objective for the Grid-forming (DG1) unit is to accurately follow the predefined voltage trajectories. Let's denote the voltage tracking error as Equation (7):

$$\mathrm{E}_v = \mathrm{V}_f^{ref} - \mathrm{V}_f, \tag{7}$$

and denote the error between the lumped uncertainties $\Theta_v$ and its estimated value $\hat{\Theta}_v$ as Equation (8):

$$\tilde{\Theta}_v = \hat{\Theta}_v - \Theta_v. \tag{8}$$

A Lyapunov function can be expressed as Equation (9):

$$W_1 = \frac{1}{2}\mathrm{E}_v^T\mathrm{E}_v + \frac{1}{2}\tilde{\Theta}_v^T\gamma_v\tilde{\Theta}_v, \tag{9}$$

where diagonal matrix $\gamma_v$ consists of positive entries that are the estimation coefficients. Let's differentiate $W_1$ with respect to time as Equation (10):

$$\frac{d}{dt}W_1 = \mathrm{E}_v^T\left(\frac{d}{dt}\mathrm{E}_v\right) + \tilde{\Theta}_v^T\gamma_v\left(\frac{d}{dt}\tilde{\Theta}_v\right), \tag{10}$$

considering (7), (8) and (4), one can be shown as Equation (11):

$$\frac{d}{dt}W_1 = E_v^T\left(\frac{d}{dt}V_f^{ref} - c\left(I_f - I_o\right) - \omega_0 V_f^{\perp} - \Theta_v\right) + \tilde{\Theta}_v^T\gamma_v\left(\frac{d}{dt}\hat{\Theta}_v\right). \tag{11}$$

Choosing the estimation law as Equation (12):

$$\frac{d}{dt}\hat{\Theta}_v = -\gamma_v^{-1}E_v, \tag{12}$$

$\frac{d}{dt}W_1$ can be reduced to Equation (13):

$$\frac{d}{dt}W_1 = E_v^T\left(\frac{d}{dt}V_f^{ref} - c\left(I_f - I_o\right) - \omega_0 V_f^{\perp} - \hat{\Theta}_v\right). \tag{13}$$

For $E_v$ to be stable, it is required that $\frac{d}{dt}W_1$ definitely be negative. By choosing Equation (14):

$$I_f^{ref} = I_o + \frac{1}{c}\left(\frac{d}{dt}V_f^{ref} - \omega_0 V_f^{\perp} - \hat{\Theta}_v + k_v E_v\right), \tag{14}$$

where diagonal matrix $k_v$ consists of positive constant elements, then, it can be obtained as Equation (15):

$$\frac{d}{dt}W_1 = -k_v E_v^T E_v + c E_v^T E_i \tag{15}$$

With Equation (16):

$$E_i = I_f^{ref} - I_f \tag{16}$$

It can be concluded from Equation (15) that the system is not yet made fully stable. According to Backstepping control theory [26], the control input $V_i$ should be designed in the next step to make $\frac{d}{dt}W_1$ negative definite. Hence, the following positive definite function can be chosen as Lyapunov function Equation (17):

$$W_2 = W_1 + \frac{1}{2}E_i^T E_i + \frac{1}{2}\tilde{\Theta}_i^T \gamma_i \tilde{\Theta}_i, \tag{17}$$

With Equation (18):

$$\tilde{\Theta}_i = \hat{\Theta}_i - \Theta_i, \tag{18}$$

where $\tilde{\Theta}_i$ is the error between lumped uncertainties $\Theta_i$ and its estimated value $\hat{\Theta}_i$. Time derivation of $W_2$ is obtained as Equation (19):

$$\frac{d}{dt}W_2 = \frac{d}{dt}W_1 + E_i^T\left\{\frac{d}{dt}E_i\right\} + \tilde{\Theta}_i^T \gamma_i\left(\frac{d}{dt}\tilde{\Theta}_i\right). \tag{19}$$

Considering (16), (18) and (3), it can be shown as Equation (20):

$$\frac{d}{dt}W_2 = -k_v E_v^T E_v + c E_v^T E_i + E_i^T\left\{\frac{d}{dt}I_f^{ref} - a\left(V_i - bI_f - V_f\right) - \omega_0 I_f^{\perp} - \Theta_i\right\} + \tilde{\Theta}_i^T \gamma_i\left(\frac{d}{dt}\hat{\Theta}_i\right). \tag{20}$$

If the estimation law is selected as Equation (21):

$$\frac{d}{dt}\hat{\Theta}_i = -\gamma_i^{-1}E_i, \tag{21}$$

where $\gamma_i$ is a diagonal matrix with positive constant elements, then $\frac{d}{dt}W_2$ becomes as Equation (22):

$$\frac{d}{dt}W_2 = -k_v E_v^T E_v + E_i^T\left\{cE_v + \frac{d}{dt}I_f^{ref} - a\left(V_i - bI_f - V_f\right) - \omega_0 I_f^{\perp} - \hat{\Theta}_i\right\}. \tag{22}$$

If the following control law is selected as Equation (23):

$$V_i = V_f + bI_f + \frac{1}{a}\left(cE_v + \frac{d}{dt}I_f^{ref} - \omega_0 I_f^{\perp} - \hat{\Theta}_i + k_i E_i\right) \tag{23}$$

where $k_i$ is a diagonal matrix with positive constant elements, then $\frac{d}{dt}W_2$ can be obtained as Equation (24):

$$\frac{d}{dt}W_2 = -k_v E_v^T E_v - k_i E_i^T E_i \le 0. \tag{24}$$

It is shown that the time derivative of the Lyapunov function $W_2$ is strictly negative, therefore it implies that the proposed voltage control system is asymptotically stable.

### *4.2. IOFL Control of Grid-following DG Units*

#### *4.2.1. Power controller design*

For Grid-following units, the primary control objective is to manage the active/reactive power supplied by the generation units. In the subsequent sections, it will delve into the detailed design procedure of the presented power controller. The instantaneous active/reactive power components produced by the DG unit can be mathematically represented as Equations (25,26) [28-29]:

$$P = V_f \cdot I_f = V_{fd}I_{fd} + V_{fq}I_{fq} \tag{25}$$

$$Q = V_f^{\perp}.I_f = V_{fq}I_{fd} - V_{fd}I_{fq} \tag{26}$$

In Equations (25,26), the symbol " $\cdot$ " represents the inner product of two vectors, and the superscript " $\perp$ " indicates a phase lag of 90° with respect to the original vector. Based on Equations (25,26), the matrix form of instantaneous power equation of DG units can be expressed as Equation (27):

$$\mathrm{S} = \mathrm{E}_f \mathrm{I}_f \tag{27}$$

With Equation (28,29):

$$S = [P \quad Q]^T, \tag{28}$$

$$E_f = \begin{bmatrix} V_{fd} & V_{fq} \\ V_{fq} & -V_{fd} \end{bmatrix}. \tag{29}$$

By differentiating (27), it can be obtained that as Equation (30)

$$ddt\boldsymbol{S} = ddt\boldsymbol{E}f\, I_f + E_f \left( \frac{d}{dt} I_f \right) \tag{30}$$

If $\frac{d}{dt}V_{f,dq}$ and $\frac{d}{dt}I_{f,dq}$ are substituted into Equation (31), it can be expressed as Equation (31):

$$\frac{d}{dt} S = G + H + aE_f V_i + \Upsilon_s, \tag{31}$$

With Equation (32):

$$G = \begin{bmatrix} c\left(I_{fd} - I_{od}\right) + \omega_0 V_{fq} & c\left(I_{fq} - I_{oq}\right) - \omega_0 V_{fd} \\ c\left(I_{fq} - I_{oq}\right) - \omega_0 V_{fd} & -c\left(I_{fd} - I_{od}\right) - \omega_0 V_{fq} \end{bmatrix} I_f, \tag{32}$$

$$H = -E_f \begin{bmatrix} a\left(bI_{fd} + V_{fd}\right) - \omega_0 I_{fq} \\ a\left(bI_{fq} + V_{fq}\right) + \omega_0 I_{fd} \end{bmatrix}, \tag{33}$$

$$\Upsilon_s = \begin{bmatrix} \Theta_{vd} & \Theta_{vq} \\ \Theta_{vq} & -\Theta_{vd} \end{bmatrix} I_f + E_f \begin{bmatrix} \Theta_{id} & \Theta_{iq} \\ \Theta_{iq} & -\Theta_{id} \end{bmatrix}, \tag{34}$$

where the vector $\Upsilon_s$ represents the lumped uncertainties affecting the dynamics of $\mathrm{S}$. Based on the IOFL control theory [27], by choosing the control input $\mathrm{V}_i$ as Equation (35):

$$\mathrm{V}_i = \tfrac{1}{a} \mathrm{U}_f^{-1} \left( -\mathrm{G} - \mathrm{H} + \mathrm{U}_i \right), \tag{35}$$

where $\mathrm{U}_i$ should be determined as a new control input, $\frac{d}{dt}\mathrm{S}$ can be expressed as Equation (36):

$$\tfrac{d}{dt}\mathrm{S} = \mathrm{U}_i + \mathrm{Y}_s \tag{36}$$

Letting the tracking error denoted by Equation (37):

$$\mathrm{E}_s = \mathrm{S}^{ref} - \mathrm{S}, \tag{37}$$

and the error between the lumped uncertainties $\Upsilon_s$ and its estimated value $\hat{\Upsilon}_s$ denoted by Equation (38):

$$\tilde{\Upsilon}_s = \hat{\Upsilon}_s - \Upsilon_s, \tag{38}$$

a positive definite Lyapunov function can be chosen as Equation (39):

$$W_3 = \frac{1}{2} E_s^T E_s + \frac{1}{2} \tilde{\Upsilon}_s^T \gamma_s \tilde{\Upsilon}_s, \tag{39}$$

where $\gamma_s$ is a diagonal matrix with all positive constant diagonal entries which are the adaptation law gains. Differentiating $W_3$ with respect to time gives Equation (40):

$$\frac{d}{dt} W_3 = E_s^T \left( \frac{d}{dt} E_s \right) + \hat{\Upsilon}_s^T \gamma_s \left( \frac{d}{dt} \tilde{\Upsilon}_s \right). \tag{40}$$

By selecting the adaptation law as Equation (41):

$$\frac{d}{dt} \hat{\Upsilon}_s = -{\gamma_s}^{-1} E_s, \tag{41}$$

then, $\frac{d}{dt}W_3$ can be given by Equation (42):

$$\frac{d}{dt} W_3 = E_s^T \left( \frac{d}{dt} S^{ref} - U_i - \hat{\Upsilon}_s \right). \tag{42}$$

Now by choosing the control input $\mathrm{U}_i$ as Equation (43):

$$U_i = \frac{d}{dt} S^{ref} - \hat{\Upsilon}_s + k_{es} E_s, \tag{43}$$

where $\mathrm{k}_{es}$ is a diagonal matrix consisting positive constant elements, $\frac{d}{dt}W_3$ can be written by Equation (44):

$$\tfrac{d}{dt} W_3 = -\mathrm{k}_{es} \mathrm{E}_s^T \mathrm{E}_s \le 0. \tag{44}$$

Hence, the time derivative of the chosen Lyapunov function is negative definite, indicating asymptotic stability of the power control system.

#### 4.2.2. Compensation of unbalanced load current

In Figure 1, it is considered that a combination of both balanced and unbalanced loads is connected to the Grid-following unit's PC buses. In addition to generate pre-specified powers, the control objective is to compensate the effect of an unbalanced load by injecting required NSCCs by the corresponding Grid-following unit. For this purpose, the instantaneous power reference of Grid-following unit is determined as Equation (45):

$$S^{ref} = S^{pre-set} + \frac{3}{2} E_f I_L^n \tag{45}$$

where, $I_L^n$ is the NSCCs of local load of Grid-following unit. In order to regulate the active/reactive of Grid-following unit and to generate the NSCCs of the local load, the obtained power reference is robustly tracked by the proposed direct power controller.

## 5. Simulation Results

To assess the effectiveness of the proposed control strategy, the MG depicted in Figure 1 is simulated using the MATLAB/Simulink software environment. The system parameters can be found in Table 1. In the studied MG, the Grid-forming ($DG_1$) unit utilizes the proposed voltage controller, while the Grid-following ($DG_2$) unit employs the proposed power controller. The study includes four simulation cases, each detailed in the subsequent subsections. The case studies provide insights into the MG performance under various scenarios, including parametric uncertainties, the black start process, energization with unbalanced loads, and the accidental outage of Grid-following units. It's important to highlight that across all case studies, the parameters and topology of the controllers remain consistent.

### 5.1. Microgrid Black-Start

The objective of this case study is twofold: 1) MG Black-Start Capability: It aims to showcase the MG's ability to black-start, which refers to the process of restoring power to the system after a complete shutdown. 2) Robustness of Proposed Control Strategy: The study evaluates the robustness of the proposed control strategy in the face of parametric uncertainties within the MG. In studies, the Grid-forming unit is black-started with $V_f^{ref} = 0$, while the power reference of Grid-following unit is set to $P_2^{ref} = 0$ and $Q_2^{ref} = 0$. Subsequently, $V_f^{ref}$ is increased to 1 p.u. with an exponentially trajectory. In this study, the robust performance of the proposed controllers is assessed under parametric uncertainties. Specifically, a $20\%$ step-mismatch is introduced in the filter resistance starting from $t = 0.3$ s.

At $t = 0.4$ s and $t = 0.8$ s, the active/reactive power components of the reference signal of DG2, are exponentially increased to 0.4 p.u. and 0.3 p.u., respectively, with 0.005 s time-constant. The response of MG to explained events is depicted in Figure 3. The voltage magnitude of DG1 is indicated in Figure 3(a). This quantity can be obtained by Equation (46):

$$V = \sqrt{(V_d)^2 + (V_q)^2} \tag{46}$$

According to Figure 3(a), the filter voltage exhibits a stable and rapid response as it closely follows its reference command. Notably, this behavior demonstrates strong robustness even in the presence of parametric uncertainties and during the black-start process of the Grid-forming unit. The active/reactive power components of DG2 and DG1 are depicted in Figure 3(b) and (c). According to Figure 3(b), the active/reactive powers of the Grid-following unit closely track their respective reference signals. Notably, there are no observable transients or inter-channel interactions. In Figure 3(d), the voltage magnitude at the point of common coupling (PCC) can be observed. Additionally, Figure 3(e) and Figure 3(f) provide zoomed views of the voltage waveform at the PCC for periods around t = 0.4 s and t = 0.8 s, respectively. Based on the information provided, the transients of the PCC voltage are practically insignificant. This case study serves as a demonstration of the robust performance of the proposed control strategy. Despite uncertainties in system parameters and the black-start process of the Grid-forming unit, the strategy effectively tracks reference commands and maintains system stability. Additionally, it validates the MG's black-start capability under the presented control method.

### 5.2. Unbalanced Load Energization

#### 5.2.1. Energization of Unbalanced Load1

In this case study, the focus is on demonstrating the robust performance of the proposed voltage controller under unbalanced load conditions. Despite the challenges posed by varying loads, the controller aims to maintain stability and effectively regulate the system. In this case study, we consider the following scenario: 1 (The MG system initially operates under the conditions described in Subsection 5.1. 2) At $t = 1.7$ s, an unbalanced load is connected to the low-voltage side of feeder $F_1$. In this case study, the unbalanced load connected to the MG system consists of a series RL circuit between phase-b and phase-c. Specifically: the load resistance is $3.6\Omega$ and the load inductance is $8.6\,mH$ .

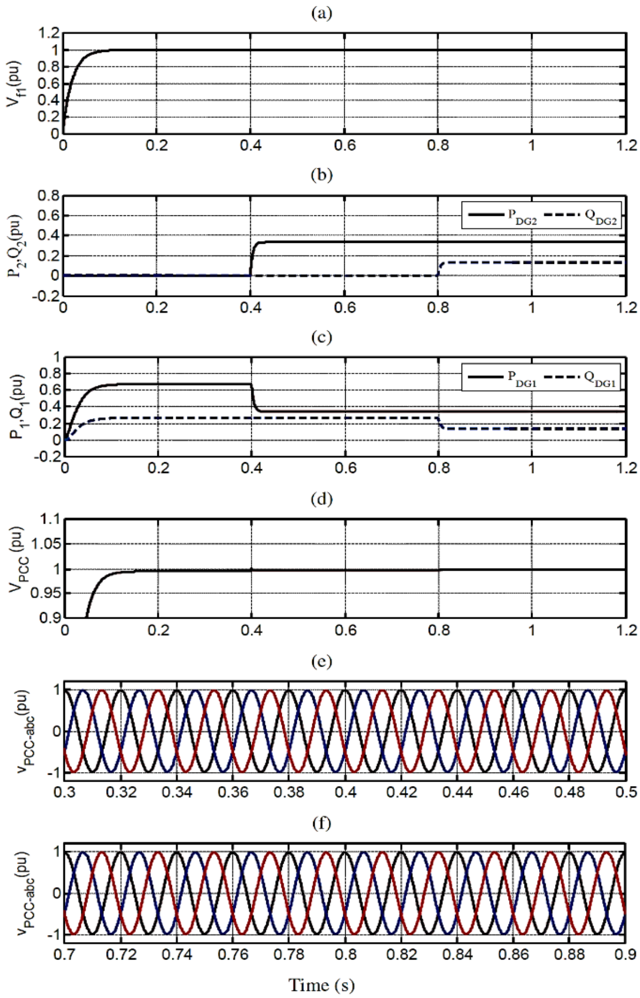


**Figure 3.** Black-start of Grid-forming unit and energization of a Grid-following unit: (a) magnitude of output voltage of DG1, (b) and (c) active/reactive power components of DG2 and DG1, (d) PCC voltage magnitude, and (e) and (f) instantaneous PCC voltage around $t = 0.4$ s and $t = 0.8$ s.

Figure 4(a)-(g) indicated the instantaneous current of load, the load current magnitude, output power components of DG1 and DG2, the voltage magnitude of the PCC and filter, and the PCC bus's instantaneous voltage, in a time-period around $t = 1.7$ s; and depicts the dynamic response of MG to energization of the explained unbalanced load. As shown in Figure 4(a) and (b), when $Load_1$ becomes unbalanced, a notable NSCC appears in the load current. This results in an increase in the current unbalance factor (CUF)—the ratio of NS to PS components—rising from zero to approximately $33.3\%$. As depicted in Figure 4(b)-(d), the NSCC of the load current becomes evident through double-frequency oscillations (DFOs) observed in both the magnitude of the load current and the instantaneous active/reactive power components of the Grid-forming unit. As depicted in Figure 4(c) and 4(d), even with the unbalanced load energization, the instantaneous active/reactive power components of the Grid-following unit exhibit robust tracking of their reference values. Notably, there are no observable transients or double-frequency oscillations (DFOs) in these components. Figure 4(e), (f) and (g) provide confirmation that even under unbalanced load conditions, the proposed voltage controller effectively and robustly regulates the voltage waveform of the MG. In this case, the voltage unbalance factor (VUF)—which represents the ratio of the NS to PS components of the filter and PCC voltage—is $0.08\%$ and $0.19\%$, respectively. These values fall well within the IEEE Standards requirement for voltage imbalance, which specifies a limit of below $2\%$ for sensitive equipment. This case study serves as verification of the stability and robustness of the proposed voltage controller under unbalanced load conditions and in the presence of parameter uncertainties.

#### *5.2.2. Energization of Unbalanced Load2*

In this case study, the purpose is to assess the effectiveness of the presented power controller against load unbalance. In this case study, the MG initially operates under the same conditions explained in Subsection 5.1. In this case, an unbalanced load is energized through the low-voltage feeder of $F_2$ at $t = 1.7$ s. The unbalanced load is composed of a resistor and an inductance connected in series with parameters of $3.6\Omega$ and 8.6 mH, connected between phase-b and phase-c.

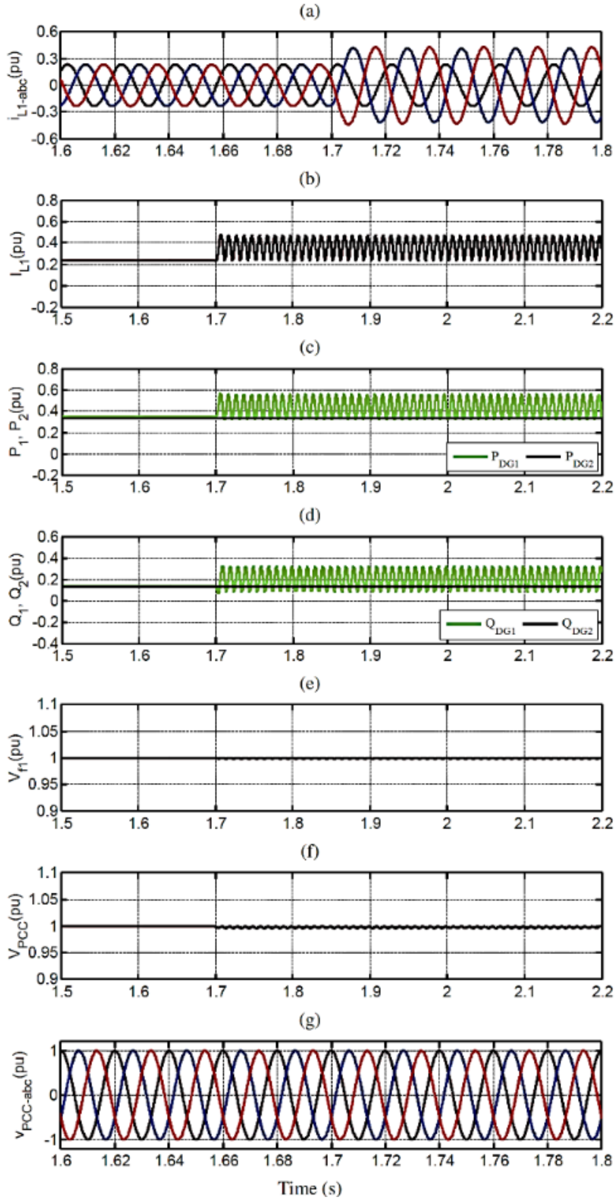


**Figure 4.** Energization of unbalanced Load1: (a) instantaneous load current, (b) load current amplitude, (c) active power component of DG1 and DG2, (d) reactive power component of DG1 and DG2, (e) and (f) amplitude of the PC1 and PCC voltage, and (g) instantaneous voltage of PCC bus.

In Figure 5, the system's response following the connection of the described unbalanced load can be observed. The time period of interest is about t = 1.7 s. Figure 5(a)-(b) indicate the load current in instantaneous form as well as magnitude form. As shown in Figure 5(a), since the Load2 becomes unbalanced, the load current is imposed with a significant NS component, such that an increase of about 33.3% has occurred in the load current CUF index. When analyzing the load current, the NSCC becomes evident through DFOs in the detected amplitude of the load current, as indicated in Figure 5(b). These oscillations are a result of the unbalanced load conditions that discussed earlier.

In Figure 5(c)-(d) the active/reactive power of both DG units are shown. From these plots, it can be observed that the average active and reactive power values of the Grid-following unit closely follow their respective references, even when dealing with load switching and unbalanced load conditions. However, under unbalanced load conditions, the instantaneous values of the active/reactive powers of Grid-following unit are influenced by DFOs. The DFOs related to DG2 is directly affected by NSCC of the load. The sudden variations observed in the average powers of Grid-forming unit are a result of step demand variation of the loads. Figure 5(e)-(g) shows the magnitude as well as the instantaneous voltage of PCC bus and filter. They indicate that when the load become unbalanced, the voltage waveform throughout the system is robustly regulated by the presented control structure. The VUF of both the filter and PCC voltage in this case are less than 0.01%. This case study demonstrates that subject to unbalanced load conditions, the control system designed in this paper is stable and robust.

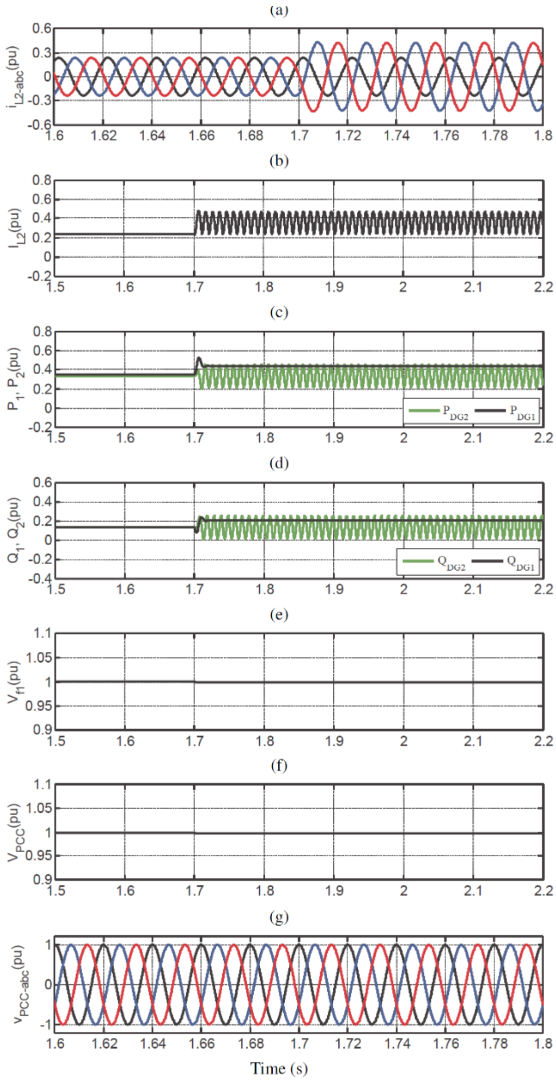


**Figure 5.** Energization of unbalanced Load2: (a) instantaneous load current, (b) load current amplitude, (c) active power component of DG1 and DG2, (d) reactive power component of DG1 and DG2, (e) and (f) amplitude of the PC1 and PCC voltage, and (g) instantaneous voltage of PCC bus.

### *5.3. Unexpected disconnection of Grid-following Unit, under unbalance conditions*

The purpose of this case study is to verify whether the proposed voltage control structure can ensure the stability of the MG following an unexpected disconnection of the Grid-following unit. This outage is considered a large-signal disturbance. The only condition for stability is that the demand of the MG must can be met by the Grid-forming unit. Before the Grid-following unit disconnection, the MG system operates according to the conditions outlined in Subsection 5.2.2. At t = 2 s, the Grid-following unit is disconnected from the MG and the loads of feeder F2 are supplied by the Grid-forming unit. Figure 6(a)-(g) shows the load current magnitude, the instantaneous active/reactive power of the both DG units, a zoomed view of $P_{DG1}$ and $Q_{DG1}$, amplitude of the filter and PCC voltage, and instantaneous value of PCC voltage. Considering these plots, it can be seen that after outage of Grid-following unit, the power generated by the Grid-forming unit is adaptively adjusted so that the absence of generation at PC2 is offset. In addition, despite the mismatched filter resistance and accidental outage of Grid-following unit, even under non-local unbalanced load condition, the proposed voltage controller robustly regulates the voltage waveform of MG with a reasonable transient, as indicated in Figure 6(e)-(g).

## 6. Conclusions

In this paper, a robust control structure is presented for islanded operation of a MG comprises several buses fed by multiple inverter-based DG units. In this proposed control strategy, the Grid-forming/Grid-following structure is utilized. Specifically, an adaptive Backstepping control method is employed to ensure that the voltage magnitude and frequency of the Grid-forming unit closely follow predefined trajectories. This approach aims to enhance stability and reliability in the operation of the multi-bus microgrid. In this paper, an adaptive direct power controller using the IOFL control method is also presented that its purpose is to regulate the active/reactive power supplied by the Grid-following units. The effectiveness of the proposed control scheme is demonstrated through various simulation case studies conducted in the MATLAB/Simulink software. These simulations confirm the robust and stable performance of the control scheme, even in the presence of MG parameter uncertainties, black-start scenarios, unbalanced load energization, and sudden accidental outages of Grid-following units under unbalanced load conditions. The important results of the article are summarized as follows:

- The proposed control scheme is designed based on local measurements and is operated independent from the MG loads characteristics.
- The lumped uncertainties respectively effects on dynamics of voltage as well as power of Grid-forming and Grid-following units, containing disturbances and parameters variations, are compensated by an adaptive estimation method.
- These adaptive terms enhance the system's robustness against measurement errors and modeling inaccuracies.

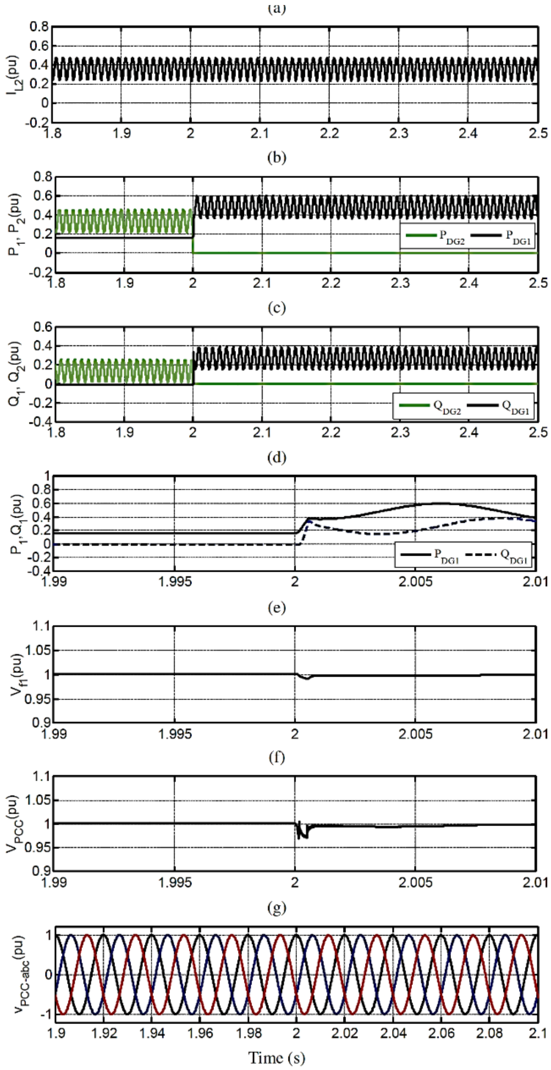


**Figure 6.** Accident outage of Grid-following unit: (a) load current amplitude, (b) active power component of DG1 and DG2, (c) reactive power component of DG1 and DG2, zoomed view of (d) $P_{DG1}$ and $Q_{DG1}$, (e) amplitude of the PC1 voltage, (f) amplitude of PCC bus voltage, and (g) instantaneous voltage of PCC bus.

## References

[1] M. M. Rezaei, and J. Soltani, "Sliding Mode Control of a Grid-Connected Distributed Generation Unit Under Unbalanced Voltage Conditions," *Automatika*, vol. 57, no. 1, pp. 89–98, 2016.

[2] H. Eshghi, J. Soltani, M. M. Rezaei, and S. Shojaeian, "A Robust Control Strategy for a Single-phase Grid-connected Multibus Microgrid Based on Adaptive Sliding Mode Control and Dynamic Phasor Concept," *International Transactions on Electrical Energy Systems*, vol. 31, no. 8, 2021.

[3] M. Sakamoto, and H. Haga, "Control Method for Universal Smart Power Module Considering Wireless Communication," *IEEJ Journal of Industry Applications*, vol. 12, no. 2, pp. 204–214, 2023.

[4] S. Abdalfatah, E. E. El-kholy, and H. Awad, "Power-Sharing in Microgrids by Adaptive Virtual Impedance and Fuzzy Logic," *Engineering Research Journal*, vol. 179, no. 0, pp. 68–74, 2023.

[5] M. K. Behera, and L. C. Saikia, "A Novel Spontaneous Control for Autonomous Microgrid VSC System Using BPF Droop and Improved Hysteresis Band Control Scheme,"

*Electric Power Systems Research*, vol. 220, 109262, 2023.
[6] M. M. Rezaei, and J. Soltani, "A Robust Control Strategy for a Grid-Connected Multi-Bus Microgrid Under Unbalanced Load Conditions," *International Journal of Electrical Power & Energy Systems*, vol. 71, pp. 68–76, 2015.
[7] M. J. Morshed, and A. Fekih, "Design of a chattering-free Integral Terminal Sliding Mode Approach for DFIG-based Wind Energy Systems," *Optimal Control Applications and Methods*, vol. 41, no. 5, pp. 1718–1734, 2020.
[8] S. Harasis, "Controllable Transient Power Sharing of Inverter-Based Droop Controlled Microgrid," *International Journal of Electrical Power & Energy Systems*, vol. 155, 109565, 2024.
[9] H. H. Goh, X. Zhang, et al., "Harmonic Virtual Impedance Control in Islanded Microgrids for Harmonic Power Sharing and Harmonic Suppression," *CSEE Journal of Power and Energy Systems*, 2024.
[10] T. John, and U. Khan, "A Control Architecture for Regulating Voltage and Power Flows in a Networked Microgrid System," *International Transactions on Electrical Energy Systems*, vol. 2024, pp. 1–14, 2024.
[11] E. Rokrok, F. Shavakhi Zavareh, J. Soltani, and M. R. Shakarami, "A Robust Control Strategy for Distributed Generations in Islanded Microgrids," *AUT Journal of Electrical Engineering*, vol. 52, no. 1, pp. 107-120, 2020.
[12] M. Zhang, Y. Han, et al., "Multi-Timescale Modeling and Dynamic Stability Analysis for Sustainable Microgrids: State-Of-The-Art and Perspectives," *Protection and Control of Modern Power Systems*, vol. 9, no. 3, pp. 1–35, 2024.
[13] S. Chen, Y. Sun, et al., "A First-Order PLL-Synchronized Voltage-Supporting Control Method for Parallel Inverters with Near-Zero Line Impedance," *IEEE Transactions on Power Electronics*, vol. 39, no. 8, pp. 9072–9078, 2024.
[14] X. Lin, R. Yu, J. Yu, and H. Wen, "Dual-Frames-Impedance-Based Analysis of Dynamic Phase Difference Effect on Grid-Forming Converter with Different Power Synchronization Controls," *International Journal of Electrical Power & Energy Systems*, vol. 158, 109928, 2024.
[15] L. S. Arunagiri, B. S. Rajpurohit, and A. Jain, "Control of Distribution Static Compensator with Active Damped Inductor-Capacitor-Inductor Filter Using Dual Loop $\alpha\beta$-Frame Current Controllers for Power Quality Improvement," *IET Energy Systems Integration*, vol. 5, no. 2, pp. 128–151, 2022.
[16] W. Pinthurat, B. Hredzak, G. Konstantinou, and J. Fletcher, "Techniques for Compensation of Unbalanced Conditions in LV Distribution Networks with Integrated Renewable Generation: An Overview," *Electric Power Systems Research*, vol. 214, 108932, 2023.
[17] S. A. Yahyaee, P. Sreekumar, and V. Khadkikar, "A Novel Decentralized Unbalance Load Sharing Approach for Islanded Microgrids," *2022 IEEE Industry Applications Society Annual Meeting (IAS)*, pp. 1–7, 2022.
[18] B. Sharma, P. K. Pankaj, et al., "Power Sharing in Three-Level NPC Inverter Based Three-Phase Four-Wire Islanding Microgrids with Unbalanced Loads," *IEEE Access*, vol. 11, pp. 20725–20740, 2023.
[19] M. Dehghani, A. Kavousi-Fard, T. Niknam, and O. Avatefipour, "A Robust Voltage and Current Controller of Parallel Inverters in Smart Island: A Novel Approach," *Energy*, vol. 214, 118879, 2021.
[20] M. J. Hossain, H. R. Pota, M. A. Mahmud, and M. Aldeen, "Robust Control for Power Sharing in Microgrids with Low-Inertia Wind and PV Generators," *IEEE Transactions on Sustainable Energy*, vol. 6, no. 3, pp. 1067–1077, 2015.
[21] B. E. Sedhom, M. M. El-Saadawi, M. A. Elhosseini, M. A. Saeed, and E. E. Abd-Raboh, "A Harmony Search-Based H-Infinity Control Method for Islanded Microgrid," *ISA Transactions*, vol. 99, pp. 252–269, 2020.
[22] M. Shafiee-Rad, Q. Shafiee, M. S. Sadabadi, and M. R. Jahed-Motlagh, "Decentralized Voltage Stabilization and Robust Performance Satisfaction of Islanded Inverter-Interfaced Microgrids," *IEEE Systems Journal*, vol. 15, no. 2, pp. 1893–1904, 2021.
[23] M. Armin, M. Rahman, et al., "Robust Extended $H_\infty$ Control Strategy Using Linear Matrix Inequality Approach for Islanded Microgrid," *IEEE Access*, vol. 8, pp. 135883–135896, 2020.
[24] M. Hamzeh, H. Karimi, and H. Mokhtari, "A New Control Strategy for a Multi-Bus MV Microgrid Under Unbalanced Conditions," *IEEE Transactions on Power Systems*, vol. 27, no. 4, pp. 2225–2232, 2012.
[25] M. M. Rezaei, and J. Soltani, "Robust Control of an Islanded Multi-bus Microgrid Based on Input–output Feedback Linearisation and Sliding Mode Control," *IET Generation, Transmission & Distribution*, vol. 9, no. 15, pp. 2447–2454, 2015.
[26] A. Sotoudeh, and M. Rezaei, "Robust Control of Isolated SCIG-Based WECS Feeding Constant Power Load Using Adaptive Backstepping and Fractional Order PI Methods," *International Journal of Dynamics and Control*, vol. 12, no. 2, pp. 452–462, 2023.
[27] J. J. E. Slotine, and W. Li, "Applied Nonlinear Control," *Englewood Cliffs*, vol. 199, no. 1, p. 705, 1991.
[28] J. A. Suul, A. Luna, P. Rodríguez, and T. Undeland, "Virtual-Flux-Based Voltage-Sensor-Less Power Control for Unbalanced Grid Conditions," *IEEE Transactions on Power Electronics*, vol. 27, no. 9, pp. 4071–4087, 2012.
[29] IEEE P 1159 Working Group, "Recommended Practice for Monitoring Electric Power Quality," *Technical Report*, Draft 5, 1994.

## Declaration of competing interest

The authors declare that they have no known competing financial interests or personal relationships that could have appeared to influence the work reported in this paper. The ethical issues, including plagiarism, informed consent, misconduct, data fabrication and/or falsification, double publication and/or submission, redundancy, have been completely observed by the authors.

## Bibliography

**Mohammad Mahdi Rezaei** received the M.Sc. degree in electrical engineering from Amirkabir University of Technology (Tehran Polytechnic), Tehran, Iran, in 2007, and the Ph.D. degree in electrical engineering from the Science and Research Branch, Islamic Azad University, Tehran, Iran, in 2015. He is currently an Associated Professor in the Department of Electrical and Computer Engineering, Khomeinishahr Branch, Islamic Azad University, Isfahan, Iran. His main areas of research are control of microgrids, distributed generations, and design, optimization and implementation of electrical drives.
**Email:** mm.rezaei@iaukhsh.ac.ir
**ORCID:** 0000-0002-8569-3170
**Contribution Statement:** Conceptualization, Funding acquisition, Investigation, Project administration, Resources, Supervision, Validation, Roles/Writing - original draft, Writing-review & editing.

Journal of Green Energy Research and Innovation

# Modeling and Optimization of The Photovoltaic System Connected to the Grid

**Yaser Ebazadeh, Reza Alayi, Eskandar Jamali Shakarab, Abdolreza Behvandi**

## Highlights

- The study focuses on a photovoltaic system with batteries for distributed generation, adjusting power flow based on the battery charge status to optimize energy use.
- The goal is to absorb the maximum power from the PV system under any temperature and radiation conditions, using part of the energy to charge the battery when needed.
- The research presents a structured design with controllers for efficient energy management, ensuring optimal power extraction from the PV system and effective integration into the grid or local load.

## Graphical Abstract

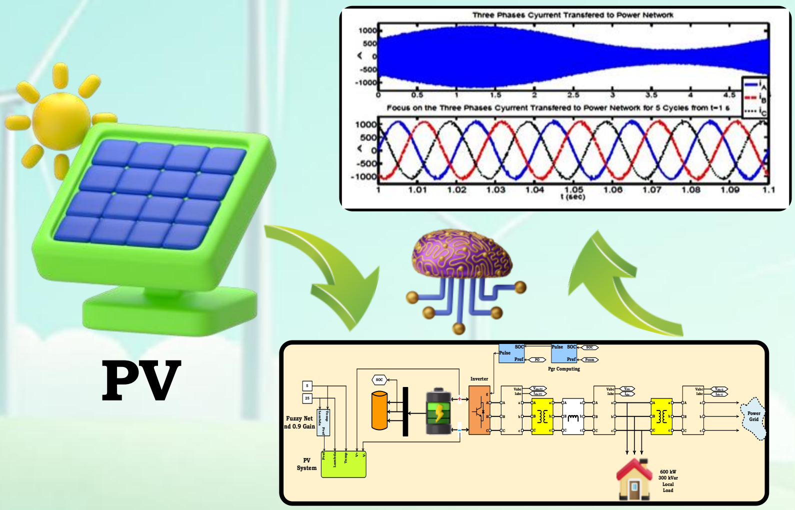


Use your device to scan and read the article online

Citation
Y. Ebazadeh, R. Alayi , E.J. Shakarab, and A. Behvandi, " Modeling and Optimization of The Photovoltaic System Connected to the Grid," *Journal of Green Energy Research and Innovation*, vol. 2, no. 1, pp. 32-43, 2025.

https://doi.org/10.61186/jgeri.2.1.32

JGERI Journal of Green Energy Research and Innovation

Journal of Green Energy Research and Innovation 2.1 (2025) 32-43

Online ISSN: 3041-9018

Journal of Green Energy Research and Innovation

Journal Homepage: www.jgeri.araku.ac.ir

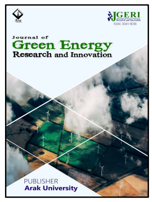


# Modeling and Optimization of The Photovoltaic System Connected to The Grid

Yaser Ebazadeh [1], Reza Alayi [2,*], Eskandar Jamali Shakarab [2], Abdolreza Behvandi [3]

[1] *Department of Computer Engineering, Germi Branch, Islamic Azad University, Germi, Iran.*
[2] *Department of Mechanical Engineering, Germi Branch, Islamic Azad University, Germi, Iran.*
[3] *Department of Electrical Engineering, Ramhormoz Branch, Islamic Azad University, Ramhormoz, Iran.*

A R T I C L E I N F O

*Keywords:*
Photovoltaic,
Controller,
On-grid,
Electrical energy.

*Article History:*
Received: 11 July 2024;
Revised: 20 August 2024;
Accepted: 11 September 2024.

***Article type:***
Research Article

* ***Corresponding author***
*E-mail address:*
reza.alayi@yahoo.com (R. Alaiy)

A B S T R A C T

In recent years, distributed production as a source of local loads and continuous economic exploitation has gathered attention. On this thread, this study focuses on distributed production using a photovoltaic package with batteries so that the power drawn from the distributed generation system for injection into the global network or receiving it is adjusted based on the battery charge status. The goal is to absorb the maximum power received from the photo-voltaic system at any temperature and hypothetical radiation. If the battery charge is not optimal, part of this power is applied to the battery for charging. By presenting a suitable structure, a photovoltaic system with a battery package is presented as a distributed generation source with the design of appropriate controllers. The results showed that at any temperature and radiation, the maximum power received from the photovoltaic system could be estimated. By controlling switching, a converter, the required amount of energy can be obtained from the photovoltaic system. It can be concluded that such a structure, as a desirable distributed generation source, is realized. With the proper design of the necessary controllers, optimal management can be done for power management.

## 1. Introduction

Distributed production as a source of local loads as well as continuous and economic exploitation have been considered by researchers in recent years. For this reason, different structures and several control algorithms have been presented in most different research [1-3]. In some research, the issue of island-building and the recognition of the necessity of island-building to continuously feed the local load has been considered [4-6] in which the island-building problem is investigated when the national network is shut down and the islandization of the distributed generation system is intelligently designed by terminal voltage and network frequency to detect transient errors from the total blackout of the system [7,8]. In the IEEE 929-2000 standard, the islanding conditions of the distributed generation system are described from the national network, but the main issue in observing this standard is the detection of transient errors and disturbances caused by local load changes from the national network blackout [9-11]. A control technique has been introduced to determine the necessity of island-building in which only local and available parameters are measured and remote signals are excluded [12,13]. Also, without the use of telecommunication signals, the connection of the scattered system and the global network is designed using a hybrid technique based on multi-inverter performance [14,15]. In addition, in [16,17] a method for safe detection of island-building based on reactive power flowing under normal conditions and its investigation during sudden changes is presented, and the same method has been carried out in [18] taking into account the power factor and its sudden changes, in which after deciding to island-building, the disconnection order is sent to the switch. In [19,20] considering the moment of a sharp drop in active and reactive power, the island-building problem was analyzed. In 2022 [21] presented a collaborative Optimization of PV Greenhouses and Clean Energy Systems in Rural Areas. The purpose of this research a novel method for optimizing the collaboration between photovoltaic greenhouse load control and rural energy systems. The combined coordination model of agriculture and energy networks is established, and the combined model involves carbon, electrical energy, and thermal energy. Fu et al. [22] have done modeling with the purpose of Stochastic Optimal Planning of Distribution Networks Considering a Dynamic Correlation and Dimension Reduction. Fu et al. [23] presented a statistical machine-learning model for capacitor planning considering uncertainties in photovoltaic power.

The results verify that the proposed model greatly improves planning performance while meeting accuracy requirements. The case study also considers a realistic power distribution system operating under stressed conditions.

This paper discusses the use of distributed production with a photovoltaic system and batteries. The power from this system is adjusted based on the battery charge status when it is either being injected into the global network or received. The goal is to maximize the power received from the photovoltaic system regardless of temperature and radiation levels. If the battery charge is not optimal, some of this power is used to charge the battery. The paper first describes the photovoltaic system model, then designs the necessary controllers. Finally, simulation results are presented to demonstrate the effectiveness of the proposed structure.

## 2. Materials and Methods

### *2.1. Structure description*

The structure introduced in this paper consists of a photovoltaic system connected to a DC/DC converter whose output is connected to a battery package with the appropriate voltage, shown in Figure 1. The output of the converter is connected to a two-level inverter and after connecting to a transformer and a harmonic filter, the local load is fed through a distributed generation system and global network. The distributed generation system is connected to the global network through a distribution transformer and the local load is combined through the distributed generation system and global network. In this structure, two separate controllers are designed as follows:

- Power controller of a photovoltaic system, which absorbs reference and determines power from the photovoltaic system at any given temperature and radiation. This will be done by adjusting the pulse switching of the dc/dc converter, and in fact, the pulse switching controller of the mentioned converter adjusts the power received from the photovoltaic system to its reference value.
- The power controller is exchanged between the distributed generation system and the global network, which is done by adjusting the pulse switching of the inverter connected to the DC/DC converter and adjusting the transmission power of the photovoltaic/battery set to the reference value. It is obvious that when the power transferred from the distributed generation system is less than the power generated by the photovoltaic system, the rest of the absorbed power from the photovoltaic system is applied to the batteries and sets them in charging conditions. When the transmission power is higher, the batteries will supply the rest of the power and will be in a discharged state.

### *2.2. Modeling photovoltaic system*

A photovoltaic system consists of several series/parallel cells as shown in Figure 2 as described in [12, 24-26] on how they are modeled. In modeling the system, a current source whose value depends on the sun's radiation is used and the relationships governing the voltage and current of this system are per Equations (1-4).

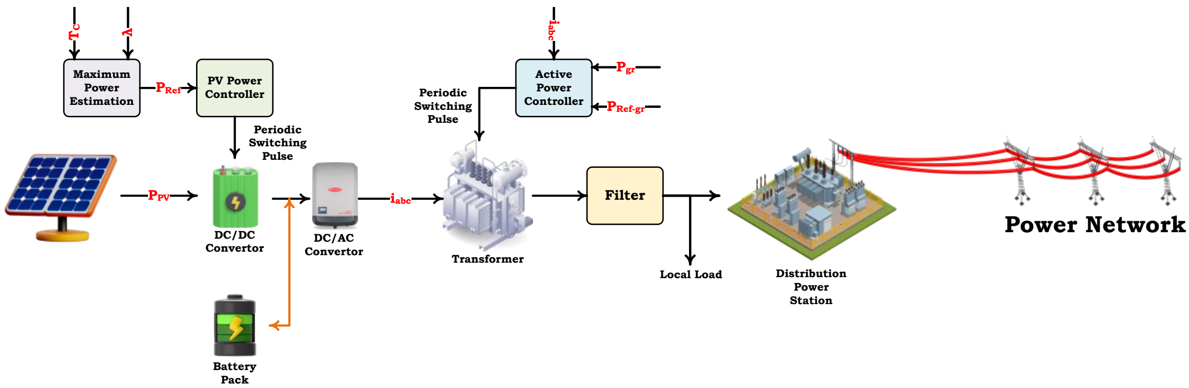


**Figure 1.** Power generation system with battery storage connected to the grid.

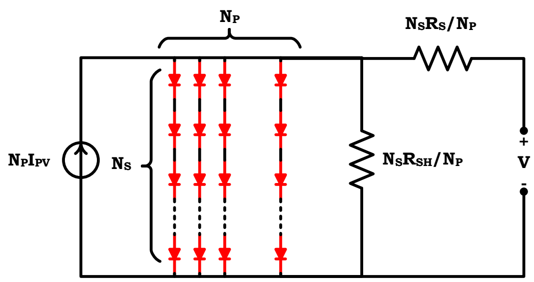


**Figure 2.** Model of the photovoltaic system consisting of series/parallel cells [12].

$$I_{PV} = \left[I_{sc} + K_l\left(T_{PV} - T_{ref}\right)\right], \lambda \tag{1}$$

$$I_{RS} = \frac{I_{sc}}{e^{\frac{q, V_{ec}}{N_s, k, A, T_{PV}}} - 1} \tag{2}$$

$$I_S = I_{RS}\left(\frac{T_{PV}}{T_{ref}}\right)^3 \cdot e^{\frac{q, G, \left(\frac{1}{T_{ref} T_{PV}}\right)}{k, A}} \tag{3}$$

$$I = N_P, I_{PV} - N_P, I_s\left[e^{\frac{q\left(\frac{V}{N_s} + \frac{R_S.I}{N_p}\right)}{k, T_{PV} \cdot A}} - 1\right] - \frac{\frac{N_p V}{N_s} + R_s, I}{R_{sh}} \tag{4}$$

According to the above equations, voltage, current, and therefore the power of the system will depend on the temperature and radiation of the environment. In Figure 3, the sample curves of a photovoltaic system whose parameters are described in Table 1 are drawn from Equations (1-4).

**Table 1.** Parameters of a photovoltaic arrays.

| Parameter | Rate |
|---|---|
| $N_s$ | 1000 |
| $N_p$ | 250 |
| $K_i$ | 0.025 |
| $V_{oc}$ | 1200 × 0.6 = 720 |
| $I_{sc}$ | 300 × 3.6 = 1090 |
| $T_{ref}$ | 25°C |
| $R_{sH}$ | 10000 Ω |
| $R_s$ | 10 μΩ |
| A | 3.3 |

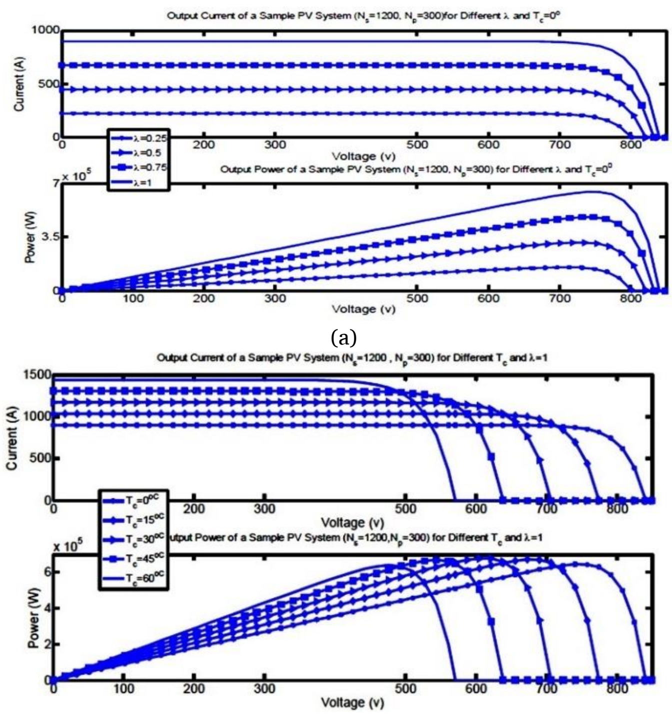


**Figure 3.** Voltage-current curve and power voltage of a sample photovoltaic package at (a) certain temperatures and different radiations, and (b) at different temperatures and certain radiations.

### 2.3. Battery modeling

A well-known battery model is the built-in resistance model [7,8,27,28], where the battery's internal resistance is resisted in charging and discharging modes and fits the charging status. Open circuit voltage is also defined according to the charging state. This model is illustrated and Figure 4 also shows the internal resistance and open-circuit voltage for a sample battery.

Battery charging mode, which is one of the most important control parameters of the system discussed in this paper, can be calculated from Equations (5-7) [7-9]:

$$SoC = \frac{A,h - Ah_{seed}}{A,h} \tag{5}$$

$$Ah_{used} = Ah \times \left(1 - SoC_{(0)}\right) + \int \frac{I_b}{3600} dt \tag{6}$$

$$I_b = \frac{V_{oc} - \sqrt{4R_{int} \cdot P_{el}}}{2R_{int}} \tag{7}$$

In which, $A,h$ and $Ah_{seed}$ are the instantaneous battery clock ampere and clock ampere consumed battery, respectively.

### 2.4. DC/DC and DC/AC inverters

According to the proposed structure of this paper, which is shown in Figure 1, a DC/DC converter is applied to control the absorbed power of the photovoltaic system, which is used through the switching pulse width of this model at a specified switching frequency. Figure 5(a) shows this incremental converter. In Figure 5(b), a two-level inverter used in the structure is shown and its output power will be controlled by switching pulses.

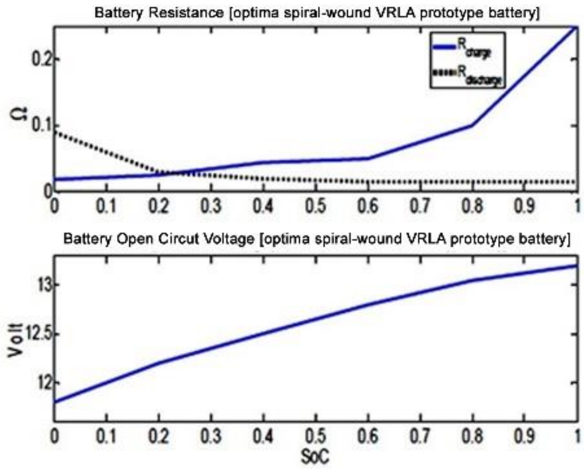


(a)

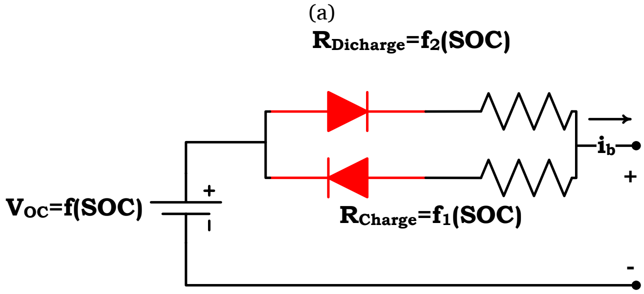


(b)

**Figure 4.** (a) Open circuit voltage and internal resistance of a sample battery, (b) Battery Internal Resistance Model.

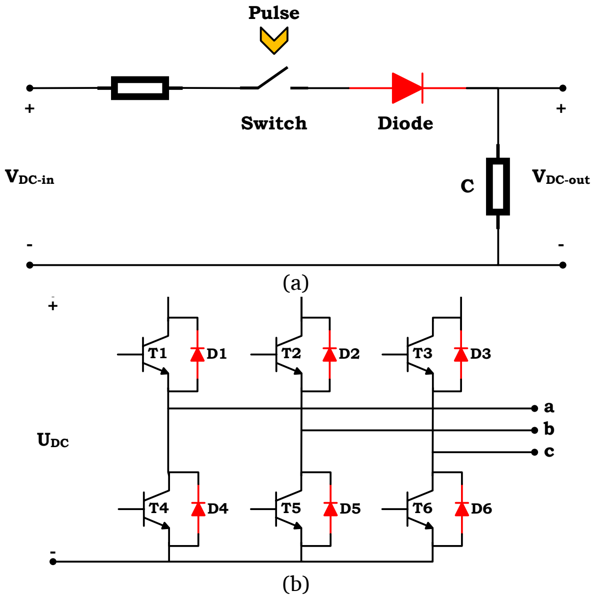


**Figure 5.** (a) Incremental DC/DC converter implemented, and (b) Two-level inverter used in the structure.

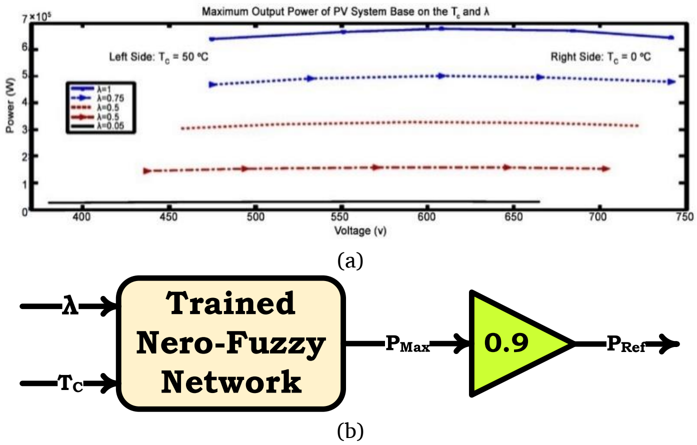


**Figure 6.** (a) Maximum power received from sample systems listed in Table 1 in terms of temperature and radiation, (b) Fuzzy-neural network.

### 2.5. *Estimation of maximum absorbable power from a photovoltaic system*

According to the previous explanations, the maximum absorbable power from the photovoltaic system depends linearly on two parameters temperature and ambient radiation. Therefore, it is necessary to estimate the maximum receivable power for each photovoltaic system with specific parameters. According to the parameters given in Table 1 used for the photovoltaic system in this paper, the maximum power received is obtained according to Figure 6(a). To estimate the maximum absorbable power, Figure 6(a) as data have been applied to a form-matching neural fuzzy network Figure 6(b). The membership functions of this network are considered by dividing radiation and temperature values into 5 different intervals according to Figure 12 and after network training, its fuzzy surface is formed according to Figure 11. To prevent damage to the photovoltaic system, after estimating the maximum power absorbed by the fuzzy neural network, 90% of this power is used as reference power and is applied to the absorbed power controller of the photovoltaic system.

### 2.6. *Design of essential controllers*

It is necessary to design two separate controllers for the whole system, which will be designed as follows.

The absorbed power controller of the photovoltaic system, which should be absorbed from the photovoltaic system at any temperature and radiation, can absorb the reference power determined by the fuzzy neural network. This controller performs power adjustment based on the DC/DC converter switching control described in the following sections.

The transfer power controller to the global network is required to adjust the transmission power to the network by the reference value. This is done by controlling the inverter switching described in the following sections.

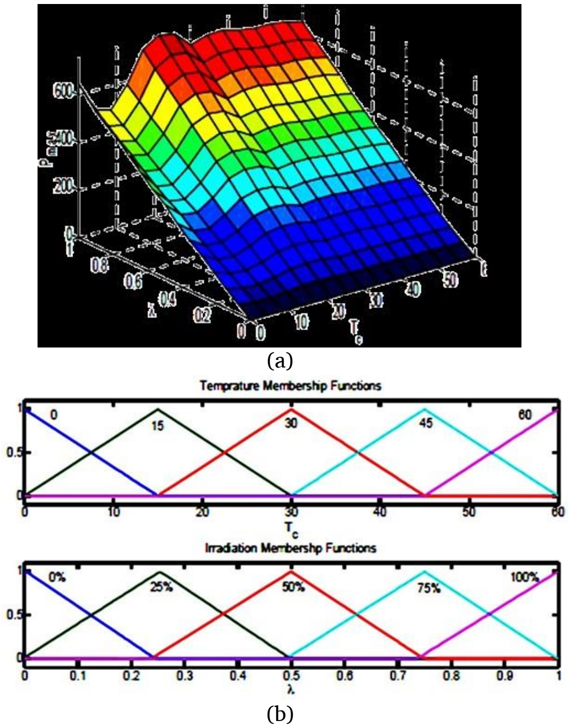


**Figure 7.** (a) Fuzzy surface of the sample fuzzy-neural network, (b) Trained network input membership functions.

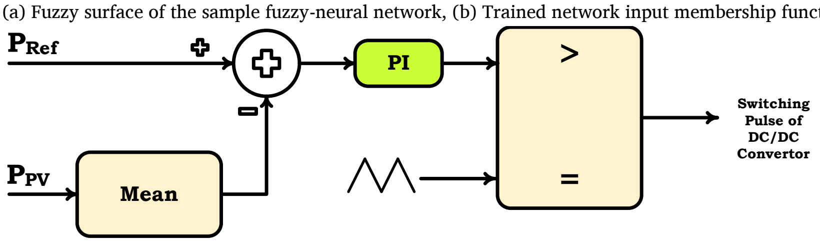


**Figure 8.** Generation procedure of pulse switching DC/DC converter to control the absorbed power of the photovoltaic system.

The transmission power will also be determined from the battery charge mode. This is in such a way that if the battery charging mode is desirable, more powerful than the nominal of the photovoltaic system is transferred to the network, which in this case means provision will be part of the power injected by the batteries. Also, if the battery charging mode is low, the power to the network is less than the available power of the photovoltaic system, which indicates the transfer of part of the power generated by the photovoltaic system to the batteries and causes them to be charged.

### *2.7. Power controller absorbed from a photovoltaic system*

This controller must adjust the power transmitted from the photovoltaic system regarding the reference value generated by the trained fuzzy neural network. For this purpose, at a specified switching frequency, the pulse width of the switching is adjusted according to Figure 8.

### *2.8. Controller transferred to the network*

For this purpose, the output current of the inverter is adjusted after converting to the dq0 frame by switching the controller with mend hysteresis. According to Figure 9, by stabilizing the two components 0 and q, the d component adjusts the current so that the transfer power to the network is equal to its reference value.

Herein, according to the control algorithm, the amount of power reference transferred to the global network should be determined according to the battery charge status, which is applied using a data table as shown in Table 2. $K_p$ is defined as the available power factor of the photovoltaic system and the transfer of power to the network is determined by Equation (8):

$$P_{\text{Ref-Tr}} = K_p, P_{\text{Ref-PV}} \tag{8}$$

## 3. Results

### 3.1. Simulation

The structure shown in Figure 1 is simulated in Simulink/ MATLAB@ environment according to Figure 10 and the parameters related to other parts of the system are under the values listed in Table 3 to 6.
To prove the proposed control performance, different conditions have been analyzed which are discussed in the next section.

### 3.2. Maximum radiation status, maximum charging mode in battery, and variable temperature

In this section, the simulation is performed for a battery with a full charge and maximum radiation ($\lambda = 1$). The ambient temperature is considered a variable temperature according to Figure 11(a). In addition, the temperature changes are considered exaggerated and at a faster rate than the actual state, which is due to the reduction of the simulation time, and, if the response to this situation is desirable, in real conditions that the speed of temperature changes is less, the desired response will surely be achieved.

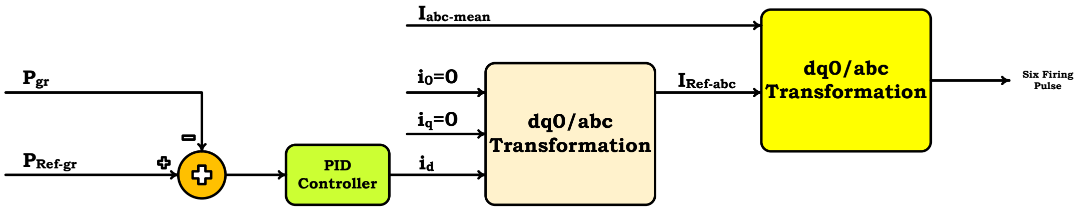


**Figure 9.** Injectable power controller to the network of the distributed generation system.

**Table 2.** Input data for battery charge status [29].

| Soc | 100% | 95% | 90% | 85% | 80% | 75% | 70% |
|---|---|---|---|---|---|---|---|
| Kp | 1.7 | 1.7 | 1.5 | 1.35 | 1.15 | 1 | 0.75 |

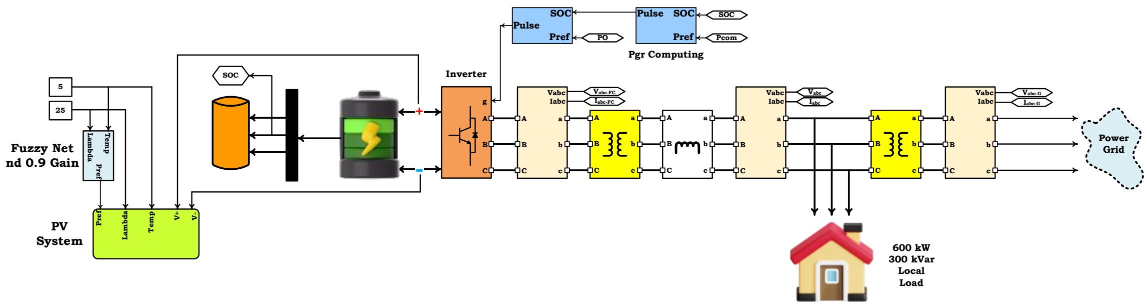


**Figure 10.** Injectable power controller to the network of the distributed generation system.

**Table 3.** Features of implemented batteries.

| Parameter | Quantity |
|---|---|
| Np | 65 |
| A.hCap | 110 |
| Vb | 10 |

**Table 4.** Transformer features connected to inverters.

| Parameter | Quantity |
|---|---|
| N1/N2 | 0.5/0.5 |
| Srate | 1 |
| Lm | 470 |
| Rc | 470 |
| L1 + L2 | 0.025 |
| R1 + R2 | 0.0015 |

**Table 5.** Transformer features connected to the grid.

| Parameter | Quantity |
|---|---|
| N1/N2 | 0.5/0.5 |
| Srate | 1 |
| Lm | 470 |
| Rc | 470 |
| L1 + L2 | 0.025 |
| R1 + R2 | 0.0015 |

**Table 6.** Features of load and overall grid.

| Parameter | Quantity |
|---|---|
| Ssc | 520 |
| V | 30 |
| F | 50 |
| PL | 750 |
| QL | 350 |
| VL | $360 \times 1.08$ |

In Figure 11(a), in addition to ambient temperature, the power drawn from the photovoltaic system ($p_{pv}$), injectable power to the global grid (pπr) as well as the reference power commanded by the controller ($p_{COM}$) are displayed. In Figure 11(b), the voltage and current of the photovoltaic system are displayed, which are changed according to the variable temperature and adjusted by the controller at 90% of its peak value. Since the battery charging status has been favorable, the power transferred to the network exceeds the power drawn from the photovoltaic system, which means that part of the power is generated by the batteries, and conspicuously in these conditions, the battery is discharging conditions. This is specified in the upper part of the Figure 11(c). In addition, the load voltage is also stabilized by the inverter on the value of 1pu as specified in the lower part of Figure 11(c).

### *3.3. Temperature and specified charging mode and different radiation*

In this section, simulation is performed for a certain temperature of 25 °C, charging status of 80% battery, and variable radiation by Figure 12(a) which, due to the reduction of simulation time, radiation changes are considered more than real conditions. According to Figure 12(a), the power transferred to the network is exactly equal to the power absorbed from the photovoltaic system, and in other words, the battery has no involvement in the transmission of power to the network. The lack of power absorption from the battery is due to the resort state that has a battery charge mode and no power is absorbed from the battery. According to these results, it can be concluded that the performance of the controller is accurate, and the transmission power to the network and absorbed from the photovoltaic system is set to the desired and predetermined values. In Figure 12(b), to show the harmonic state of the system and the function of the embedded filter, the current waveform is shown along with a small part of it, and as it is known, the harmonic state of the flowing current is appropriate.

### *3.4. Specified temperatures and radiation and different modes of battery charge*

In this section, simulation is performed for constant temperature and radiation, but different charging conditions have been performed. The injectable active power is shown in the global network in Figure 13(a). It is seen that when the charging situation is better, due to the battery's participation in the injection of active power, more power is transferred to the network. In addition, in Figure 13(b), the battery charging status is shown. Due to this, when the battery is charged more, the battery's discharge is done more quickly. Also, as is evident in the lower part of Figure 13(b), in 70% of the charge, the battery is in charge and the charging mode is incremental.

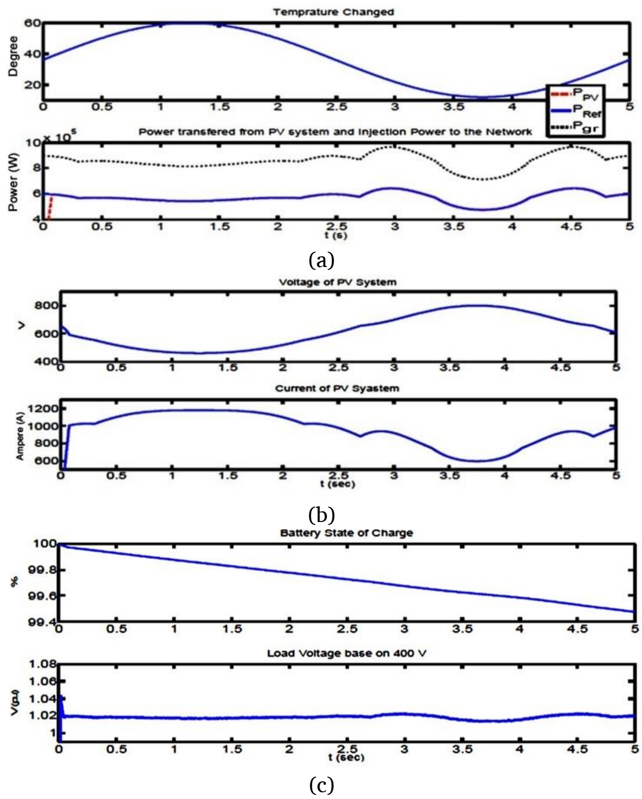


**Figure 11.** Maximum radiation status, maximum charging mode in battery, and variable temperature.

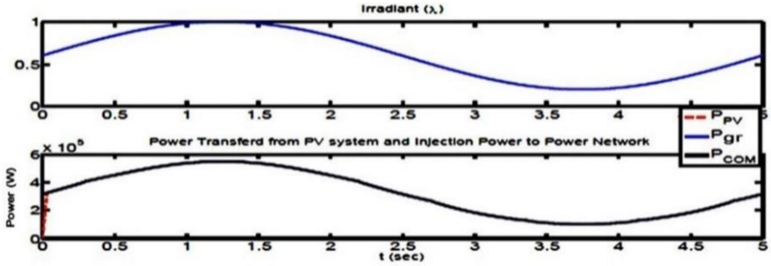


(a)

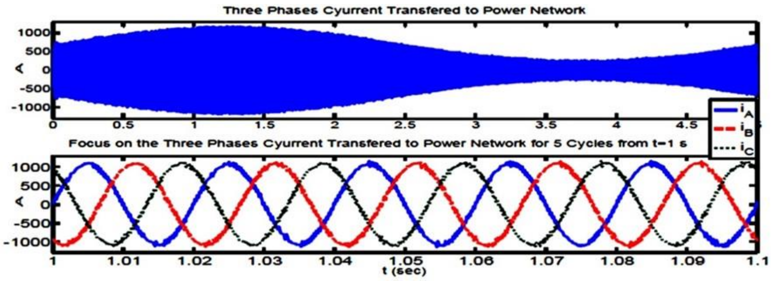


(b)

**Figure 12.** (a) Injectable power to the network and drawn from photovoltaic systems under variable radiation conditions, (b) Current waveform and part of it under variable radiation conditions.

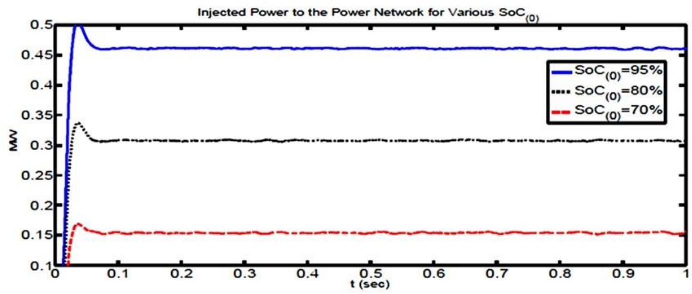


(a)

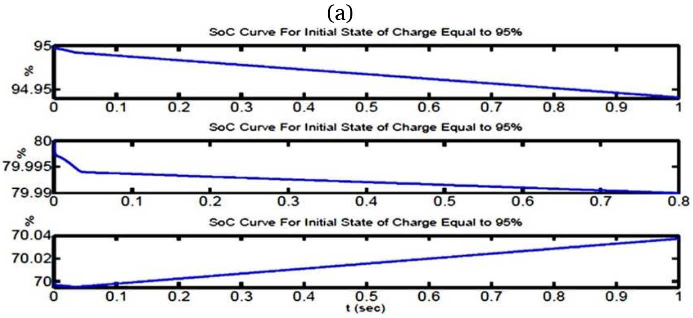


(b)

**Figure 13.** (a) Injectable power to the network in different battery charge situations, (b) Changes in battery charging mode under different battery mode conditions.

## 4. Conclusions

In this paper, by presenting a suitable structure, a photovoltaic system with a battery package is presented as a distributed generation source with the design of appropriate controllers. The results of this paper showed that at any temperature and radiation, the maximum power received from the photovoltaic system can be estimated, and by controlling switching, a converter, the required amount of power can be obtained from the photovoltaic system. On the other hand, by designing another control, and controlling the inverter switching, it managed the power transmitted from the battery set and the photovoltaic system and divided between the two sources of battery and photovoltaic in a way that the battery charge mode always remained in the above-mentioned state. According to the results, it can be concluded that such a structure, as a desirable distributed generation source, is realized, and with the proper design of the necessary controllers, optimal management can be done for power management. To continue the process of studying, it is recommended to provide different structures for controllers for better performance as well as different switching structures of converters to reduce switching losses, or to use multilevel inverters.

## Nomenclature

| | |
|---|---|
| The ideal coefficient related to the photovoltaic cell model | $A$ |
| Current battery (A) | $I_b$ |
| Current source related to photovoltaic system model (A) | $I_{PV}$ |
| Short circuit current in diode used in photovoltaic cell model (A) | $I_{sc}$ |
| Reverse saturation current in diode used in photovoltaic cell model (A) | $I_{RS}$ |
| Boltzmann's constant | $K$ |
| The temperature effect coefficient on the current of the diode used in the photovoltaic cell model | $K_I$ |
| The number of cells in series in the photovoltaic system | $N_s$ |
| Photovoltaic system power (kW) | $P_{PV}$ |
| The power injected from the distributed generation system to the network (kW) | $P_{gr}$ |
| The maximum power available from the photovoltaic system (kW) | $P_{Max\text{-}PV}$ |
| The numerical value of the electron | $q$ |
| The number of parallel cells in the photovoltaic system | $N_P$ |
| The series resistance of each diode in the photovoltaic system (Ω) | $R_s$ |
| The parallel resistance of each diode in the photovoltaic system (Ω) | $R_{sh}$ |
| Internal resistance of the battery model (Ω) | $R_{int}$ |
| The temperature of the environment around the photovoltaic system (°C) | $T_{PV}$ |
| Reference temperature in the photovoltaic system model (°C) | $T_{ref}$ |
| Open circuit voltage in the battery model (V) | $V_{oc}$ |
| Radiation coefficient in the photovoltaic system model | $\lambda$ |
| The intensity of the sun's radiation (W/m²) | $G$ |
| Number of batteries | $N_p$ |
| Capacity of each battery (A.h) | $A.h_{Cap}$ |
| Nominal voltage of each battery (V) | $V_b$ |
| Nominal voltage on both sides (kV) | $N_1/N_2$ |
| Nominal power (MVA) | Srate |
| Magnetization Endoctanus (Pu) | $L_m$ |
| Resistance of core losses (Pu) | $R_c$ |
| Endoctans Dispersion (Pu) | $L_1+L_2$ |
| Resistance of two coils (Pu) | $R_1+R_2$ |
| The magnitude of the short circuit of the grid (MVA) | $S_{sc}$ |
| Nominal voltage (kV) | $V$ |
| Frequency (Hz) | $F$ |
| Local Active Load Power (kW) | $P_L$ |
| Local reactive Load Power (kVAR) | $Q_L$ |
| The nominal voltage of local loads (V) | $V_L$ |

## References


[1] R. Alayi, F. Zishan, et al., "A Sustainable Energy Distribution Configuration for Microgrids Integrated to the National Grid Using Back-To-Back Converters in a Renewable Power System," *Electronics*, vol. 10, no. 15, 1826, 2021.
[2] L. Mehigan, J. Deane, B. Gallachóir, and V. Bertsch, "A Review of the Role of Distributed Generation (DG) in Future Electricity Systems," *Energy*, vol. 163, pp. 822–836, 2018.
[3] P. D. Huy, V. K. Ramachandaramurthy, J. Y. Yong, K. M. Tan, and J. B. Ekanayake, "Optimal Placement, Sizing and Power Factor of Distributed Generation: A Comprehensive Study Spanning From the Planning Stage to the Operation Stage," *Energy*, vol. 195, 117011, 2020.
[4] L. F. Fuentes-Cortés, and A. Flores-Tlacuahuac, "Integration of Distributed Generation Technologies on Sustainable Buildings," *Applied Energy*, vol. 224, pp. 582–601, 2018.
[5] M. Azmy, "Management of Distributed Generation for Smart Buildings," *Advances in Control Techniques for Smart Grid Applications*, pp. 173–199, 2022.
[6] Fleischhacker, H. Auer, G. Lettner, and A. Botterud, "Sharing Solar PV and Energy Storage in Apartment Buildings: Resource Allocation and Pricing," *IEEE Transactions on Smart Grid*, vol. 10, no. 4, pp. 3963–3973, 2019.
[7] F. Wei, Z. Bo, and X. Fuqiang, "Evaluation on Load Restoration of Distribution System Based on Distributed Generation in Smart Buildings After Extreme Disasters," *Power Generation Technology*, vol. 40, no. 5, p. 440, 2019.
[8] A. D. Georgakarakos, M. Mayfield, and E. A. Hathway, "Battery Storage Systems in Smart Grid Optimised Buildings," *Energy Procedia*, vol. 151, pp. 23-30, 2018.
[9] S. M. Mirbagheri, D. Falabretti, and M. Merlo, "Voltage Control in Active Distribution Grids: A Review and a New Set-Up Procedure for Local Control Laws," *2018 International Symposium on Power Electronics, Electrical Drives, Automation and Motion (SPEEDAM)*, pp. 1203–1208, 2018.
[10] R. Alayi, F. Zishan, et al., "Optimal Load Frequency Control of Island Microgrids Via a PID Controller in the Presence of Wind Turbine and PV," *Sustainability*, vol. 13, no. 19, 10728, 2021.
[11] J. Babqi, Z. Yi, and A. H. Etemadi, "Centralized Finite Control Set Model Predictive Control for Multiple Distributed Generator Small-Scale Microgrids," *2017 North American Power Symposium (NAPS)*, pp. 1–5, 2017.

[12] Vukojevic, and S. Lukic, "Microgrid Protection and Control Schemes for Seamless Transition to Island and Grid Synchronization," *IEEE Transactions on Smart Grid*, vol. 11, no. 4, pp. 2845–2855, 2020.
[13] R. Bisht, A. Suresh, and S. Kamalasadan, "Multiple Single Phase Inverters Based Combined Active Power Management and Voltage Regulation of Power Distribution System Based on A Novel Optimal Control Architecture," *2019 North American Power Symposium (NAPS)*, pp. 1–6, 2019.
[14] X. Guo, and W. Chen, "Control of Multiple Power Inverters for More Electronics Power Systems: A Review," *CES Transactions on Electrical Machines and Systems*, vol. 2, no. 3, pp. 255–263, 2018.
[15] K. Naraghipour, K. Ahmed, and C. Booth, "A Comprehensive Review of Islanding Detection Methods for Distribution Systems," *2020 9th International Conference on Renewable Energy Research and Application (ICRERA)*, pp. 428–433, 2020.
[16] R. Sedaghati, and M. R. Shakarami, "A Novel Control Strategy and Power Management of Hybrid PV-FC-SC-Battery Renewable Power System-Based Grid-Connected Microgrid," *Sustainable Cities and Society*, vol. 44, pp. 830–843, 2019.
[17] M. Bajaj, and A. K. Singh, "Grid Integrated Renewable DG Systems: A Review of Power Quality Challenges and State-of-the-art Mitigation Techniques," *International Journal of Energy Research*, vol. 44, no. 1, pp. 26–69, 2019.
[18] S. Kumar, K. K. Mandal, and N. Chakraborty, "Optimal DG Placement by Multi-Objective Opposition Based Chaotic Differential Evolution for Techno-Economic Analysis," *Applied Soft Computing*, vol. 78, pp. 70–83, 2019.
[19] M. N. AlMallahi, M. El Haj Assad, S. AlShihabi, and R. Alayi, "Multi-Criteria Decision-Making Approach for the Selection of Cleaning Method of Solar PV Panels in United Arab Emirates Based on Sustainability Perspective," *International Journal of Low-Carbon Technologies*, vol. 17, pp. 380–393, 2022.
[20] Shaqour, H. Farzaneh, Y. Yoshida, and T. Hinokuma, "Power Control and Simulation of a Building Integrated Stand-Alone Hybrid PV-Wind-Battery System in Kasuga City, Japan," *Energy Reports*, vol. 6, pp. 1528–1544, 2020.
[21] X. Fu, and Y. Zhou, "Collaborative Optimization of PV Greenhouses and Clean Energy Systems in Rural Areas," *IEEE Transactions on Sustainable Energy*, vol. 14, no. 1, pp. 642–656, 2023.
[22] X. Fu, Q. Guo, and H. Sun, "Statistical Machine Learning Model for Stochastic Optimal Planning of Distribution Networks Considering a Dynamic Correlation and Dimension Reduction," *IEEE Transactions on Smart Grid*, vol. 11, no. 4, pp. 2904–2917, 2020.
[23] X. Fu, "Statistical Machine Learning Model for Capacitor Planning Considering Uncertainties in Photovoltaic Power," *Protection and Control of Modern Power Systems*, vol. 7, no. 1, 2022.
[24] R. Alayi, H. Harasii, and H. Pourderogar, "Modeling and Optimization of Photovoltaic Cells with GA Algorithm," *Journal of Robotics and Control (JRC)*, vol. 2, no. 1, 2020.
[25] R. Alayi, A. Sevbitov, M. E. H. Assad, R. Akhmadeev, and M. Kosov, "Investigation of Energy and Economic Parameters of Photovoltaic Cells in Terms of Different Tracking Technologies," *International Journal of Low-Carbon Technologies*, vol. 17, pp. 160–168, 2021.
[26] N. Ganjei, F. Zishan, et al., "Designing and Sensitivity Analysis of an Off-Grid Hybrid Wind-Solar Power Plant with Diesel Generator and Battery Backup for the Rural Area in Iran," *Journal of Engineering*, vol. 2022, pp. 1–14, 2022.
[27] R. Alayi, M. Jahangiri, et al., "Modelling and Reviewing the Reliability and Multi-Objective Optimization of Wind-Turbine System and Photovoltaic Panel with Intelligent Algorithms," *Clean Energy*, vol. 5, no. 4, pp. 713–730, 2021.
[28] M. Jahangiri, F. Karimi Shahmarvandi, and R. Alayi, "Renewable Energy-Based Systems on a Residential Scale in Southern Coastal Areas of Iran: Trigeneration of Heat, Power, and Hydrogen," *Journal of Renewable Energy and Environment*, vol. 8, no. 4, pp. 67-76, 2021.
[29] D. Azuatalam, K. Paridari, et al., "Energy Management of Small-Scale PV-Battery Systems: A Systematic Review Considering Practical Implementation, Computational Requirements, Quality of Input Data and Battery Degradation," *Renewable and Sustainable Energy Reviews*, vol. 112, pp. 555–570, 2019.

## Declaration of competing interest

The authors declare that they have no known competing financial interests or personal relationships that could have appeared to influence the work reported in this paper.

## Bibliography

**Yaser Ebazadeh** received the BS.c. in Computer Science from Tabriz University, Iran in 2004, MS.c. in Computer Engineering from Tabriz Branch, Islamic Azad University, Tabriz, Iran in 2017, and is currently pursuing the full-time Ph.D. degree in Computer Engineering of Qazvin Branch, Islamic Azad University, Qazvin, Iran. His major research interests include the resource management, task scheduling, and security of Cloud and Fog computing.
**Email:** Yaser_ebazadeh@yahoo.com
**ORCID:** 0000-0002-6106-6682
**Contribution Statement:** Data curation, Software, Validation, Visualization.

**Reza Alayi** holds a MSc. and a PhD in energy systems engineering from science and research branch Islamic Azad University (IAU) in Iran. He is leading the "Energy engineering" group the Saveh for Energy institute of higher education. He currently works Assistant Professor at the Department of Mechanical Engineering, Islamic Azad University Germi Branch. Dr. Alayi research is mainly focused energy systems analysis of renewable energy, especially solar energy and energy management in buildings and industry.
**Email:** reza.alayi@yahoo.com
**ORCID:** 0000-0003-2190-1185
**Contribution Statement:** Conceptualization, Project administration, Supervision.

**Eskandar Jamali Shakarab** received the BS.c. in Mechanical Engineering-design of solids from Tabriz University, Iran in 1999, MS.c. in Mechanical Engineering-energy conversion from Tabriz University, Iran in 2005, and Ph.D. degree in Mechanical Engineering-energy conversion of Science & Research Branch, Islamic Azad University, Tehran, Iran in 2024. His major research interests include the Thermodynamics, Renewable energies, Energy optimization in thermal systems, Design of heat exchangers, Design and analysis of power plants, Computational Fluid Dynamics (CFD) and Fluids Mechanic.
**Email:** Jamali917@yahoo.com
**ORCID:** 0000-0003-1193-6552
**Contribution Statement:** Conceptualization, Funding acquisition, Investigation, Project administration, Resources, Supervision, Validation, Roles/Writing - original draft, Writing-review & editing.

**Abdolreza Behvandi** was born in 1987 in Iran. He received his B.Sc., M.Sc., and Ph.D. degrees all in Electrical Engineering (Power Systems) in 2010, 2012, and 2019 from Isfahan University of Technology, Isfahan University, and Shahid Chamran University of Ahvaz, respectively. Currently, he is an Assistant Professor at Department of Electrical Engineering, Ramhormoz Branch, Islamic Azad University, Ramhormoz, Iran. His special interests are power system studies, power system protection, renewable energy, and microgrids.
**Email:** rezabehvandi@gmail.com
**ORCID:** 0000-0002-4879-1994
**Contribution Statement:** Data curation, Formal analysis, Investigation, Resources, Validation.

Journal of Green Energy Research and Innovation

# An Electricity Market Pricing Model Based on Load Demand in a Microgrid Using a Community Peer-To-Peer Approach

Arash Rahimi

## Highlights

- Proposes an energy exchange method and models energy pricing.
- Balances user and microgrid interests using game theory to encourage microgrid participation.
- Accounts for uncertainties in wind and solar energy production, impacting market pricing.
- Assigns fair prices for energy loads based on the unique characteristics and facilities of each microgrid.

## Graphical Abstract

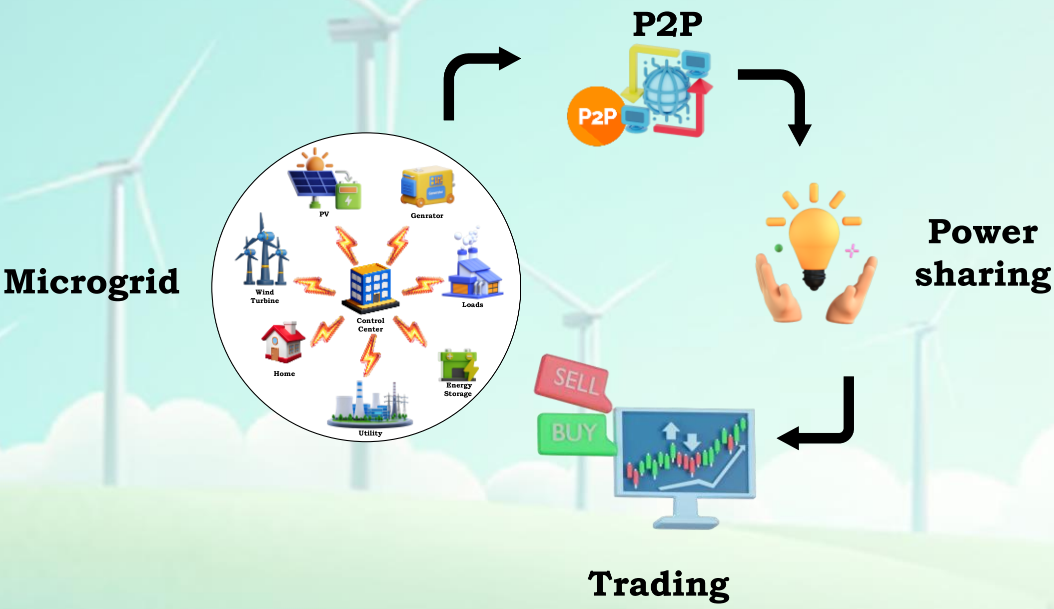


Use your device to scan and read the article online

Citation
A. Rahimi, " An Electricity Market Pricing Model Based on Load Demand in a Microgrid Using a Community Peer-To-Peer Approach," *Journal of Green Energy Research and Innovation*, vol. 2, no. 1, pp. 44-56, 2025.

https://doi.org/10.61186/jgeri.2.1.44

JGERI Journal of Green Energy Research and Innovation

Journal of Green Energy Research and Innovation 2.1 (2025) 44-56

Online ISSN: 3041-9018

Journal of Green Energy Research and Innovation

Journal Homepage: www.jgeri.araku.ac.ir

# An Electricity Market Pricing Model Based on Load Demand in A Microgrid Using a Community Peer-To-Peer Approach

Arash Rahimi *

*Electricity Market Department, Electricity Distribution Company of Khuzestan, Ahvaz, Iran.*

A R T I C L E I N F O

*Keywords:*
Electricity market,
Microgrid,
Peer-to-Peer (P2P),
Energy management,
Demand response.

*Article History:*
Received: 30 May 2024;
Revised: 26 July 2024;
Accepted: 28 July 2024.

***Article type:***
Research Article

* ***Corresponding author***
*E-mail address:*
Arash.rahimi68@gmail.com (A. Rahimi)

A B S T R A C T

In this paper, a new peer-to-peer (P2P) pricing mechanism based on Flexi User and Pool Hub schemes is proposed in a community of buyers using battery storage systems to ensure that all customers in a community enjoy economic benefits. The proposed mechanism does not only consider the power surplus and shortage relationship, but also considers the power grid Real-Time Price (RTP) and Feed-in Tariff (FiT), which reflects the power system demand, where the price is high during peak demand and lower during off-peak. Demand is then implemented by a demand response (DR) program to encourage consumers to manage energy consumption, reduce stress on the power grid, and ensure that energy exchange between peers does not violate grid constraints. Results show that in addition to demand response in the grid, in the Flexi User scenario, the total savings to society from the combination of storage and P2P collaboration lead to a 24.25% reduction in electricity bills compared to a reference case (neither storage nor P2P trading). While the monetary savings in the Pool Hub market is up to 25.53%, this requires more direct P2P trading of distributed energy resources.

## 1. Introduction

Due to the requirements of sustainable development and reducing the emission of environmental pollutants, today's power grids have undergone huge changes and developments to provide a new low-carbon decentralized infrastructure [1]. The use of distributed energy resources, jointly with information and communication technology and energy system management for homes and residential buildings, has forced us to rethink our approach to the operation of the power system. In particular, going down to the lower levels of the network, a new type of agent appears, i.e., sellers, with the ability to produce and consume (and most likely store in the very near future) [2]. Renewable energy, which is also called reversible energy, refers to a type of energy that, unlike non-renewable or fossil energy, has the source of producing that type of energy with the ability to be regenerated in a short period of time by nature [3]. The warming of the earth and the depletion of fossil fuels have caused the electrical energy systems to become new systems and use renewable energy. Over the past ten years, the cumulative global wind energy capacity has increased 6.58 times, from 74 GW in 2006 to 487 GW in 2016, while photovoltaic (PV) power has also increased by 43.14 times from 7.0 GW in 2006 to 302 gigawatts increased in 2016. Therefore, the unique characteristics of renewable and clean energy sources compared to fossil fuels, such as compatibility with the environment and relatively unlimited resources, have caused an increase in the demand for the use of such new energies. So that it is predicted that the use of clean energy will surpass other traditional methods in the coming years [4]. On the other hand, the flexibility of distribution networks is an issue that has been further enhanced by the evolution of these networks from a unidirectional flow of electricity (from large centralized generators) to a system of bidirectional power flow between traditional generators and increasingly small-scale producers. Manufacturers often use distributed energy resources (DER), which are intermittent and allow them to play a more active and dynamic role in electricity consumption and production. In the meantime, electric energy storage devices will play a significant role in increasing the flexibility of the network [5].

Today, vast changes are emerging in power systems. Day by day, the presence of solar resources, wind farms and geothermal resources at the transmission level and small renewable energy sources such as fuel and solar cells at the distribution level is increasing. This presence of renewable resources in distribution systems has created a new structure of networks called microgrids [6].

Microgrids (MGs) are introduced as DER, energy storage systems (ESSs) and a group of controllable and uncontrollable loads. MGs can be used in different modes including grid connection and island mode. By connecting to the grid and taking power from the grid or giving power to the grid, MG plays a key role in adjusting the power balance as well as supply and demand. In stand-alone mode, MG is located away from the grid and customers buy power from MG according to DG offers [7,8]. In Figure 1, a schematic of a microgrid is shown.

One of the new platforms for economic exploitation in microgrids is energy exchange between self-production consumers, which can be peer-to-peer (P2P) with other self-production consumers or with the upstream network. Produced renewable energy can be used for self-consumption, storage or exchange with others [9]. One of the new topics raised in relation to self-production consumers is P2P energy exchange, in such a way that consumers can provide for their required power. They should use the products of self-producing consumers in the network whose energy production is more than their required power consumption [10]. P2P energy exchange is more economical than energy exchange only with the upstream network. In [11], a local electricity market for P2P energy exchange is presented. Consumers self-determine residential generation, generation capacity or consumption capacity to minimize their electricity bills and dependence on the upstream grid. Two types of competition in P2P energy exchange are discussed. First, the competition to determine the appropriate price between the sellers, which is determined according to the solar energy purchase tariff and the energy purchase price from the upstream network, and it should be such that the first choice of the buyers is to buy from the self-produced consumers. The second is the competition between buyers to choose the right seller to make the most economical choice [12]. In general, the research conducted in the field of peer-to-peer approach can be divided into two categories: double auction model [13-17] and analytical model [18-21]. The research conducted using the dual auction (DA) model is such that peers (sellers and buyers) can interact with each other to trade their energy in a step-by-step manner. On the other hand, the researches based on the analytical model are focused on estimating the energy generated from DERs in a local market based on specific rules.

Also, in [22] the concentrates were on the planning of price-based unit commitment (PBUC) managed by Virtual Power Plants (VPPs) over a day. The proposed framework effectively formulates strategies for VPP market production and consumer engagement, particularly with load-shedding capabilities. The research crucially investigates the effects of uncertainties on VPP strategies using probability density functions and the Monte Carlo method. The model proves effective for strategizing VPP market production and consumer interaction in simulations without energy price and demand uncertainties. However, when these uncertainties are included, VPP profits are impacted by market volatility, and increased price and demand fluctuations can significantly alter VPP strategies, occasionally leading to losses.

A P2P energy network can be defined as a network, where network members can share part of their resources (for example, renewable energy and storage space and information) to achieve energy-related goals such as maximizing renewable energy consumption, electricity cost reduction, load modification, network operation reduction and investment cost minimization. Each member can be an energy provider or receiver and communicate directly with the network without any intervention from a third controller. In addition, a new peer can be added to an old peer without changing the operational structure of the system. Today, the presence of the consumer in the load supply chain can play an important role in reducing costs and increasing the stability of the network, and the consumer is in two situations of virtual production and consumption.


**Figure 1.** The general structure of a microgrid [7].

Therefore, by increasing the storage, the load is provided faster. In order to participate in the load in the chain, the demand side resources should be used. Reducing the cost of electricity supply, reducing the cost of electricity consumed by consumers, reducing investment to build new power plants, preserving the environment, improving reliability is a suitable tool for providing system security in emergency situations and reducing blackouts among the benefits of demand side management programs. Demand side management programs are either short-term or long-term. Among these resources, we can mention load response programs. Load response programs are short-term programs whose effects are visible both in the short term and in the long term. In general, load response programs are divided into two main categories: time-based programs and price-based programs [23,24].

The main purpose of this paper is to encourage subscribers to install renewable systems for self-consumption, storage and their participation in electricity markets to earn money by selling excess energy to the upstream grid or other consumers. The participation of consumers in the production side brings many benefits both for the network and for the consumers themselves. Consumers in a smart micro-grid using renewable systems can have on-site production and in addition to supplying the electrical energy, they can also supply the energy of their neighbors and reduce their dependence on the upstream network. The goal is to determine the appropriate energy prices according to the renewable energy purchase tariff by the upstream network and encourage participation in P2P production and energy exchange programs and self-consumption, which ultimately leads to the minimization of self-produced consumer costs. Therefore, the main contributions and novelty of this paper can be stated as follows:

- Providing an energy exchange method and modeling energy pricing
- Considering the benefits of microgrids in addition to the interests of the user, that is, taking into account the interests of the user and microgrids at the same time, using game theory, which encourages microgrids to participate in these projects.
- Considering the uncertainty for the production of wind and solar systems, which causes changes in market pricing.
- Considering different prices for the load being exchanged between each of the microgrids and the operator based on the different characteristics of each microgrid, which makes the prices assigned to the microgrids fairer according to their different facilities.
- The use of energy storage devices along with the transmission network and by determining the optimal planning under the Flexi User and Pool Hub strategies

The structure of this paper is as follows: In section 2, system modeling and problem formulation are discussed. In section 3, the formulation of energy sharing by P2P method is proposed. In section 4, the simulation results are presented, and in section 5, the conclusion will be expressed.

## 2. Problem model

In order to efficiently use renewable resources in the microgrid and improve the performance of P2P trading, we use two distinct local electricity market designs in the producer and consumer communities. Therefore, we use two different systems in using the battery for storage and subsequently we consider the rules for prices, P2P trading and the amount of battery consumption. For this purpose, we consider a set of n consumers who are connected through a local electricity distribution network. In this model, each customer has wind energy production technology or solar panel. The purpose of this market is to minimize the cost of electricity consumption from the transmission network by prioritizing self-sufficiency. This is possible by incentivizing direct P2P trading within the community (marketplace) or using batteries for balancing. Figure 2 schematically shows a community of four houses where a battery storage is either decentralized at the house level (a) or centrally located in the community (b). Also Figure 3, shows the flowchart of proposed model of study.

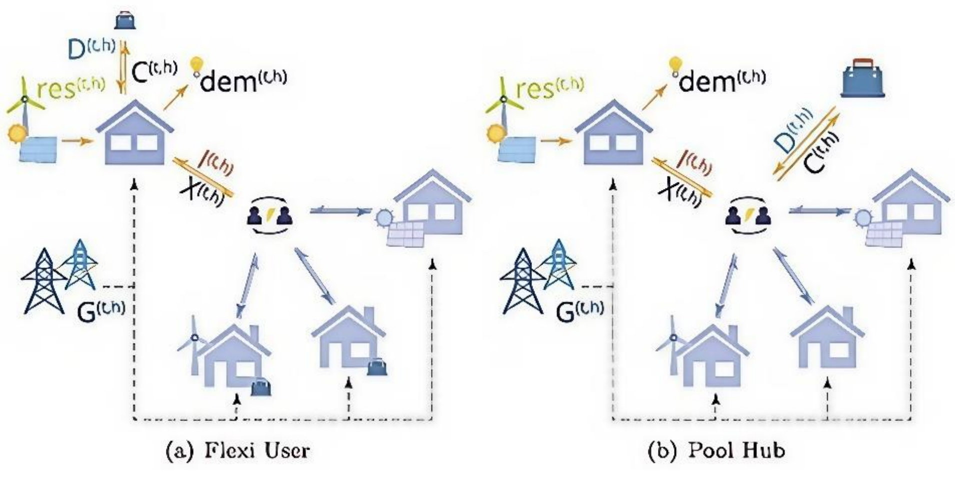


**Figure 2.** Schematic of the proposed problem [2].

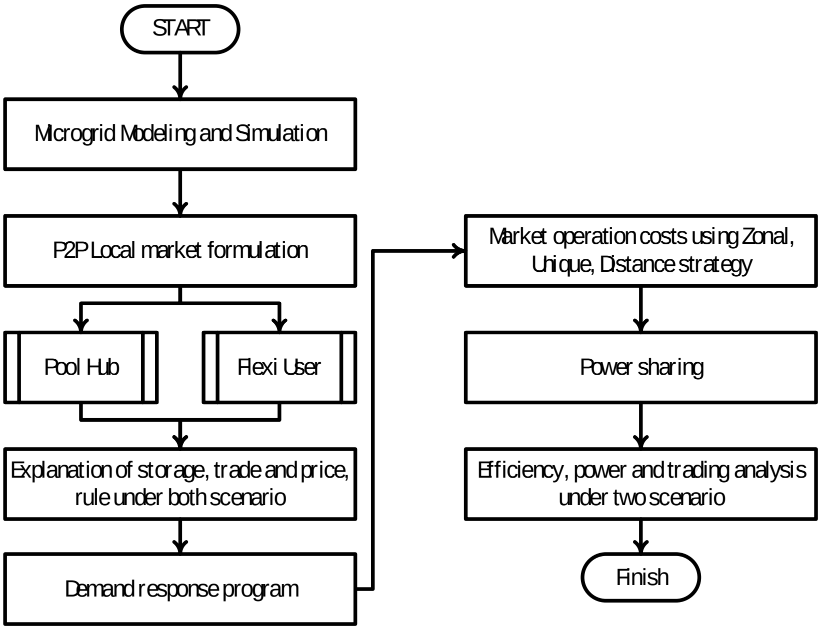


**Figure 3.** The flowchart of proposed model of study.

Designing the market includes determining the rules of market operation and checking its actions. This design lays down rules that aim to ensure the efficient and fair functioning of the market. Hence, to examine the value of storage and P2P trading in a local market, we define and compare trading rules and how to manage storage according to different sets of rules to bring the most benefit to the community. These two separate plans are called Flexi User and Pool Hub in the market [25,26].

As seen in Figure 2, the Flexi User strategy is designed for individual battery configurations at the consumer level; This is while the existing structure in Pool Hub considers a large battery at the community level. For both plans, trading of locally generated electricity within the community is allowed, with the ability to sell excess electricity from renewable energy sources to peers. Each of these two settings gives a specific role to the storage entity, which leads to distinct market design definitions as follows:

**Decentralized storage - Flexi User market:**

This market design imposes rules on system setup with individual batteries. Producers and consumers in a community can dynamically trade locally generated energy at a local P2P price. Private storage is also recharged by DG from producers within the community.

**Centralized storage - Pool Hub Market:**

This market design applies the rules in setting up a system with a common battery. Producers and consumers can trade locally with the same dynamic local P2P pricing as with User Flexi. Unlike User Flexi, there is only one large storage unit that is centrally located and owned by the community. Battery charging can only be done and compensated by renewable energy producers in the community. Battery discharge is available to all - producers and consumers - at a slightly higher charge compensation rate.

In order to create a fair market, these two plans include special rules for prices. To incentivize local trade, introduce a price mechanism for P2P trade in a way that guarantees low electricity prices at the local level. Apart from the main rules in determining the price and accessibility of storage, the battery is allowed to be charged only from DG sources and it is assumed that the producers cannot feed into the grid. On the one hand, the arbitrage potential that can be obtained when changing network consumption using batteries is reduced. On the other hand, this reduction comes with limitations. In addition to the rules related to storage, trading and prices defined in market design, assumptions should also be considered due to the complexity of the model and computational effort. Hence, we assume unlimited supply from the network at any time. Physically, battery degradation and power distribution characteristics such as load current are ignored. DG investment costs are also not included in the calculation model. Although we are aware of the uncertainty in power generation through RES, no certainty is assumed in production or prices.

## 3. Formulation

### *3.1. P2P market-based problem formulation*

The problem model for load distribution between network components using P2P is expressed as follows which directly expresses the limitations of microgrid, according to [27], in the context of a P2P market [2]. Equations (1-9) represent a mathematical model for the problem of load distribution in P2P networks. The model includes an objective function for cost optimization and a set of constraints related to power balance, network limitations, and operational conditions of various network components.

$$\min_{P, p_{n\in\Omega}, \theta_{i\in N}} \sum_{n\in\Omega} f_n(p_n) \tag{1}$$

$$P = -P^T \tag{2}$$

$$p_n = \sum_{m\in\omega_n} p_{nm} \qquad n\in\Omega \tag{3}$$

$$\underline{p_n} \le p_n \le \overline{p_n} \qquad n\in\Omega \tag{4}$$

$$p_{nm} \ge 0 \qquad n\in\Omega_g \tag{5}$$

$$p_{nm} \le 0 \qquad n\in\Omega_c \tag{6}$$

$$\underline{p_n} \le p_{nm} \le \overline{p_n} \qquad n\in\Omega_p \tag{7}$$

$\omega_n$

$p_n = \sum_{m\in\omega_n} p_{nm}$

$p_{nm} = 0$

$$q_{ij} = Y_{ij}(\theta_j - \theta_i) \le C_{ij} \qquad (i,j)\in L \tag{8}$$

$$\sum_{n\in N_i} p_n = \sum_{(i,j)\in L} q_{ij} \qquad i\in N \tag{9}$$

In the proposed network, the entry of electric lines *L*, which $Y_{ij}$ is mentioned for the connecting node of line *i* and *j*. It is classically assumed to be driven by their inductance in the presence of pure sinusoidal voltage and current. This assumption leads to real power currents $q_{ij}$ is proportional to the voltage angle difference, which $\theta_i$ at node i, is noted between the two ends of the line as in Equation (8). To prevent any damage to the transmission lines, their flow is limited by thermal limits related to the heat they can dissipate. In addition, a power balance Equation (9) must be maintained at each node *N* of the network between the line currents and the power injection of the agents connected to it, so $N_i$ at node *i*.

The objective of the P2P market, $\Omega$, with size of $N_\Omega$, is to minimize the total cost, which sums all the individual cost functions as in Equation (1). To minimize the cost function $f_n$, agent (customer) *n* can optimize its transaction volume $p_n$ within the flexibility range defined by a lower $\underline{p_n}$ and an upper bound $\overline{p_n}$, as expressed in Equation (4-7). If agent *n* sells electricity, the value of the transaction is positive and when buying, it becomes negative. Considering multilateral transactions requires the division of net powers, according to [28], into a set of multiple bilateral transactions $p_{nm}$. Every possible bilateral power trade within the market can be condensed into a matrix *P* such that in Equation (10):

$$P = \begin{pmatrix} p_{11} & \cdots & p_1 N_\Omega \\ \vdots & \ddots & \vdots \\ pN_\Omega 1 & \cdots & pN_\Omega N_\Omega \end{pmatrix} \tag{10}$$

It is necessarily $p_{nm}$ equal to zero if *m* in the business partnership set is not representative of *n* in the set $\omega_n$. Then the net power $p_n = \sum_{m\in\omega_n} p_{nm}$ is obtained as in Equation (3). As seen in Equation (2), *P* is symmetric to guarantee the power balance of each transaction, so $p_{nm} = 0$. This allows prices to potentially be customized in each equation.

### *3.2. P2P energy sharing mechanism*

The P2P energy exchange mechanism is designed to motivate residents to participate in the energy market. Accordingly, in this paper, a new P2P pricing mechanism is presented to ensure all customers that they will enjoy more economic benefits, unlike the traditional electricity market. The proposed pricing mechanism can be applied to any P2P energy sharing model. The proposed mechanism does not only consider the power surplus and shortage relationship, but also considers the power grid RTP and FiT, which reflects the power system demand, where the price is high during peak demand and lower during off-peak. A Demand Response (DR) program is then implemented to encourage consumers to manage energy consumption, reduce stress on the power grid, and ensure that energy exchanges between peers do not violate grid constraints. Accordingly, for each time period, the total surplus energy to the P2P market that is imported by n customers is equal to Equation (11):

$$E_S(t) = \sum_{i=1}^{n} E^i_{surplus}(t), \ \forall t\in[0,T] \tag{11}$$

Also, the lack of energy purchased by customers is also defined as follows in Equation (12):

$$E_D(t) = \sum_{i=1}^{m} E^i_{deficiency}(t), \ \forall t\in[0,T] \tag{12}$$

Since P2P prices depend on the relationship between the shortage and surplus of energy to be traded in the P2P market, this measure is defined by the ratio $\alpha$ as follows in Equation (13):

$$\alpha = \frac{E_D - E_S}{E_D + E_S} \quad , \alpha \in [-1,1] \tag{13}$$

When $\alpha = 0$, excess energy is equal to deficiency ($E_S(t) = E_D(t)$). Also, when $\alpha \approx -1$, there is no shortage ($E_D(t) = 0$)or the surplus is much greater than the shortage ($E_S(t) \gg E_D(t)$). Also, when $\alpha \approx 1$ there is no excess energy ($E_S(t) = 0$) or the excess is much smaller than the deficiency ($E_S(t) \ll E_D(t)$).

In the proposed model, according to the reality of electricity consumption, the energy price of the main grid fluctuates during the day. Demand is higher in peak periods and lower in off-peak periods, which affects domestic P2P prices. Therefore, the relationship between import price and FiT can be expressed as Equation (14):

$$\beta = \frac{r_{ex}}{r_{ex} + r_g} \quad , r_{ex} < r_g \tag{14}$$

In this equation, $r_g$ is equal to RTP of the main network and $r_{ex}$ is equal to FiT. Therefore, the P2P market price is calculated according to the values ($\alpha$) and ($\beta$)as Equation (15-16) [1]:

$$r_b = \begin{cases} \left(\frac{r_g - r_{ex}}{2}\right)\frac{(2-\beta)e^{2\alpha} + \beta e^{-2\alpha}}{e^{2\alpha} + e^{-2\alpha}} + r_{ex} & , \alpha \geq 0 \\ \left(\frac{r_g - r_{ex}}{2}\right)\frac{(1+\beta)e^{2\alpha} + (1-\beta)e^{-2\alpha}}{e^{2\alpha} + e^{-2\alpha}} + r_{ex} & , \alpha < 0 \\ r_g & , E_s(t) = 0 \end{cases} \tag{15}$$

$$r_s = \begin{cases} \left(\frac{r_g - r_{ex}}{2}\right)\frac{(1+\beta)e^{2\alpha} + (1-\beta)e^{-2\alpha}}{e^{2\alpha} + e^{-2\alpha}} + r_{ex} & , \alpha \geq 0 \\ \left(\frac{r_g - r_{ex}}{2}\right)\frac{(2-\beta)e^{2\alpha} + (\beta)e^{-2\alpha}}{e^{2\alpha} + e^{-2\alpha}} + r_{ex} & , \alpha < 0 \\ r_{ex} & , E_D(t) = 0 \end{cases} \tag{16}$$

### 3.3. Problem formulation

To model the characteristics of local business interactions, we focus on the interaction of four main operational supply-demand decisions:

- Consumers/vendors demand electricity from the main grid
- Vendors use their own distributed resources
- P2P trading takes place within the community
- Battery storage is balanced

Hence, a community of producers (sellers) and consumers face business decisions based mainly on RES surplus power, battery flexibility, network and commercial prices. Therefore, using a multi-period linear programming model, these decisions are optimized in half-hour intervals (t) in a time horizon. The objective function includes electricity costs for the entire community and is subject to supply, battery, and trade constraints.

In this model, houses ($h \in H$) have diversity in demand and production profiles. Every house needs to balance supply and demand. This means that supply from renewable resources $res^{(t,h)}$, network consumption $G^{(i,h)}$, battery discharge $D^{(i,h)}$ and direct P2P purchase means $I^{(i,h)}$ must be combined with the sum of demand $dem^{(i,h)}$, battery charge $C^{(i,h)}$ and P2P sales i.e. $X^{(i,h)}$ for each house $h \in H$ in Each time step $t \in T$ is considered. In short, based on Equation (17), more supply than demand is considered [29]:

$$\begin{aligned} &RES + Grid + Battery\ discharge + P2P\ \ purchase \geq \\ &Demand + Battery\ \ charge + P2P\ \ sale \\ &res^{(t,h)} + G^{(t,h)} + D^{(t,h)} + I^{(t,h)} \geq dem^{(t,h)} + C^{(t,h)} + X^{(t,h)} \end{aligned} \tag{17}$$

**- Specific market restrictions:**

The battery decisions and objective functions of these two different schemes assume distinct rules for the availability, capacity, and pricing of storage in the community. Therefore, the models of each scheme optimize slightly different objectives under different constraints for the storage entity. For all considered models, the general objective is to minimize the cost subject to supply-demand, P2P trading and various storage constraints [29].

**- Flexi User scenario**

In the User Flexi market with decentralized storage, costs are incurred when a customer buys from the network or buys from a peer. However, in P2P trading, the selling peer earns money, thereby reducing electricity costs for the entire community. Since an amount is paid by one person and an amount is received by another person, we exclude these conditions from optimization.

Therefore, the objective function for this case, which minimizes the total consumption costs of the network $G^{(t,h)}$, is equal to Equation (18) [29]:

$$\min \sum_{h} \sum_{t}^{\text{Grid consumption}} [p_G^{(t)} . G^{(t,h)}] \tag{18}$$

Minimizing the cost of this model depends on the balance of supply and demand, i.e. Equation (17), commercial constraints Equations (19-22), and the constraint for private batteries. Based on this, the community is continuously designed to allow producers to communicate directly with their peers. Active trading must follow certain rules. The total amount of sales $X^{(t,h)}$ for each house h ∈ H as the sum of electric currents $X_p^{(t,h\to p)}$ from this house h ∈ H to its counterparts p ∈ H, as Equation (19) is defined as [29]:

$$X^{(t,h)} = \sum_{p \neq h} X_p^{(t,h\to p)} \tag{19}$$

Where

$$I_p^{(t,h\to p)} = \psi^{P2P} . X_p^{(t,p\to h)}) \quad \forall p \neq h \tag{20}$$

The change in flow direction indicates the purchase of $I_p^{(t,h\leftarrow p)}$ of a house h ∈ H from its counterpart p ∈ H. The total amount purchased in each house, $I^{(t,h)}$ is defined by Equation (21) [29]:

$$I_p^{(t,h)} = \sum_{p \neq h} I_p^{(t,h\leftarrow p)} \tag{21}$$

Since no grid input is considered, the amount of energy sold and purchased can only remain in the community. The total sales in all houses must be equal to the purchases of that house, which is expressed as Equation (22) [28]:

$$\sum_{h} \psi^{P2P} . X^{(t,h)} = \sum_{h} I^{(t,h)} \quad \forall t \in T \tag{22}$$

Private batteries form the basis of certain physical characteristics. The lower limit s and the upper limit s of the storage level $S^{(t,h)}$ in each battery are limited according to Equation (23) [29]:

$$\underline{s} \leq S^{(t,h)} \leq \bar{s} \tag{23}$$

The charging and discharging of the battery are limited to a certain amount of α and β, respectively. These rates are shown mathematically in Equations (24,25) [29]:

$$0 \leq C^{(t,h)} \leq \alpha \tag{24}$$

$$0 \leq D^{(t,h)} \leq \beta \tag{25}$$

The total storage level of the battery in a time step t is determined by Equation (26) with charge $C^{(t,h)}$ and discharge $D^{(t,h)}$. This period depends on the efficiency coefficients $\eta^c$ and $\eta^d$.

$$S^{(t,h)} = S^{(t-1,h)} + \eta^c . C^{(t,h)} - (1-\eta^d) . D^{(t,h)} \tag{26}$$

**- Pool Hub scenario**

In the Pool Hub scenario with a centralized storage, the total cost in the cost vector is three components: network consumption, P2P trading and centralized battery drain. In addition, we deduct the fees charged to customers and consider their income from P2P trading. Hence the Pool Hub objective function, Equation (27), requires two additional components that add the battery discharge costs $D^{(t,h)}$ and the charge compensation $C^{(t,h)}$ [29].

$$\min \sum_{h} (\sum_{t} [p_G^{(t)} . G^{(t,h)}] + \sum_{t} [p_D^{(t)} . D^{(t,h)}] - \sum_{t} [p_C^{(t)} . C^{(t,h)}]) \tag{27}$$

The large battery is limited to the physical constraints formulated in Equations (23-25) with constants $\underline{s}$ ،$\bar{s}$ ،$\alpha$ ،$\beta$ ،$\eta^c$ and $\eta^d$ for a more centralized storage entity. The total storage level will not depend on the charging or discharging of a house, but will take into account the total current from the battery to the houses. Equation (28) includes the amount of discharge $D^{(t,h)}$ and charge $C^{(t,h)}$ of the concentrated battery and adds these to the total storage level $S^{(t)}$ [29]:

$$S^{(t)} = S^{(t-1)} + \eta^c . \sum_{h} C^{(t,h)} - (1-\eta^d) . \sum_{h} D^{(t,h)}, \; \forall t \in T \tag{28}$$

### 3.4. Case study

In order to implement the proposed method, we use a case study that includes the basic information of the problem. The case study is a 500-unit residential complex in Italy with a total volume of 230,000 cubic meters, the energy supply of its facilities and equipment throughout the year is specifically provided by the grid. In these buildings, a number of houses are equipped with solar panels, in addition to this, the possibility of storing energy in batteries (due to their capacity and erosiveness) is also available for subscribers. Also, digital technologies and smart grids are assumed to be installed and capable of P2P trading. The main energy supply system in this complex is CHP. The generating unit (CGU) consists of an internal combustion engine (ICE) that is fueled by natural gas. These engines are the most common prime movers for medium-scale (100-5000 kW) CHP applications [30].

The nominal electrical power capacities considered for this motor (Pcgu) are from 600 kW to 1600 kW, with discrete intervals of

100 kW. Therefore, the lower power capacity is equal to 50% of the nominal power capacity and the load efficiency is considered according to the Equations (29,30):

$$\eta_{E,CGU} = \eta_{E,CGU,nom}\left(1.126L - 0.126\right) \quad (29)$$

$$\eta_{H,CGU} = \eta_{Q,cguCGU,nom}\left(0.8253L + 0.1747\right) \quad (30)$$

The load factor is defined as $L = F_{CGU} \cdot \eta_{E.CGU,nom} / P_{CGU}$. Also, nominal efficiency and heat rate to power of CGU are given in Table 1.

The investment cost of combustion units is significantly affected by the "scale effect". For this reason, the cost relationship of CGU according to its size is considered as Equation (31):

$$C_{TI,CGU} = 15460 P_{CGU}^{0.7247} \quad (31)$$

where $C_{TI,CGU}$ should be in Euros and power ($P_{cgu}$) in kilowatts.

As stated above, hourly average values are adopted to represent energy load demand. Figure 4 shows the load length curves of electrical and thermal demands of the residential complex. This data is obtained from 12 typical days, corresponding to 4 typical weeks. For each week, representing seasonal weather periods, one weekday and two weekend days (Saturday and Sunday) are considered. It is necessary to explain that the residential complex in this simulation plays the role of supplying energy and ancillary services. Therefore, by using new technologies such as blockchain, which are based on P2P behavior in the electricity market, it is possible to reduce the annual energy costs in addition to providing the amount of load required for supply to customers. From this roof, the uncertainty in the annual energy load demand is considered through normal distributions. Therefore, 20% relative standard deviation is used for both electrical and thermal requirements. Such a value corresponds to 8 consecutive years of energy demand data measured in the tested residential complex.

As mentioned, the use of energy storage devices along with the transmission network and by determining the optimal planning in both Flexi User and Pool Hub scenarios is an innovation of this research. In the following, the results of this issue will be examined.

## 4. Results

Simulation results for all CGU sizes and operational strategies are shown in this section. 10,000 iterations were performed for each combination of design configuration and operational strategy, so that reliable results and limited uncertainty in the output indicators can be obtained. On the other hand, in Table 2, the specifications of the electrical energy storage system are presented in order to receive renewable energy, store it, and sell it to the grid (interaction with the grid).

**Table 1.** Main specifications of the production unit.

| Parameter | Value |
|---|---|
| $\eta_{E,CGU,nom}$ | 38.5% |
| $\eta_{Q,CGU,nom}$ | 34.4 % |
| $HPR_{nom}$ | 0.894 |
| CGU Design Lifetime | 20 years |
| Nominal power of natural gas boiler | $\eta_{boi} = 0.9$ |
| Fuel cost per unit of thermal energy | $c_F = 0.04\ €/kWh$ |
| Price of buying and selling electricity based on P2P transactions | $c_{PEG} = 0.15€/kWh$<br>$c_{SEG} = 0.05\ €/kWh$ |

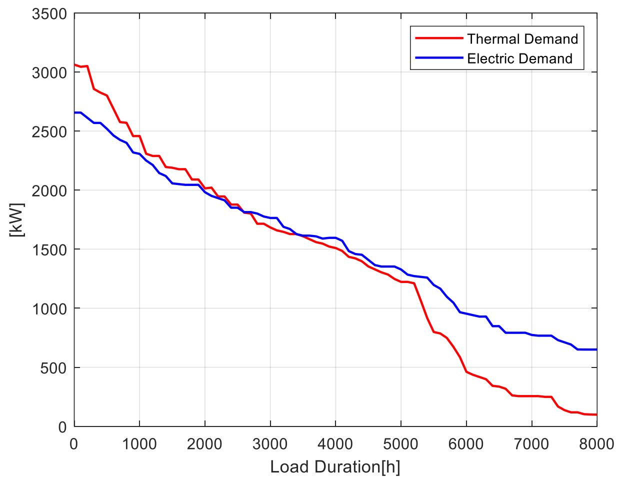


**Figure 4.** Length curve of electrical and thermal demand.

**Table 2.** Specifications of electric energy storage devices.

| Parameter | Value |
|---|---|
| Capacity | 100 Kw.h |
| Charging power | 50 Kw |
| Discharging power | 50 kw |
| Charging efficiency | 0.85 % |
| Discharging efficiency | 0.85 % |

In the following, we have presented the model's supply and demand decisions on how to cover each of the sample houses (customers) on a day in spring. In this simulation, the following are observed:

- Interaction and storage reduce network consumption
- P2P transactions allow the community to cover all demand through renewable energy sources for many parts of the day.
- Storage covers a large share of demand, especially at peak times

This spring sample day shows how P2P trading and energy storage are used by the community to cover their demand. A pure consumer (House 1) covers the demand mainly with P2P purchases due to the exploitation of cheaper local P2P prices. Figures 5 and 6 show the problem results for both Flexi User and Flexi User scenarios, respectively. Pool Hub is presented in the first house and in terms of using all three conditions of PV, Wind and Battery in interaction with the grid. In economics, a graph of supply and demand serves as an instrument to comprehend the correlation between the amount of a product that sellers are willing to offer and the volume that buyers intend to purchase. This concept is rooted in the principle of supply and demand, which posits that the cost of a product or service will recalibrate until the demanded quantity aligns with the supplied quantity. Figures 5, and 6 illustrates the consumption sources for the houses exemplified, captured on a typical spring day under two mentioned scenarios. The following observations can be made:

- A significant portion of the demand in the Pool Hub market is met through interaction and storage.
- Prosumers exhibit a tendency to deplete the battery at varying times.
- Consumption from the grid during peak hours is substantially reduced and rescheduled to late night or early morning.
- During the evening peak, the house utilizes the battery or DG to evade high grid prices. On the selected day, which sees substantial wind-generated electricity, house 1 has the opportunity to sell and recharge the battery at high compensations during the morning and evening, and deplete it at low rates during the day. The consumer largely meets its demand through P2P purchases and draws from the grid during times of high demand and low generation. It is only during periods of intense demand that it becomes necessary to draw from the grid at the highest rate.

The two suggested market models, Flexi User and Pool Hub, integrate market regulations concerning prices, P2P transactions, and battery utilization. The variation in rules originates from the difference in ownership of the deployed battery storage. The enforcement of these rules encourages the use of different market features (battery storage or direct P2P trade) within their configurations. Consequently, the supply-demand decisions of the community vary among the cases examined. Figures 5, and 6 display the average source of supply for the exemplified community over a single day, considering the total time span of nine months. Under the Flexi User market rules, the community predominantly consumes directly from the renewable sources during the day, and employs the storage in the evening to decrease grid consumption (Figure 5). The regulations of a Pool Hub market design result in slightly different supply-demand decisions (Figure 6). The community consistently discharges a minor amount of electricity from the centralized battery during the day and a marginally larger share in the evening. This subsequently leads to a higher demand for grid consumption in the evening. The direct consumption from renewable generation is more substantial during the day as P2P trade is also extensively utilized.

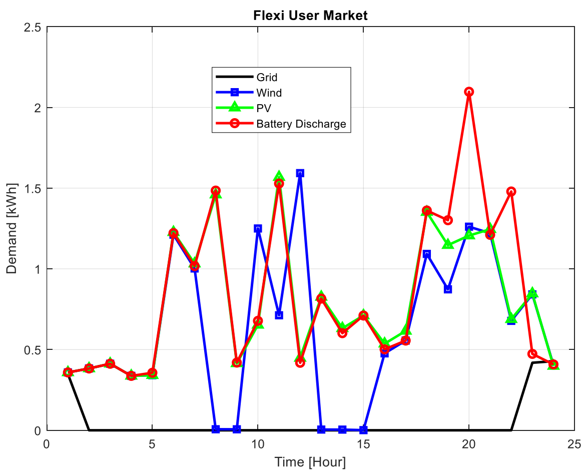


**Figure 5.** Demand supply graph for house 1 on a spring day in the Flexi User market.

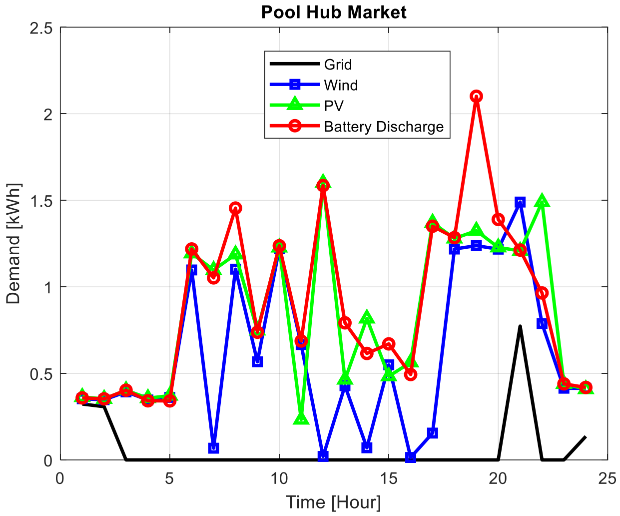


**Figure 6.** Demand supply graph for House 1 on a spring day in the Pool Hub market.

All producers can use their own production and store surplus electricity for later use. Offloading power from the grid is only necessary during the evening peak when local power generation, particularly from the PV source, is relatively low or absent. At night, when prices are low, buyers also cover the demand by consuming from the grid and use their own production to charge the battery. Since the selected day provides a good supply of wind, it can be seen that House 1 has met a major part of the demand in the community. The generation from DG will vary between seasons, thereby greatly affecting storage utilization, as charging is assumed to be possible only from local DG.

Figures 7 and 8 also show typical examples of how the simulated energy system works and the detailed outputs of the simulations by considering energy storage devices in planning the load demand in the studied residential complex. Figure 7 shows the electricity demand in 72 consecutive hours. Figure 8 also shows the same type of result for thermal demand. As we can see in Figure 7, the demand fluctuates significantly, reaching peaks that align with the CGU production at several points, suggesting moments when production meets demand. CGU production also shows fluctuations but maintains a level close to the peaks of the blue line, indicating a correlation between demand and CGU production capacity. In other hands, the energy purchased by the grid has smaller peaks compared to the other lines, showing less frequent and lower quantity purchases from the grid. Also, the energy sold to grid has even smaller peaks than the red one, indicating infrequent and low-quantity sales to the grid. This graph visually represents how energy production compares with consumption over time and how much energy is traded with the electrical grid.

Figure 8, shows output thermal power exchanged in the P2P market over the 72-hours. As we can see, ehe ‘Demand’ line has sharp peaks and troughs, indicating significant fluctuations over time. The ‘CGU Production’ line has a more consistent pattern with slight undulations around the middle of the y-axis range. The ‘Boiler Production’ line shows a trend that generally increases and then decreases, with its peaks being much lower than those of the demand.

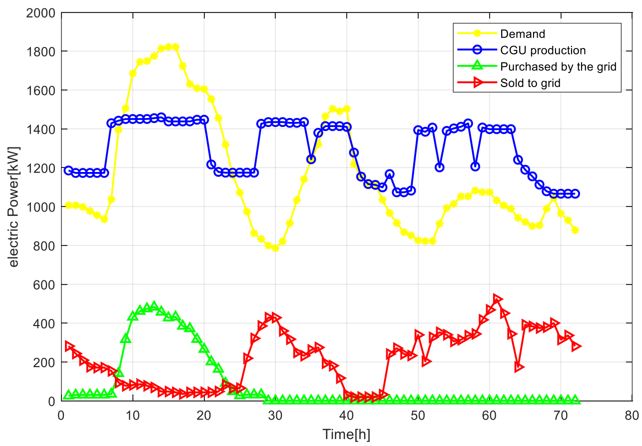


**Figure 7.** Output electrical power exchanged in the P2P market.

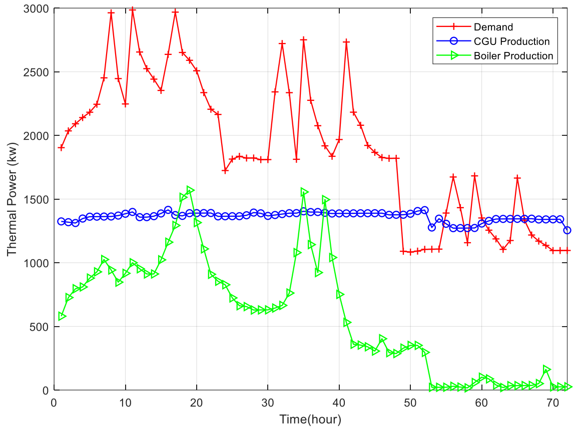


**Figure 8.** Output thermal power exchanged in the P2P market.

In the following, using the peer-to-peer or P2P approach, modeling of the electricity market and determination of the power level and the exchange of electrical energy sales have been discussed. P2P markets rely on the matching of supply and demand based on multilateral negotiations between all agents (or agent actions). These markets can transmit a complete map of exchanges to the network, and hence enable the sharing of costs related to the use of shared infrastructure and services. In this article, such costs are attributed through exogenous network loads to several alternative methods, uniformly, based on the electrical distance between agents and regions. This covers a variety of basic network physical and regulatory settings. Since attribution mechanisms are defined in an exogenous manner to affect any P2P business, they ultimately change the subject of the market to cover the costs of operating the network. It should be noted that the market fee is modeled based on the following three approaches:

- Zonal: Based on this plan, the power grid is divided into several areas associated with distinct regional unit costs. Each zone can be managed by a different system operator. A high-price area encourages foreign agents not to trade with domestic agents and drives domestic agents to self-consumption. In this sense, regional cost allocation policy allows to isolate a region economically. However, its effectiveness is highly dependent on the design of the areas.
- Unique: According to this plan, the way to allocate costs is to divide them equally among the members of the community.
- Distance: Based on this plan; in order to make the allocation of costs more accurate, network charges can be used according to the electrical distance between agents.

Figure 9 shows that when unique and regional network costs are too high, agents tend to leave the market. Because, the electrical distance policy does not guide transactions between partners connected to an electrical node. Hence, Agents 21 and 31 continue to trade with each other, even with high distance unit costs. In Figure 10 also, as expected, the costs of electrical distance and regional unit allow eliminating all power exchanges between regions. This clearly shows that, unlike unique cost allocation, electrical distance and regional cost allocation allow economic separation of regions. It was also found that the proposed network costs affect bilateral transactions in a way that may lead to sub-optimates. According to Figure 11, considering network costs, if possible, worsens the optimality of the settlement compared to the free market without network restrictions.

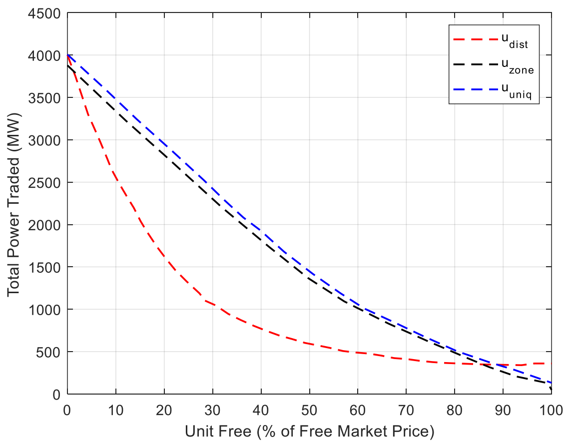


**Figure 9.** The total amount of power traded in the market.

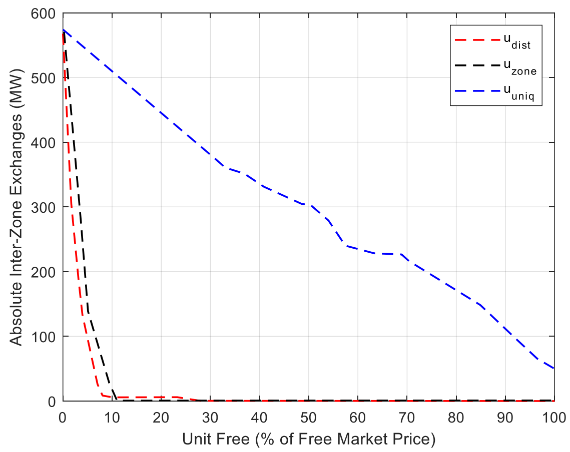


**Figure 10.** Total amount of power exchanged between different regions.

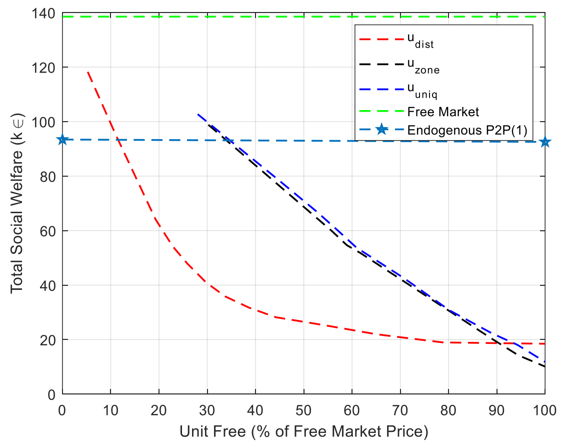


**Figure 11.** Exogenous P2P market efficiency.

## 5. Conclusion

A P2P energy network can be defined as a network, where network members can share part of their resources (for example, renewable energy and storage space and information) to achieve energy-related goals such as maximizing renewable energy consumption, electricity cost reduction, load modification, network operation reduction and investment cost minimization. Each member can be an energy provider or receiver and communicate directly with the network without any intervention from a third controller. In addition, a new peer can be added to an old counterpart without changing the operational structure of the system. In this paper, a load demand-based electricity market pricing model is presented in an integrated microgrid using a community-based P2P market model. The design of a community manager that manages business activities within the community as well as communication between the community and the rest of the system is formed. In this paper, the end-user benefits of electricity storage in the presence of P2P trading in local electricity markets with smart grid features are evaluated. Two market designs, Flexi User and Pool Hub, have been used in a community of buyers using battery storage systems. The results show a very interesting trade-off between the independence of the main network and the use of two added features - peer-to-peer trading and storage - for a community of customers. In the Flexi User scenario, the total savings to society from the combination of storage and peer-to-peer collaboration reached a 24.25% reduction in electricity bills compared to a reference case (neither storage nor peer-to-peer trading). While the monetary savings in the Pool Hub market is up to 25.53%, this requires more direct peer-to-peer trading of distributed energy resources.

## References

[1] F. Alfaverh, M. Denai, and Y. Sun, "A Dynamic Peer-To-Peer Electricity Market Model for a Community Microgrid with Price-Based Demand Response," *IEEE Transactions on Smart Grid*, vol. 14, no. 5, pp. 3976–3991, 2023.

[2] T. Baroche, P. Pinson, R. L. G. Latimier, and H. B. Ahmed, "Exogenous Cost Allocation in Peer-To-Peer Electricity Markets," *IEEE Transactions on Power Systems*, vol. 34, no. 4, pp. 2553–2564, 2019.

[3] Z. Wang, Q. Bui, B. Zhang, C. L. K. Nawarathna, and C. Mombeuil, "The Nexus Between Renewable Energy Consumption and Human Development in BRICS Countries: The Moderating Role of Public Debt," *Renewable Energy*, vol. 165, pp. 381–390, 2021.

[4] E. Du, N. Zhang, et al., "The Role of Concentrating Solar Power Toward High Renewable Energy Penetrated Power Systems," *2019 IEEE Power & Energy Society General Meeting (PESGM)*, 2019.
[5] M. S. Javadi, K. Firuzi, et al., "Optimal Sizing and Siting of Electrical Energy Storage Devices for Smart Grids Considering Time-Of-Use Programs," *IECON 2019 - 45th Annual Conference of the IEEE Industrial Electronics Society*, pp. 4157–4162, 2019.
[6] J. Li, R. Xiong, et al., "Design-Test of a Hybrid Energy Storage System for Primary Frequency Control Using a Dynamic Droop Method in an Isolated Microgrid Power System," *Applied Energy*, vol. 201, pp. 257–269, 2017.
[7] Y. Arya, "A New Optimized Fuzzy FOPI-FOPD Controller for Automatic Generation Control of Electric Power Systems," *Journal of the Franklin Institute*, vol. 356, no. 11, pp. 5611–5629, 2019.
[8] Q. Jiang, M. Xue, and G. Geng, "Energy Management of Microgrid in Grid-Connected and Stand-Alone Modes," *IEEE Transactions on Power Systems*, vol. 28, no. 3, pp. 3380–3389, 2013.
[9] Z. Li, and T. Ma, "Peer-to-Peer Electricity Trading in Grid-Connected Residential Communities with Household Distributed Photovoltaic," *Applied Energy*, vol. 278, 115670, 2020.
[10] M. Khorasany, Y. Mishra, and G. Ledwich, "Market Framework for Local Energy Trading: a Review of Potential Designs and Market Clearing Approaches," *IET Generation, Transmission & Distribution*, vol. 12, no. 22, pp. 5899–5908, 2018.
[11] B. H. Rao, S. L. Arun, and M. P. Selvan, "Framework of Locality Electricity Trading System for Profitable Peer-to-peer Power Transaction in Locality Electricity Market," *IET Smart Grid*, vol. 3, no. 3, pp. 318–330, 2020.
[12] Paudel, K. Chaudhari, C. Long, and H. B. Gooi, "Peer-To-Peer Energy Trading in a Prosumer-Based Community Microgrid: A Game-Theoretic Model," *IEEE Transactions on Industrial Electronics*, vol. 66, no. 8, pp. 6087–6097, 2019.
[13] H. T. Doan, J. Cho, and D. Kim, "Peer-To-Peer Energy Trading in Smart Grid Through Blockchain: A Double Auction-Based Game Theoretic Approach," *IEEE Access*, vol. 9, pp. 49206–49218, 2021.
[14] C. Mullaney, A. Aijaz, N. Sealey, and B. Holden, "Peer-To-Peer Energy Trading Meets IOTA: Toward a Scalable, Low-Cost, and Efficient Trading System," *2022 IEEE/ACM 15th International Conference on Utility and Cloud Computing (UCC)*, pp. 399–406, 2022.
[15] C. Zhang, T. Yang, and Y. Wang, "Peer-To-Peer Energy Trading in a Microgrid Based on Iterative Double Auction and Blockchain," *Sustainable Energy, Grids and Networks*, vol. 27, 100524, 2021.
[16] U. R. Barbhaya, L. Vishwakarma, and D. Das, "Etradechain: Blockchain-Based Energy Trading in Local Energy Market (LEM) Using Modified Double Auction Protocol," *IEEE Transactions on Green Communications and Networking*, vol. 8, no. 1, pp. 559–571, 2024.
[17] P. Angaphiwatchawal, P. Phisuthsaingam, and S. Chaitusaney, "A K-Factor Continuous Double Auction-Based Pricing Mechanism for the P2P Energy Trading in a LV Distribution System," *2020 17th International Conference on Electrical Engineering/Electronics, Computer, Telecommunications and Information Technology (ECTI-CON)*, pp. 37–40, 2020.
[18] Y. Zhou, and P. D. Lund, "Peer-To-Peer Energy Sharing and Trading of Renewable Energy in Smart Communities — Trading Pricing Models, Decision-Making and Agent-Based Collaboration," *Renewable Energy*, vol. 207, pp. 177–193, 2023.
[19] X. Luo, W. Shi, Y. Jiang, Y. Liu, and J. Xia, "Distributed Peer-To-Peer Energy Trading Based on Game Theory in a Community Microgrid Considering Ownership Complexity of Distributed Energy Resources," *Journal of Cleaner Production*, vol. 351, 131573, 2022.
[20] S. Malik, M. Duffy, S. Thakur, B. Hayes, and J. Breslin, "A Priority-Based Approach for Peer-To-Peer Energy Trading Using Cooperative Game Theory in Local Energy Community," *International Journal of Electrical Power & Energy Systems*, vol. 137, 107865, 2022.
[21] G. Li, Q. Li, X. Yang, and R. Ding, "General Nash Bargaining Based Direct P2P Energy Trading Among Prosumers Under Multiple Uncertainties," *International Journal of Electrical Power & Energy Systems*, vol. 143, 108403, 2022.
[22] H. Hanif, M. Zand, M. Azimi Nasab, S. M. S. Ghiasi, and S. Padmanaban, "Scenario-Based Planning of Participation of Virtual Power Plants in Storage and Energy Markets in Terms of Load Response and Market Price Uncertainty," *Journal of Green Energy Research and Innovation*, vol. 1, no. 3, pp. 77–95, 2024.
[23] J. Dong, C. Song, et al., "Decentralized Peer-To-Peer Energy Trading Strategy in Energy Blockchain Environment: A Game-Theoretic Approach," *Applied Energy*, vol. 325, 119852, 2022.
[24] W. Tushar, T. K. Saha, et al., "A Motivational Game-Theoretic Approach for Peer-to-Peer Energy Trading in the Smart Grid," *Applied Energy*, vol. 243, pp. 10–20, 2019.
[25] J. Ebrahimi, and M. Abasi, "Design of a Power Management Strategy in Smart Distribution Networks with Wind Turbines and EV Charging Stations to Reduce Loss, Improve Voltage Profile, and Increase Hosting Capacity of the Network," *Journal of Green Energy Research and Innovation*, vol. 1, no. 1, pp. 1–15, 2024.
[26] Kazemi, and A. Morsagh Dezfuli, "Optimal Placement of Distributed Energy Resources to Reduce Losses, Improve Voltage Profile, and Convert It Into a Self-Healing Smart Grid," *Journal of Green Energy Research and Innovation*, vol. 1, no. 1, pp. 16–33, 2024.
[27] F. Wu, P. Varaiya, P. Spiller, and S. Oren, "Folk Theorems on Transmission Access: Proofs and Counterexamples," *Journal of Regulatory Economics*, vol. 10, no. 1, pp. 5–23, 1996.
[28] E. Sorin, L. Bobo, and P. Pinson, "Consensus-Based Approach to Peer-To-Peer Electricity Markets with Product Differentiation," *IEEE Transactions on Power Systems*, vol. 34, no. 2, pp. 994–1004, 2019.
[29] Lüth, J. M. Zepter, P. Crespo del Granado, and R. Egging, "Local Electricity Market Designs for Peer-To-Peer Trading: the Role of Battery Flexibility," *Applied Energy*, vol. 229, pp. 1233–1243, 2018.
[30] U. Arnold, and Ö. Yildiz, "Economic Risk Analysis of Decentralized Renewable Energy Infrastructures – A Monte Carlo Simulation Approach," *Renewable Energy*, vol. 77, pp. 227–239, 2015.


## Declaration of competing interest

The author declare that they have no known competing financial interests or personal relationships that could have appeared to influence the work reported in this paper.

## Bibliography


**Arash Rahimi** was born in Ahvaz, Iran in 1989. He received his bachelor's and master's degrees in Power Systems Engineering from Shahid Chamran University of Ahvaz in 2012 and 2015. He is currently a Ph.D. student of Power Systems Engineering at Shahid Chamran University of Ahvaz. His main interests include Electrical Energy Distribution Systems, Electricity Market, Operation, Microgrids, and Protection of Power Systems.
**Email:** Arash.rahimi68@gmail.com
**ORCID:** 0009-0009-4314-1966
**Contribution Statement:** Conceptualization, Data curation, Formal analysis, Funding acquisition, Investigation, Methodology, Project administration, Resources, Software, Supervision, Validation, Visualization, Roles/Writing - original draft, Writing-review & editing.

Journal of Green Energy Research and Innovation

# Application of Remote Sensing in Wind Power Plant Location

Mostafa Davodabadi Farahani, Saeed Sharafi, Ali Farahani

## Highlights

- Using remote sensing knowledge to locate the wind power plant.
- Using Google Earth Enchain for remote sensing.
- Checking the wind condition including wind speed and direction.
- Investigating environmental conditions including temperature, pressure and air density.

## Graphical Abstract

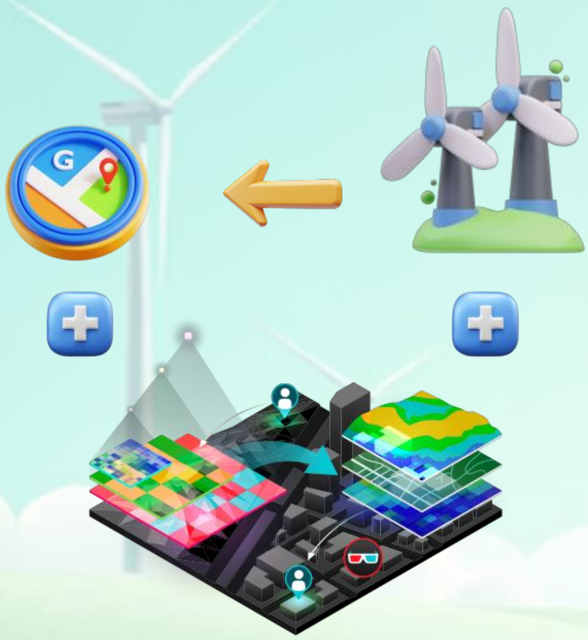


Use your device to scan and read the article online

Citation
M. D. Farahani, S. Sharafi, and A. Farahani " Application of Remote Sensing in Wind Power Plant Location," *Journal of Green Energy Research and Innovation*, vol. 2, no. 1, pp. 57-65, 2025.

https://doi.org/10.61186/jgeri.2.1.57

JGERI Journal of Green Energy Research and Innovation

Journal of Green Energy Research and Innovation 2.1 (2025) 57-65

Online ISSN: 3041-9018

Journal of Green Energy Research and Innovation

Journal Homepage: www.jgeri.araku.ac.ir

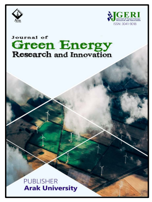


# Application of Remote Sensing in Wind Power Plant Location

Mostafa Davodabadi Farahani [1], Saeed Sharafi [2], Ali Farahani [3,*]

[1] *Department of Environmental Systems Engineering, Faculty of Agriculture and Environment, Arak University, Arak 38156-8-8349, Iran.*

[2] *Department of Environmental Science and Engineering, Faculty of Agriculture and Environment, Arak University, Arak 38156-8-8349, Iran.*

[3] *Department of Electrical Engineering, Faculty of Engineering, Arak University, Arak 38156-8-8349, Iran.*

ARTICLE INFO

*Keywords:*
Wind power plant,
Remote sensing,
Google earth engine,
Power system planning.

*Article History:*
Received: 07 April 2024;
Revised: 07 May 2024;
Accepted: 10 May 2024.

***Article type:***
Research Article

* ***Corresponding author***
*E-mail address*
Alifarahani372@yahoo.com (A. Farahani)

ABSTRACT

Today, the attention to energy security, the increase in the need for electrical energy and the need to create new power plants, especially the power plants that use renewable energy, has increased significantly both in Asia and globally. Wind power is expected to make the largest contribution to global decarburization, ranking first or second in terms of projected capacity by 2050. This type of power plant directly uses natural energy as fuel. And as a result, climate change affects the efficiency of these power plants. Two parameters of the natural phenomenon of wind, which include wind speed and direction, are the main factors of wind power plant efficiency. The science of remote sensing is the process of identifying and monitoring the physical characteristics of a remote area by means of satellites. Google Earth Engine is an artificial intelligence to use this knowledge. Google Earth Engine combines a multi-petabyte catalog of satellite imagery and geospatial datasets with planetary-scale analysis capabilities. Google Earth Engine provides us with these parameters. In this article, by collecting and then analyzing these data, we try to choose suitable candidate locations for the establishment of these two types of power plants, and based on priority, we provide a list for the establishment of solar and wind power plants.

## 1. Introduction

Fossil fuels are running out, and their extraction is very expensive, which has made humanity look for sustainable energy. Wind energy as a renewable and sustainable energy source and most importantly without pollution is one of the sustainable energies of interest [1]. The energy generated by wind power conversion frameworks (WECS) varies with environmental meteorology and wind speed [2,3], so we need to predict and manage these changes [4]. Wind power plants or wind farms use wind energy to produce electricity. This type of power plant plays an important role in the development of power plants in many countries.

Wind power plants are a group of wind turbines that are used to produce electricity [5]. We also know these power plants as wind farms or wind parks. Wind power plants can consist of one or a thousand wind turbines. Wind farms can be either onshore or offshore. It can be said that the largest onshore wind farms are located in China and the United States. For example, Gansu Wind Farm is the largest wind farm in the world with a capacity of more than 6000 MW located in China. Location is very important for establishing a wind farm. In general, a place to establish a wind power plant should be chosen that has suitable wind conditions, access to the electricity transmission network, and physical access. Electricity production has a direct relationship with wind speed and wind direction [6], which is explained in the section of wind conditions.

Wood Mackenzie analysts expect China to install more than 400 gigawatts of new wind capacity between 2021 and 2030, 73 gigawatts offshore, and the rest of the world to connect nearly 600 gigawatts to the grid. The wind power capacity forecast for the rest of Asia and the Pacific is 126 GW of new capacity between 2021 and 2030, half of which will be provided by India. Meanwhile, analysts expect Europe to connect 248 gigawatts of new wind capacity to the grid over the next decade, 34% of which will be offshore. US wind capacity is projected at 114 GW of new wind power capacity, including 35 GW due to increased PTC development between 2021-2023. In Latin America, there is a forecast of 42 GW of new grid-connected capacity between 2021 and 2030, with the vast majority (90%) of this capacity in Brazil, Chile, Colombia, and Mexico. Analysts also predict that 47 gigawatts of new wind capacity will be added in the Middle East and Africa by 2030Considering the amount of planning and construction that must be done to reach the predicted capacities, the study is necessary to determine the best place to install wind power plants.

One strategy for mitigating the variability of wind power is by aggregating wind farms that cover a large geographical area. The aggregation of wind farms creates a smoothing effect: individual wind farms with different wind utilization rates are grouped into a synthesized system, thereby producing a single output with minimal variability compared to each generation unit or wind farm prior to aggregation [7,8]. Another strategy for mitigating the variability of wind power is by using energy storage systems (ESSs). ESSs can be applied to the power system in a variety of forms (e.g., CAES, electrochemical batteries, and flow batteries) and can provide a variety of services (e.g., renewable power output smoothing, peak shaving, and frequency regulation). Also, ESS can improve the operational reliability of wind power systems and aid in the reduction of electricity production costs [9-12]. reference [6] By incorporating Geographic Information System (GIS) tools and the Analytical Hierarchy Process (AHP) offers a comprehensive solution to balance energy production, cost factors, and environmental impacts.

Remote sensing is the process of identifying and monitoring the physical properties of an area by measuring its reflected and emitted radiation at a distance (usually from a satellite or aircraft) [13]. Today, remote sensing has different uses, including the discovery and mapping of the topography of the unevenness of the earth and oceans and temperature changes without the need for travel [14]. Tracking the growth of a city and changes in agricultural land or forests over several years or decades. Tracking clouds and dust storms and tracking pollution. Google Earth Engine is an artificial intelligence that uses satellite data and is considered a practical tool for remote sensing with the support of Google information. Google Earth Engine (GEE) is a cloud-based platform that facilitates geoprocessing, making it a tool of great interest to the academic and research world. reference [15] proposes a bibliometric analysis of the GEE platform to analyze its scientific production. Reference [16] examines trends and applications of the Google Earth engine in remote sensing and earth science research. and [17] performs planetary-scale geospatial analysis by Google Earth Engine.

Usually, to increase the efficiency of wind power plants, the structure of the turbine, including the structure of the blades and the generator, is examined, and the turbines are installed in the places desired by the operators without a general survey of the area. So that first an area is selected, then with the help of the wind atlas, the amount of wind in the area is checked and if it is suitable, it is installed, but this place is not necessarily the best place to install the power plant, and this is a big bug in the installation of wind turbines. The main goal of this article is to remove this bug by choosing the best place to install wind turbines for establishing a wind power plant.

In this article, we will first examine the effect of wind sources on the performance of wind turbines. Also used GEE as a remote sensing knowledge toolbox. First, the method of using GEE is explained, and then the exact location of a wind power plant is discussed, and all the necessary environmental conditions, including wind speed and direction, and the temperature of the area, are checked, and the best place for the establishment of the power plant is selected.

The rest of the structure of the article is as follows: In section 2, wind power plants are discussed and wind resources are also examined. Also, in section 3, we will discuss remote sensing and how it works, and finally, we will examine a case study in section 4.

## 2. Wind power plant

Wind turbines work on a simple principle, instead of using electricity to generate wind, they use wind to generate electricity. The wind spins the turbine blades around the rotor, and the blades spin the generator, producing electricity. First, we need to understand wind power, wind is a form of solar energy that is created by a combination of three simultaneous events:

The sun unevenly heats the atmosphere, the irregularity of the earth's surface and the rotation of the earth. The flow and speed of the wind varies greatly across the globe and is modified by flowing water, vegetation and the unevenness of the land. Wind current is a clean and renewable kinetic energy that can be used for many purposes such as sailing, flying kites, and even generating electricity. The terms "wind energy" and "wind power" both describe the process by which the wind It is used to generate mechanical power or electricity. This mechanical power can be used for specific tasks (such as grinding grain or pumping water) or a generator can convert this mechanical power into electricity. A wind turbine converts wind energy into electricity using the aerodynamic force of rotor blades that act like airplane wings or helicopter rotor blades. As the wind flows across the blade, the air pressure is reduced on one side of the blade. The difference in air pressure on both sides of the blade causes it to rise and stretch. The lift force is stronger than the drag and this causes the rotor to rotate. The rotor is connected to the generator either directly (if it is a direct drive turbine) or through a shaft and a series of gears (gearbox) which speeds up the rotation and allows for a physically smaller generator. This conversion of aerodynamic force into the rotation of the generator creates electricity.

### 2.1. Wind Resource

Several different factors influence the potential wind resource in an area. The three main factors that influence power output are: wind speed, wind condition, air density, and blade radius. Wind turbines need to be in areas with a lot of wind on a regular basis, which is more important than having occasional high winds.

Wind speed largely determines the amount of electricity generated by a turbine. Higher wind speeds generate more power because stronger winds allow the blades to rotate faster. Faster rotation translates to more mechanical power and more electrical power from the generator. The relationship between wind speed and power for a typical wind turbine is shown in Figure 1. Turbines are designed to operate within a specific range of wind speeds. The limits of the range are known as the cut-in speed and cut-out speed. The cut-in speed is the point at which the wind turbine is able to generate power. Between the cut-in speed and the rated speed, where the maximum output is reached, the power output will increase cubically with wind speed. For example, if wind speed doubles, the power output will increase 8 times. This cubic relationship is what makes wind speed such an important factor for wind power.

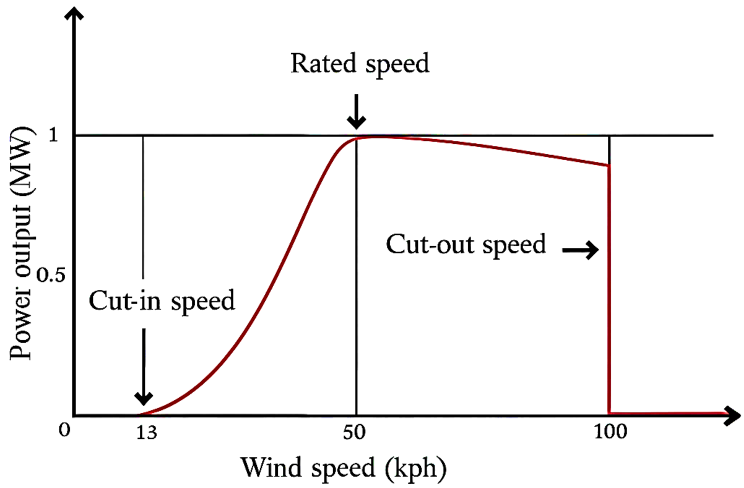


**Figure 1.** Arbitrary power curve of a 1 MW wind turbine compared to wind speed.

This cubic dependence does cut out at the rated wind speed. This leads to the relatively flat part of the curve in Figure 1, so the cubic dependence is during the speeds below 15 m/s (54 kph). The cut-out speed is the point at which the turbine must be shut down to avoid damage to the equipment. The cut-in and cut-out speeds are related to the turbine design and size and are decided on prior to construction.

The balancing factor is that strong gusts and high turbulence require more powerful and more expensive turbines, otherwise there is a risk of damage. The average power in the wind is not proportional to the average wind speed. The closer the angle of the wind with the blades is to 90 degrees, the more wind power is needed to move the blades. For this reason, ideal wind conditions would be strong but steady winds with little turbulence from one direction. Mountain passes are ideal places for wind power plants in these conditions. Wind turbines are designed to maximize the rotor blade radius to maximize power output. Larger blades allow the turbine to capture more of the kinetic energy of the wind by moving more air through the rotors. However, larger blades require more space and higher wind speeds to operate. As a general rule, turbines are spaced out at four times the rotor diameter. This distance is necessary to avoid interference between turbines, which decreases the power output. It should also be noted that power output of wind power plant is related to the local air density, which is a function of altitude, pressure, and temperature. Dense air exerts more pressure on the rotors, which results in higher power output. Also, high humidity and temperatures below zero and above 40 degrees have a negative effect on turbine performance. So, in general, we need to know the wind speed and wind direction, the density of the environment (temperature, altitude and air pressure) and the humidity of the environment to study the suitable location of the wind power plant.

## 3. Remote Sensing

Remote sensing provides information about objects at or near the surface of the Earth and atmosphere based on radiation reflected or emitted from those objects. The information is usually captured at a distance from above in the form of image data. Such data allow us to determine the composition and nature of the Earth's surface and atmosphere from local to global scales, and assess changes by analyzing images captured at different points in time. In this sense, remote sensing is useful in providing spatial information that is otherwise difficult or impossible to obtain. In the social sciences remote sensing is useful for visualizing (providing alternative and synoptic views) and classifying human environments. Social science researchers commonly integrate remotely sensed data or its derivatives with other socioeconomic data sets within geographic information systems to conduct spatial analyses. We said that remote sensing is the process of identifying and monitoring the physical characteristics of an area by measuring its reflected and emitted radiation at a distance (usually from a satellite or aircraft) [13]. And Google Earth Engine is a powerful tool for using remote sensing knowledge. In the following, we will explain the performance of GEE. According to the classification of moisture concepts carried out by UNESCO, Iran's climate is divided into four types: humid, dry, semi-arid and ultra-arid. Based on this, the Tehran with humid climate is considered. In Figure 2 show flowchart of the research process is shown. Using GEE, the desired satellites are selected first, the sentinel-5p satellite is selected to receive and process data. One of the uses of this satellite is weather forecasting and it has the ability to calculate temperature, wind speed, air pressure, etc. Then the desired areas are selected using them that it is shown in Figure 3. Then the desired coding is done to obtain the desired parameters such as the speed and direction of the wind and the density of the environment. Each parameter has its own wavelengths and information, the task of satellites is to identify this information, and the desired parameters are calculated in two medium-term and long-term intervals. Mid-term data of about one year to examine all seasons and examine current environmental conditions. The long-term data of about ten years are analysed to examine the climate changes of the region from the past to the present, so that we can have a general view of the future of the region.

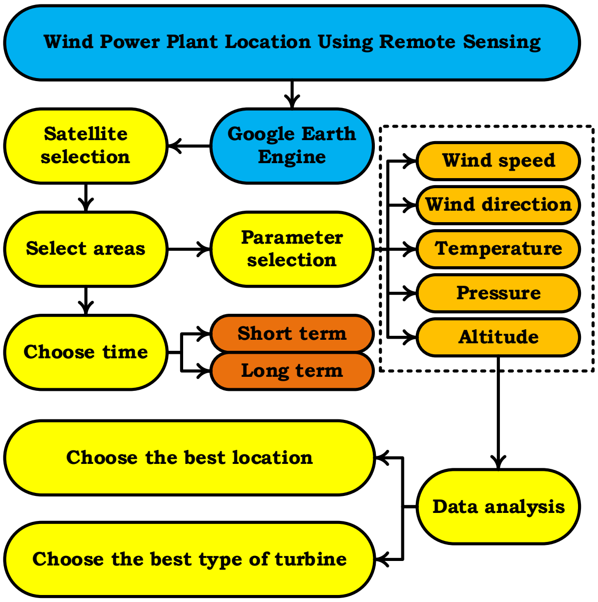


**Figure 2.** The flowchart methodology of this research.


**Figure 3.** The Geographical location of desired place.

## 4. Results

We conduct the desired research on the city of Tehran in two short-term and long-term periods. The short-term period is one year and the year 2020 has been selected. First, we calculate the wind speed. The wind speed is measured in meters per second with the amount of recorded data of 196 data per year, which is one measurement data almost every two days. and this amount of data is reliable. The results of measuring the wind speed in Tehran in year 2020 in terms of meters per second are shown in Figure 4. The wind speed in 2020 fluctuated between 0.31 and 3.247 meters per second. Also, the average wind speed was 1.35 meters per second, which you can see in Table 1.

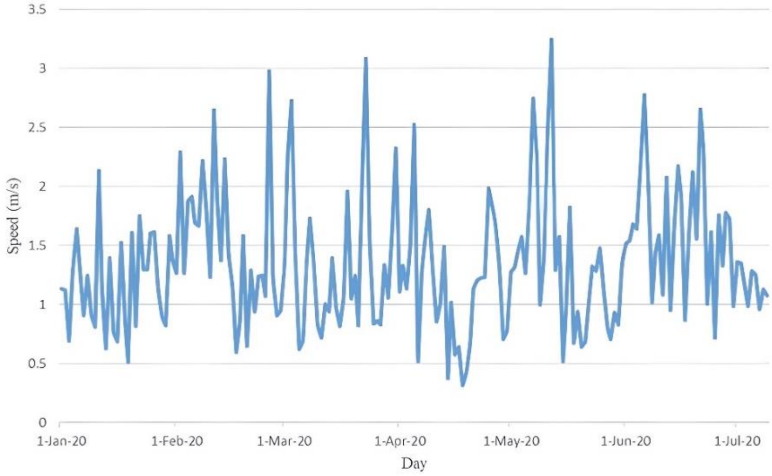


**Figure 4.** Wind speed chart in (m/s) in 2020 in Tehran city.

Figure 5 is a graphic representation of the amount of wind blowing in different areas of Tehran. Warmer colors show higher wind speeds, and on the contrary cooler colors show lower wind speeds. As you can see, the south, southwest and west of Tehran are the places where the wind speed is higher than other areas. Also, in the north and east of Tehran, the wind speed is lower than in other regions.

In Figure 6, you can see a column chart of wind direction for Tehran city in year 2020. The amount of wind blowing in all directions is expressed separately and as a percentage. The amount of wind blowing in the northeast direction of is 64% as the lowest value. Also, western winds account for 24% of the total wind gusts, which is the highest amount. South, southwest, and northwest winds each account for 14% percent. Southeast winds account for 13% percent, and finally, north and east winds account for 9% and 7% percent are assigned to themselves, respectively. According to the values provided, the best direction to install the turbine blades is in the direction of the west winds so that maximum wind power can be used.

**Table 1.** Minimum, maximum and average of wind speed in (m/s) in Tehran city in the year 2020.

| Average | Maximum | Minimum |
|---|---|---|
| 1.350 | 3.247 | 0.319 |

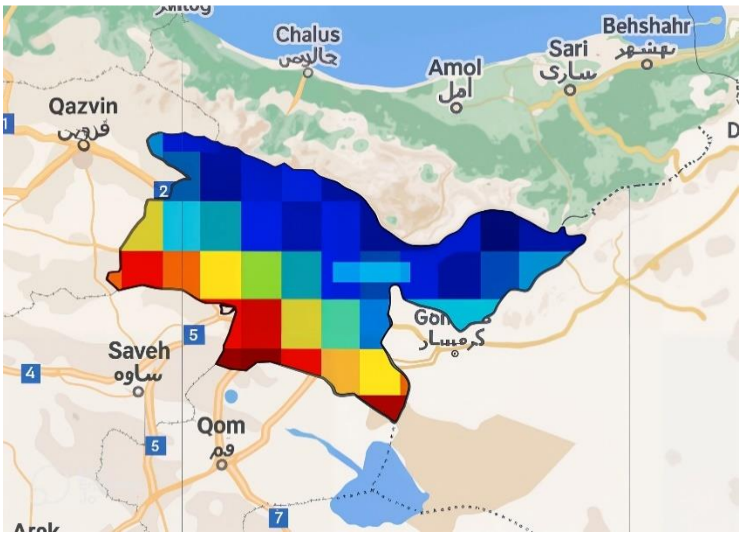


**Figure 5.** Graphic representation of the amount of wind blowing in different areas of Tehran. Warmer colors show higher wind speeds, and on the contrary cooler colors show lower wind speeds.

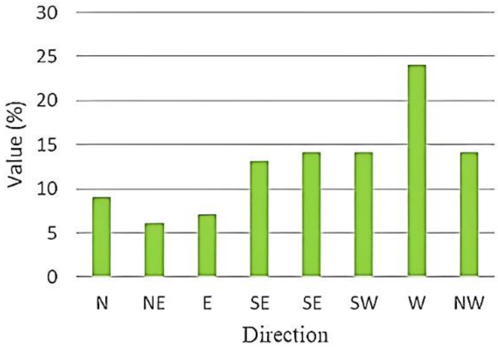


**Figure 6.** Bar chart of wind direction values in percentage in Tehran city for 2020 (including main and secondary directions).

After the short-term surveys (one-year period) of the wind condition, we will move on to the long-term studies (10-year period from 2010 to 2020). As you can see in Figure 7, the wind condition in Tehran is relatively has been stable and the average wind speed in these ten years is about 1.3 (m/s). As you can see in the Figure 8, the average wind speed in 2020 is higher than the annual average, and the 10-year average speed is a more reasonable number for predicting the coming years. As a result, the best value for estimating the wind speed is the ten-year average.

Figure 9 is a graphic representation of the amount of wind blowing in different areas of Tehran for the period of 2010 to 2020. Warmer colors indicate higher wind speed and on the contrary, cooler colors indicate lower wind speed. As you can see, the southwest of Tehran has had the highest amount of wind during these ten years. The 10-year survey was able to show a more accurate location than the 1-year survey.

Figure 10 shows the temperature changes of Tehran city in 2020. The temperature is displayed during the day and night. You can see that in the months of August and July, the daily temperature reaches 50 degrees Celsius. On the other hand, the air temperature at night in December and February reaches below ten degrees Celsius. As a result, the components of the turbine must be selected in such a way that they can work easily in this temperature range and can withstand freezing nights for about 2 months without being damaged. Also, Figure 11 shows the temperature of Tehran in August. You can see that the southern part of Tehran has a higher temperature and the northern part of Tehran has a more moderate temperature.

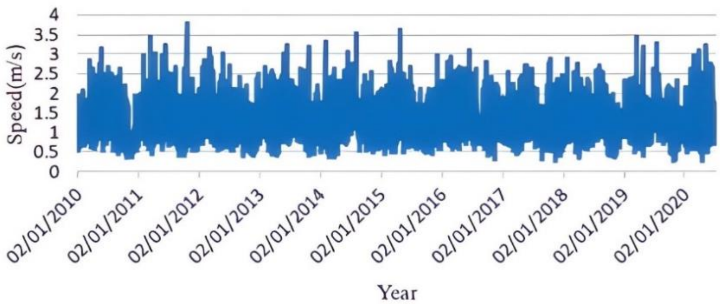


**Figure 7.** Wind speed chart in (m/s) in years 2010 to 2020 in Tehran city.

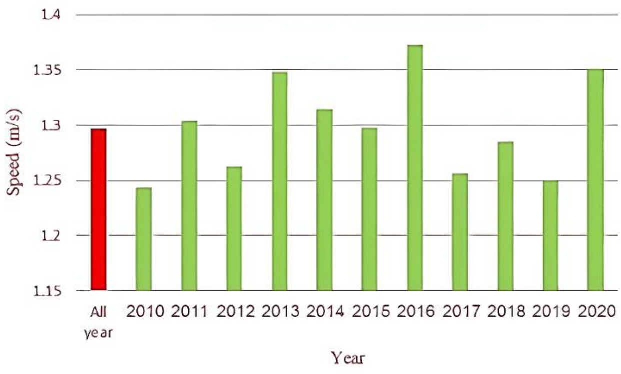


**Figure 8.** Average wind speed chart in (m/s) in years 2010 to 2020 in Tehran city.

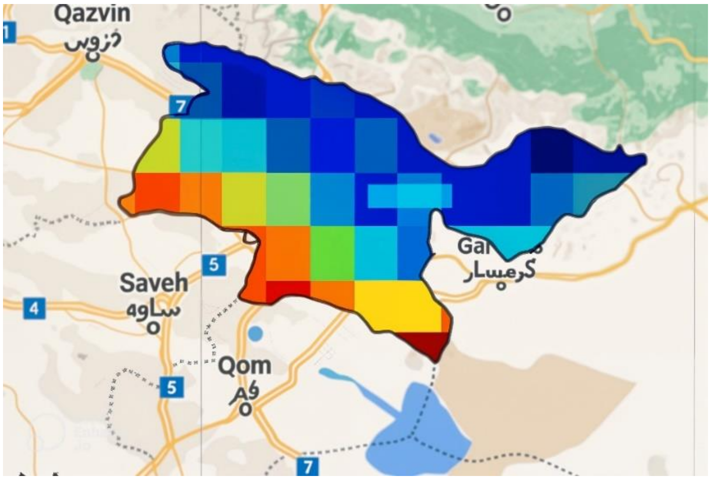


**Figure 9.** Graphic representation of the amount of wind blowing in different areas of Tehran for year 2010 to 2020. Warmer colors show higher wind speeds, and on the contrary cooler colors show lower wind speeds.

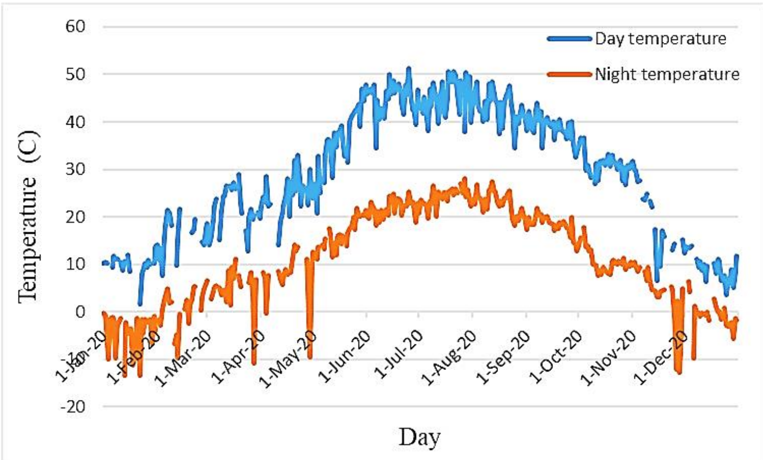


**Figure 10.** Shows the temperature changes of Tehran in 2020 in Celsius.

One of the advantages of GEE is the remote measurement of parameters, especially the measurement of air pressure. Table 2 shows the average surface air pressure of Tehran city in 2020. It means air surface pressure at heights near the ground (wind turbine installation height). The measurement has been done for 6 months. Also, Figure 12 shows the graphic view of surface air pressure in Tehran in 2020. The south of Tehran has more air pressure and the air pressure decreases as you move to the north of Tehran and increase the height above the sea level.

The purpose of measuring air temperature and pressure is to find air density. Air density is the ratio of mass to volume of air in the earth's atmosphere. Air density decreases with increasing altitude, which is an indication of air pressure. Also, changes in temperature and humidity change the density of the air. The density of air at sea level at 15 degrees Celsius and according to the international standard atmosphere is about 1.225 kg/m3 and 0.075 lb/m3. As a result, in terms of air density, south of Tehran is a more favourable area for establishing a wind power plant.

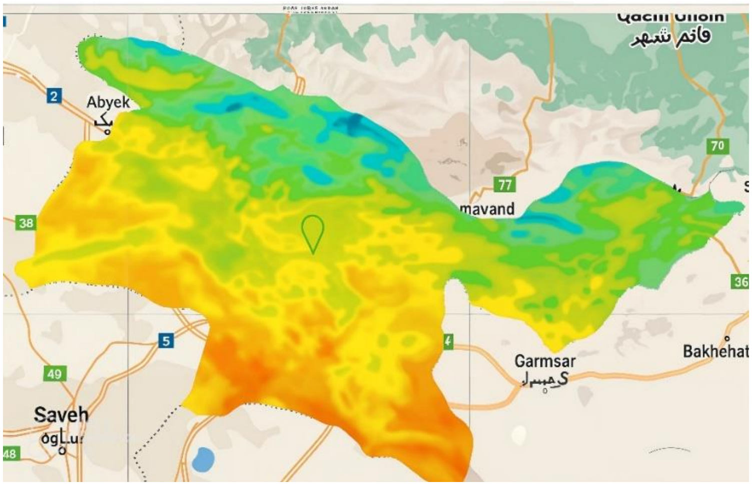


**Figure 11.** Shows the temperature of Tehran in August graphically for year 2020.

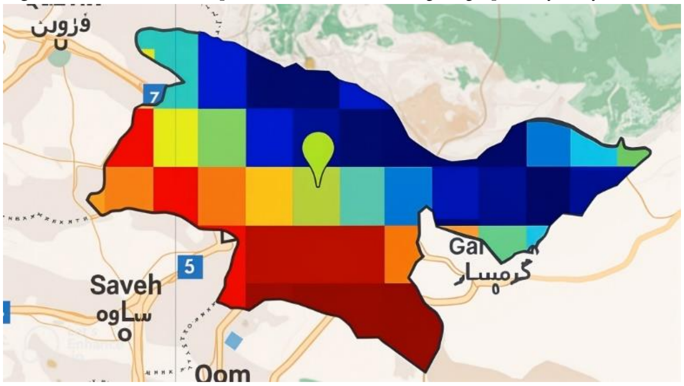


**Figure 12.** Shows the graphic view of surface air pressure in Tehran in 2020.

**Table 2.** Shows the average surface air pressure of Tehran city in 2020.

| Day | Surface pressure (Pa) |
|---|---|
| 1-Jan-2020 | 83,466.96 |
| 1-Feb-2020 | 83,445.59 |
| 1-Mar-2020 | 83,362.64 |
| 1-Apr-2020 | 83,393.91 |
| 1-May-2020 | 83,528.11 |
| 1-Jun-2020 | 83,213.36 |

## 5. Conclusion

Remote Sensing is a new science that is growing rapidly with the development of satellites and its applications are increasing. We were able to investigate the environmental conditions of the target area by using this knowledge and using GEE. In addition to the mentioned parameters, with GEE, it is easy to look at the geographical situation of the region (lowlands and highlands) and also other parameters, such as the level of air, land and water pollution, to check fossil fuel power plants. In this article, we presented a method for locating the wind power plant according to the environmental conditions to increase the efficiency of the turbines using remote sensing knowledge. One of the advantages of using this method is access to remote area information in all places, including inaccessible places such as the highest mountains to the deepest valleys. Also, high speed and easy access to data and finally large amount of data for long periods of time can be considered as advantages of this method. High accuracy is another advantage of this method. Also, this method can be used to make decisions in the area of choosing the location of other power plants, including solar power plants in the whole country or at the level of a small city.

## References


[1] X. Wang, P. Guo, and X. Huang, "A Review of Wind Power Forecasting Models," *Energy Procedia*, vol. 12, pp. 770–778, 2011.
[2] Z. Dongmei, Z. Yuchen, and Z. Xu, "Research on Wind Power Forecasting in Wind Farms," *2011 IEEE Power Engineering and Automation Conference*, pp. 175–178, 2011.
[3] M. Lei, S. Shiyan, C. Chuanwen, L. Hongling, and Z. Yan, "A Review on the Forecasting of Wind Speed and Generated Power," *Renewable and Sustainable Energy Reviews*, vol. 13, no. 4, pp. 915-920, 2009.
[4] W. C. Tsai, C. M. Hong, et al., "A Review of Modern Wind Power Generation Forecasting Technologies," Sustainability, vol. 15, no. 14, p. 10757, 2023.
[5] R. Gasch, and J. Twele, "Wind Power Plants: Fundamentals, Design, Construction and Operation," *Springer Science & Business Media*, 2011.
[6] Dinçer, A. Demir, and K. Yılmaz, "Multi-Objective Turbine Allocation on a Wind Farm Site," *Applied Energy*, vol. 355, 122346, 2024.
[7] P. Hayes, I. Ilie, A. Porpodas, S. Z. Djokic, and G. Chicco, "Equivalent Power Curve Model of a Wind Farm Based on Field Measurement Data," *2011 IEEE Trondheim PowerTech*, pp. 1–7, 2011.
[8] M. Pei, L. Ye, et al., "Short-Term Regional Wind Power Forecasting Based on Spatial–temporal Correlation and Dynamic Clustering Model," *Energy Reports*, vol. 8, pp. 10786–10802, 2022.
[9] P. Denholm, J. Jorgenson, et al., "Value of Energy Storage for Grid Applications," *National Renewable Energy Laboratory (NREL)*, USA, 2013.
[10] F. Díaz-González, A. Sumper, O. Gomis-Bellmunt, and R. Villafáfila-Robles, "A Review of Energy Storage Technologies for Wind Power Applications," *Renewable and Sustainable Energy Reviews*, vol. 16, no. 4, pp. 2154–2171, 2012.
[11] M. Khalid, and A. Savkin, "Minimization and Control of Battery Energy Storage for Wind Power Smoothing: Aggregated, Distributed and Semi-Distributed Storage," *Renewable Energy*, vol. 64, pp. 105–112, 2014.
[12] M. C. Such, and C. Hill, "Battery Energy Storage and Wind Energy Integrated into the Smart Grid," *2012 IEEE PES Innovative Smart Grid Technologies (ISGT)*, pp. 1–4, 2012.
[13] J. Si, X. Li, H. Chen, and L. Han, "A Novel CNN-Based Radar Reflectivity Retrieval Network Using Geostationary Satellite Observations," *IEEE Geoscience and Remote Sensing Letters*, vol. 21, pp. 1–5, 2024.
[14] N. Kussul, M. Lavreniuk, S. Skakun, and A. Shelestov, "Deep Learning Classification of Land Cover and Crop Types Using Remote Sensing Data," *IEEE Geoscience and Remote Sensing Letters*, vol. 14, no. 5, pp. 778–782, 2017.
[15] Velastegui-Montoya, N. Montalván-Burbano, et al., "Google Earth Engine: A Global Analysis and Future Trends," *Remote Sensing*, vol. 15, no. 14, 3675, 2023.
[16] B. Pham-Duc, H. Nguyen, H. Phan, and Q. Tran-Anh, "Trends and Applications of Google Earth Engine in Remote Sensing and Earth Science Research: a Bibliometric Analysis Using Scopus Database," *Earth Science Informatics*, vol. 16, no. 3, pp. 2355–2371, 2023.
[17] "Google Earth Engine: Planetary-Scale Geospatial Analysis for Everyone," *Remote Sensing of Environment*, vol. 202, pp. 18–27, 2017.


## Declaration of competing interest

The authors declare that they have no known competing financial interests or personal relationships that could have appeared to influence the work reported in this paper.

## Bibliography


**Mostafa Davodabadi Farahani** He completed his bachelor's degree from Arak Azad University in Arak, Iran in 2020 and his master's degree in environmental systems engineering from Arak University in Arak, Iran in 2024. His research interests include remote sensing, environmental systems, and clean energy.
**Email:** Mstafa.farahani@gmail.com
**ORCID:** 0009-0001-2900-1264
**Contribution Statement:** Conceptualization, Data curation, Funding acquisition, Investigation, Methodology, Software, Writing-review & editing.



**Saeed Sharafi** Completed his PHD in department of environment science and engineering. currently, he is an assistant professor at Arak University. His research interests include hydrology, abiotic stress and environment science.
**Email:** sharafi.saeed@gmail.com
**ORCID:** 0000-0003-2644-5924
**Contribution Statement:** Conceptualization.



**Ali Farahani** graduated with a B.S. in Electrical Engineering from Arak Azad University, Arak, Iran in 2015. He completed his M.S. in Electrical Engineering from Arak University, Arak, Iran in 2018-2020. He is currently pursuing a Ph.D in Electrical Engineering from Tafresh University, Tafresh, Iran. His research interests include state estimation, control, and planning in power systems.
**Email:** Alifarahani372@yahoo.com
**ORCID:** 0009-0003-1437-808X
**Contribution Statement:** Conceptualization, Formal analysis, Investigation, Resources, Software, Roles/Writing-original draft, Writing-review & editing.